

LA-UR-09-02442

Approved for public release;
distribution is unlimited.

Title: Advances in Monte Carlo
Criticality Methods

Author(s): Forrest Brown, Brian Kiedrowski,
William Martin, Gokhan Yesilyurt

Intended for: ANS Mathematics & Computation Topical Meeting
Saratoga, NY
May 3-7, 2009



Los Alamos National Laboratory, an affirmative action/equal opportunity employer, is operated by the Los Alamos National Security, LLC for the National Nuclear Security Administration of the U.S. Department of Energy under contract DE-AC52-06NA25396. By acceptance of this article, the publisher recognizes that the U.S. Government retains a nonexclusive, royalty-free license to publish or reproduce the published form of this contribution, or to allow others to do so, for U.S. Government purposes. Los Alamos National Laboratory requests that the publisher identify this article as work performed under the auspices of the U.S. Department of Energy. Los Alamos National Laboratory strongly supports academic freedom and a researcher's right to publish; as an institution, however, the Laboratory does not endorse the viewpoint of a publication or guarantee its technical correctness.

M&C 2009
Monte Carlo Workshop
Saratoga Springs, NY
May 3-7, 2009

Advances in Monte Carlo Criticality Methods

Forrest Brown ^a, Brian Kiedrowski ^b, William Martin ^c, Gokhan Yesilyurt ^c

^a *Los Alamos National Laboratory, Los Alamos, NM, USA*

^b *University of Wisconsin, Madison, WI, USA*

^c *University of Michigan, Ann Arbor, MI, USA*



THE UNIVERSITY
of
WISCONSIN
MADISON



Advances in Monte Carlo Criticality Methods

Workshop for M&C-2009, Saratoga Springs, NY, May 3-7, 2009

Forrest Brown (LANL), Brian Kiedrowski (U. Wisc/LANL),
William Martin (U. Mich), Gokhan Yesilyurt (U. Mich)

Monte Carlo criticality calculations are performed routinely on large, complex models for reactor physics and criticality safety applications. This tutorial includes a thorough review of best practices for calculations, alongwith in-depth coverage of several important R&D areas. It should benefit both Monte Carlo practitioners and developers.

I. Best Practices for Monte Carlo Criticality Calculations

A review of the theory & practice of Monte Carlo criticality calculations, including best practices for assuring convergence, avoiding bias in Keff and tallies, and assessing bias in confidence intervals. Includes numerous practical examples with MCNP and recent advances.

II. Adjoints, Importance, and Reactor Kinetics Parameters

A review of adjoint calculations and the need for importance weighting in computing reactor kinetics parameters. The iterated fission probability and its use in Monte Carlo calculations is discussed at length. Numerous examples are presented, along with an overview of current efforts to develop a continuous-energy importance weighting method for MCNP.

III. Temperature Dependence

For realistic, detailed reactor calculations, Monte Carlo codes are part of a multiphysics simulation involving thermal-hydraulic feedback to adjust temperatures and densities. This process can result in 1000s of material temperatures for which broadened cross-sections are needed. Existing codes (eg, MCNP) were not designed to accommodate this need. This tutorial reviews the broadening temperature dependence and discusses a novel new on-the-fly broadening scheme that would permit an unlimited number of temperatures for only a modest computing cost

Agenda

I. Best Practices for Monte Carlo Criticality Calculations (Brown)

- Bias, convergence, dominance ratio, confidence intervals
- Examples for 1/4-core PWR & criticality safety

II. Adjoints, Importance, & Reactor Kinetics Parameters (Kiedrowski)

- Adjoint calculations, importance weighting, reactor kinetics parameters.
- Iterated fission probability and its use in Monte Carlo calculations
- Examples & results
- Continuous-energy importance weighting for MCNP

III. Temperature dependence

(Martin, Yesilyurt)

- Multi-physics simulations
- Doppler broadening temperature dependence
- On-the-fly broadening scheme & results

Introduction

Perspective

- As computing power has increased, the use of Monte Carlo methods for reactor analysis has grown
- Also, since more histories give better localized statistics, the principal uses of Monte Carlo have evolved:

| | |
|---------------|--|
| 1960s: | K-effective |
| 1970s: | K-effective, detailed assembly power |
| 1980s: | K-effective, detailed 2D whole-core |
| 1990s: | K-effective, detailed 3D whole-core |
| 2000s: | K-effective, detailed 3D whole-core, depletion, reactor design parameters |

→ Recent Monte Carlo R&D is focussed on advanced methods for modeling, depletion, & design parameters

Monte Carlo for Reactor Applications

- **Monte Carlo strengths**
 - Very general & accurate geometry modeling
 - Direct use of best cross-section data (ENDF/B, JEF, JENDL, ...)
 - Continuous-energy neutron transport & physics
 - Readily adapted to parallel computers

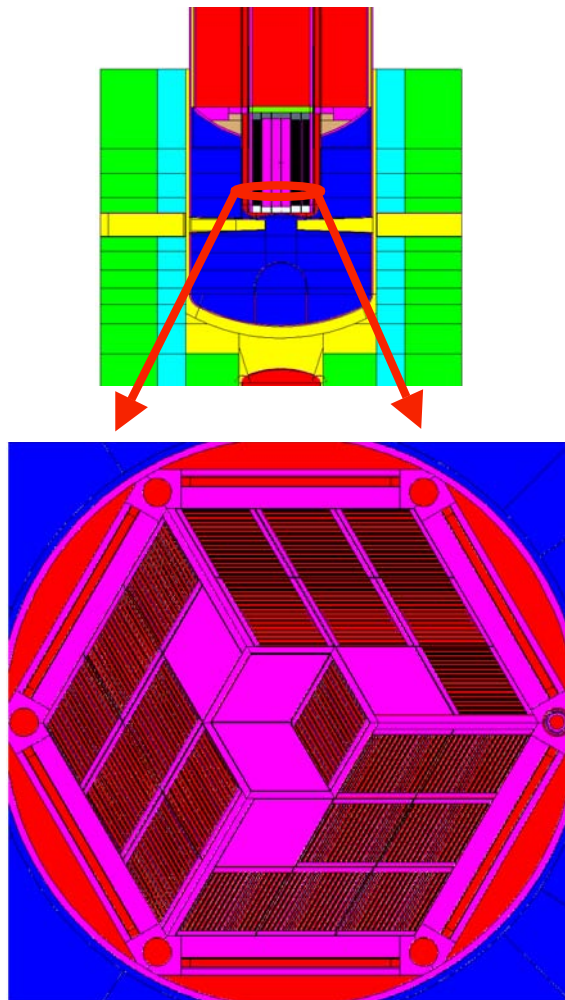
 - Examples on next few slides

- **This workshop:**
 - **Review the current challenges & advances**

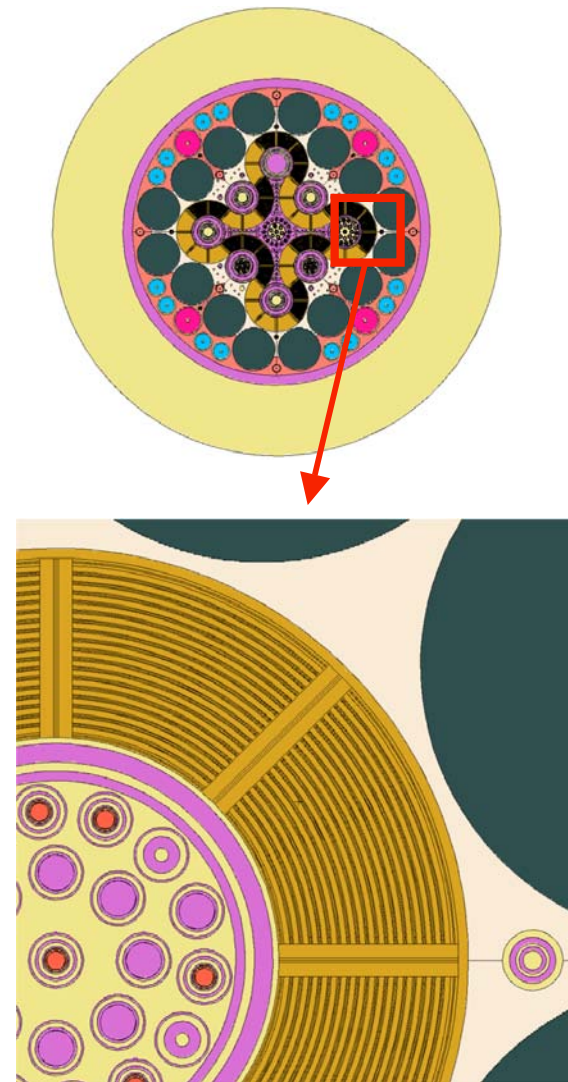
 - **Consider both theory & computations**

Research Reactors

MIT research reactor, with beam ports



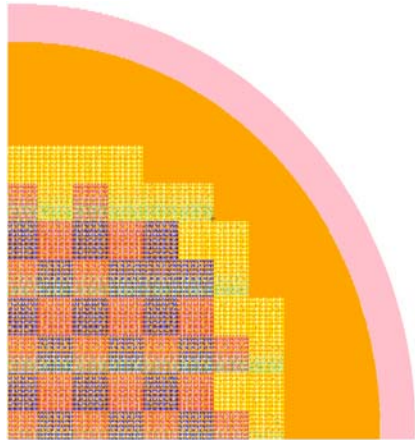
Advanced Test Reactor (ATR)



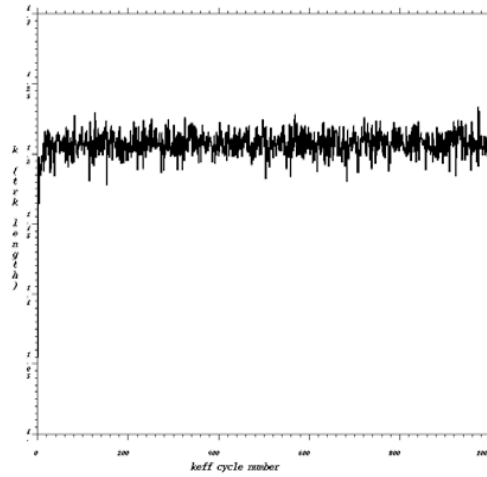
Pictures from mcnp plotter

Commercial Reactors - PWR, BWR

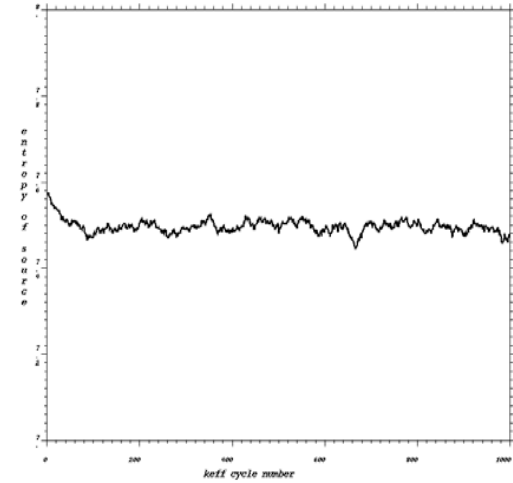
Geometry Model (1/4)



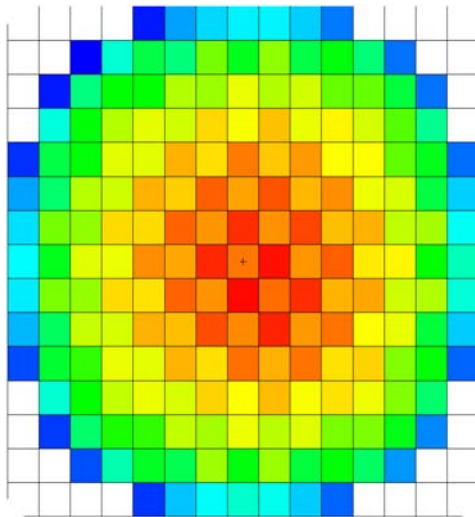
K vs cycle



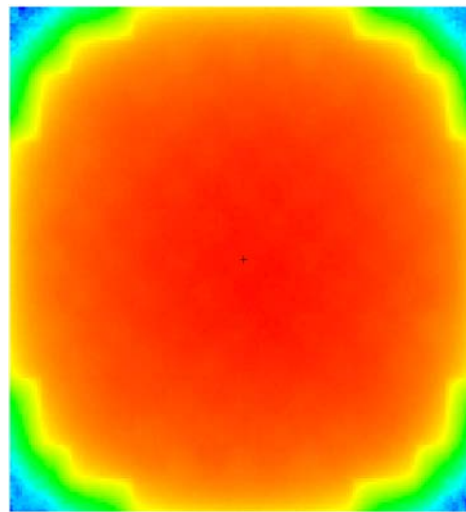
H_{src} vs cycle



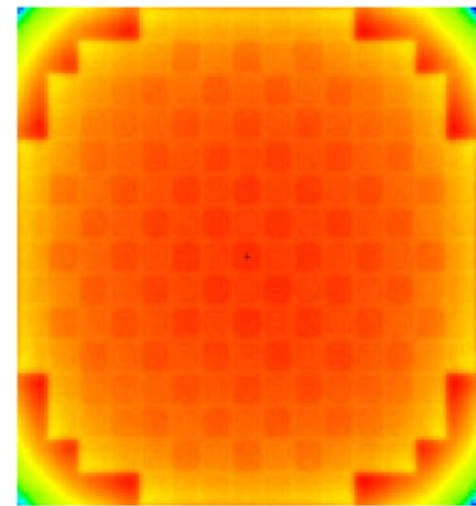
Assembly Powers



Fast Flux

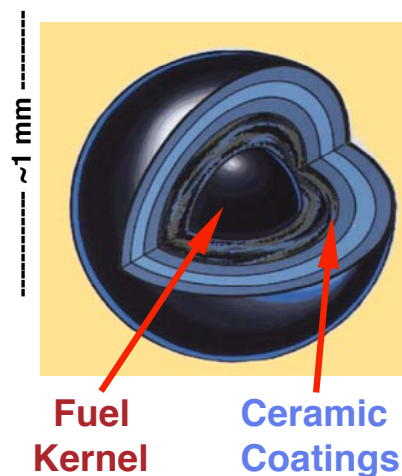


Thermal Flux



Pictures from mcnp plotter

Advanced Reactors - VHTR, HTGR, ...

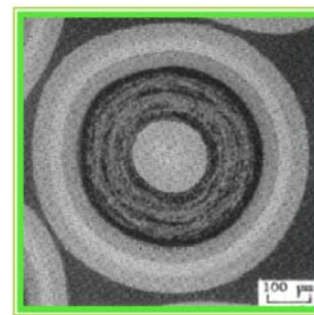


TRISO Fuel Particles:

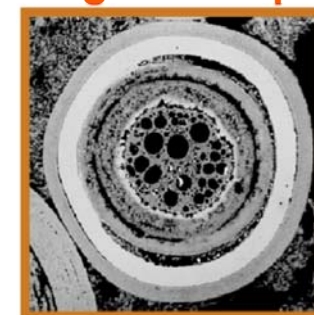
- Fission product gases trapped within coatings
- Coatings remain intact, even with high T & burnup

Fuel concept is same for block or pebble bed

Fresh Fuel



High Burnup



(From General Atomics)



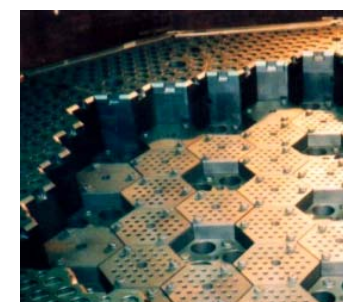
PARTICLES



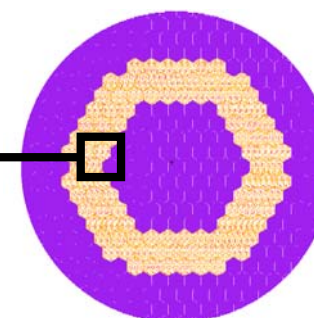
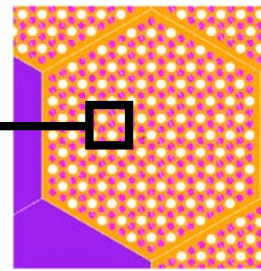
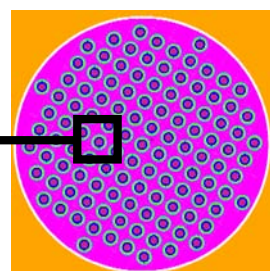
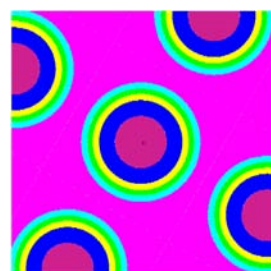
COMPACTS



FUEL BLOCK



CORE



Accurate & explicit modeling at multiple levels

Challenges in Monte Carlo Criticality Calculations

Longstanding problems with the fundamental theory:

1. **Bias in Keff**
2. **Convergence of source distribution**
3. **Underprediction bias in confidence intervals**
4. **Lack of adjoint weighting for tallies**
5. Determining adequate population size
6. Propagation of error (xsecs, depletion, etc.)
7. Existence & completeness of higher modes (Keff calculations)
8.

Current computational difficulties:

1. Fission products for depletion calculations
2. Scaling of codes to extreme problem sizes
3. **Multiphysics - coupling to T/H, heat transfer, & structural codes**
4. Multicore threading vs GPGPU vectors
5. Particle parallelism vs domain decomposition
6. Uncertainties in nuclear data
7. Validation of codes & nuclear data
8. Run-time needed for pin powers & depletion
9.

Best Practices for Monte Carlo Criticality Calculations

Fundamental problems & practical solutions for:

- Bias in Keff & tallies
- Convergence of Keff & source distribution
- Underprediction bias in confidence intervals

Introduction

- **Several fundamental problems with the MC solution of k-eigenvalue problems were identified in the 1960s - 1980s:**

- Bias in Keff & tallies
- Convergence of Keff & source distribution
- Underprediction bias in confidence intervals

(see Lieberoth, Gelbard & Prael, Gast & Candelore, Brissenden & Garlick)

- **Prior to now, all examples were toy problems that gave no guidance to MC practitioners**

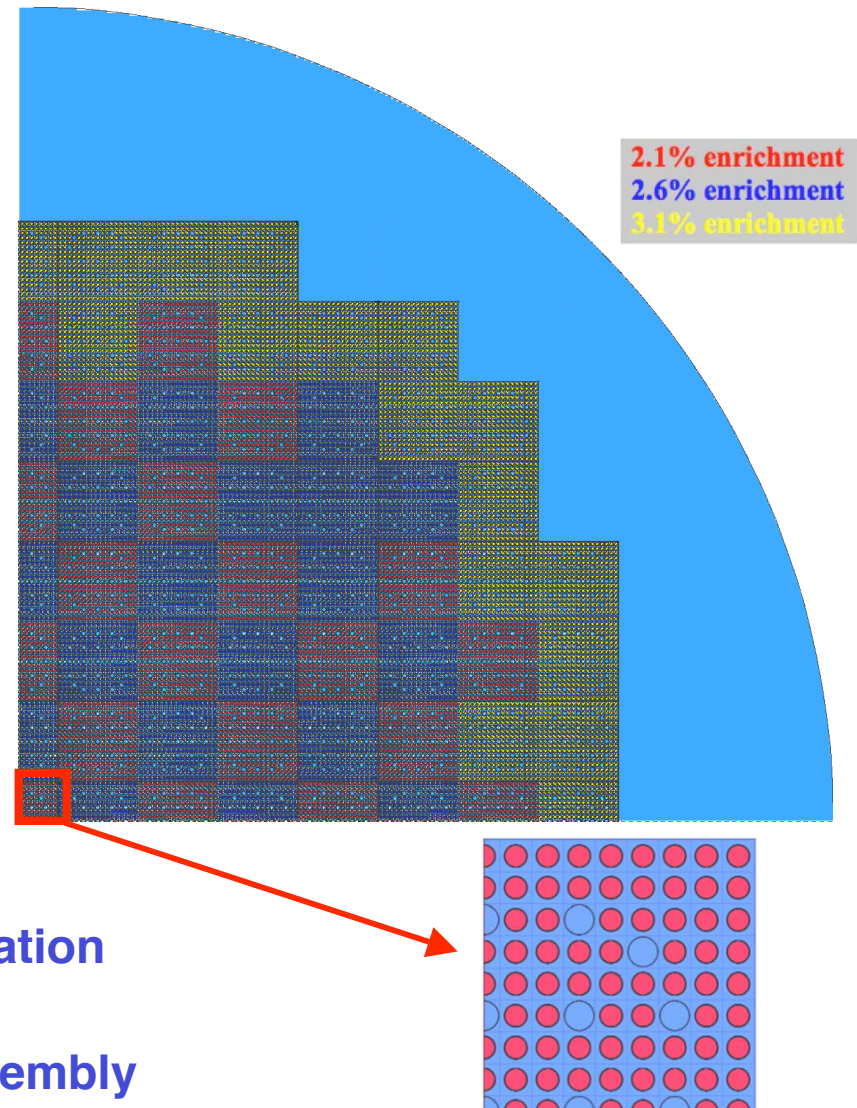
- **This talk:**

- Brief description & explanation for each concern
- Illustrate magnitude using
 1. Reactor: **realistic PWR quarter-core**
 2. Criticality Safety: **array of Pu-nitrate solution tanks**
- Discuss practical approaches to avoid the problems

Example Problem - Reactor

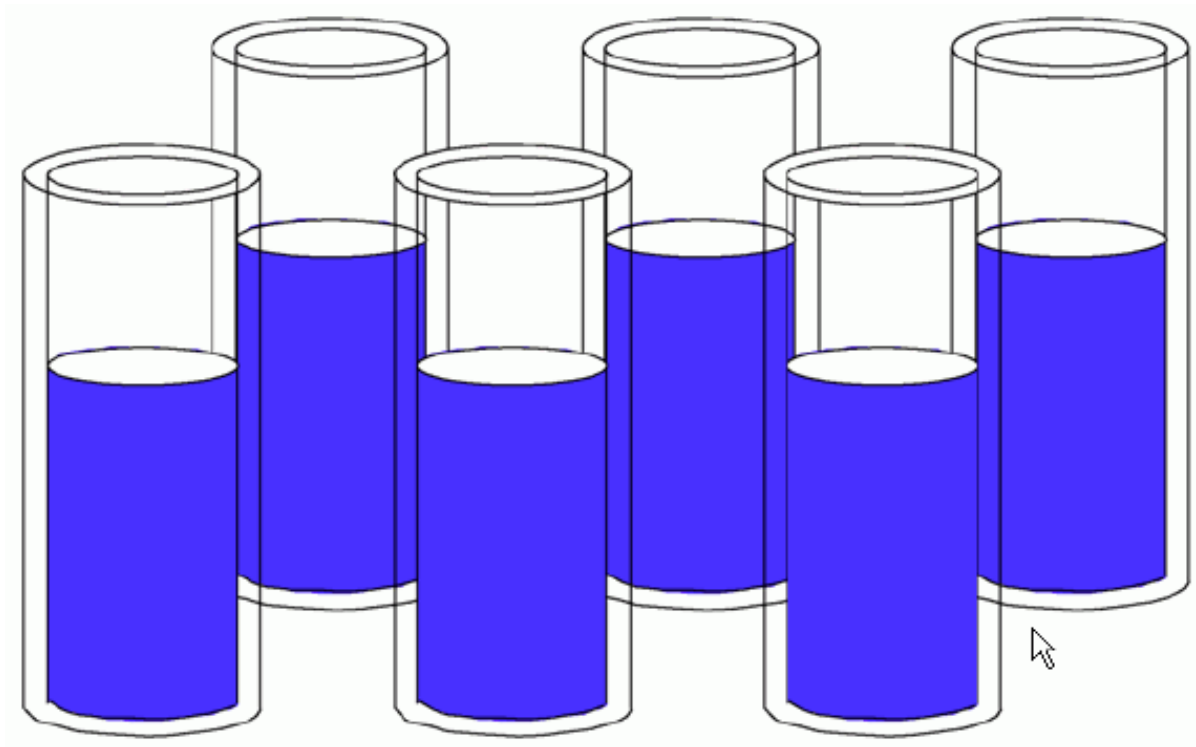
2D quarter-core PWR (Nakagawa & Mori model)

- **48 1/4 fuel assemblies:**
 - 12,738 fuel pins with cladding
 - 1206 1/4 water tubes for control rods or detectors
- **Each assembly:**
 - Explicit fuel pins & rod channels
 - 17x17 lattice
 - Enrichments: 2.1%, 2.6%, 3.1%
- **Dominance ratio $\sim .96$**
- **125 M active neutrons for each calculation**
- **ENDF/B-VII data, continuous-energy**
- **Tally fission rates in each quarter-assembly**



Example Problem - Criticality Safety

2 x 3 array of steel cans containing
plutonium nitrate solution



Power Method for Monte Carlo Criticality Calculations

K-eigenvalue equation

$$(L + T)\Psi = S\Psi + \frac{1}{K_{\text{eff}}}M\Psi$$

where

L = leakage operator

S = scatter-in operator

T = collision operator

M = fission multiplication operator

→ This eigenvalue equation is solved by power iteration

$$(L + T - S)\Psi^{(n+1)} = \frac{1}{K_{\text{eff}}^{(n)}}M\Psi^{(n)}$$

run MC histories
to get $\Psi^{(n+1)}$ & $K_{\text{eff}}^{(n+1)}$

fixed source
from cycle (n)

Power Iteration

Diffusion Theory or Discrete-ordinates Transport

Initial guess: $K_{\text{eff}}^{(0)}, \Psi^{(0)}$

Outer iterations (n)

- **Inner iterations** to solve for $\Psi^{(n+1)}$

$$(L + T - S)\Psi^{(n+1)} = \frac{1}{K_{\text{eff}}^{(n)}} M\Psi^{(n)}$$

- Solve linear equations or sweep through space/angle mesh

- Compute new K_{eff}

$$K_{\text{eff}}^{(n+1)} = K_{\text{eff}}^{(n)} \cdot \frac{1 \cdot M\Psi^{(n+1)}}{1 \cdot M\Psi^{(n)}}$$

- Renormalize $\Psi^{(n+1)}$

- If converged → stop

.....

Monte Carlo

Initial guess: $K_{\text{eff}}^{(0)}, \Psi^{(0)}$

Outer iterations (n)

- **Follow histories** to solve for $\Psi^{(n+1)}$

$$(L + T - S)\Psi^{(n+1)} = \frac{1}{K_{\text{eff}}^{(n)}} M\Psi^{(n)}$$

- During histories, save fission sites to use for source in next iteration

- Compute new K_{eff}

- **Tally $K_{\text{eff}}^{(n+1)}$ during histories**

- Renormalize $\Psi^{(n+1)}$

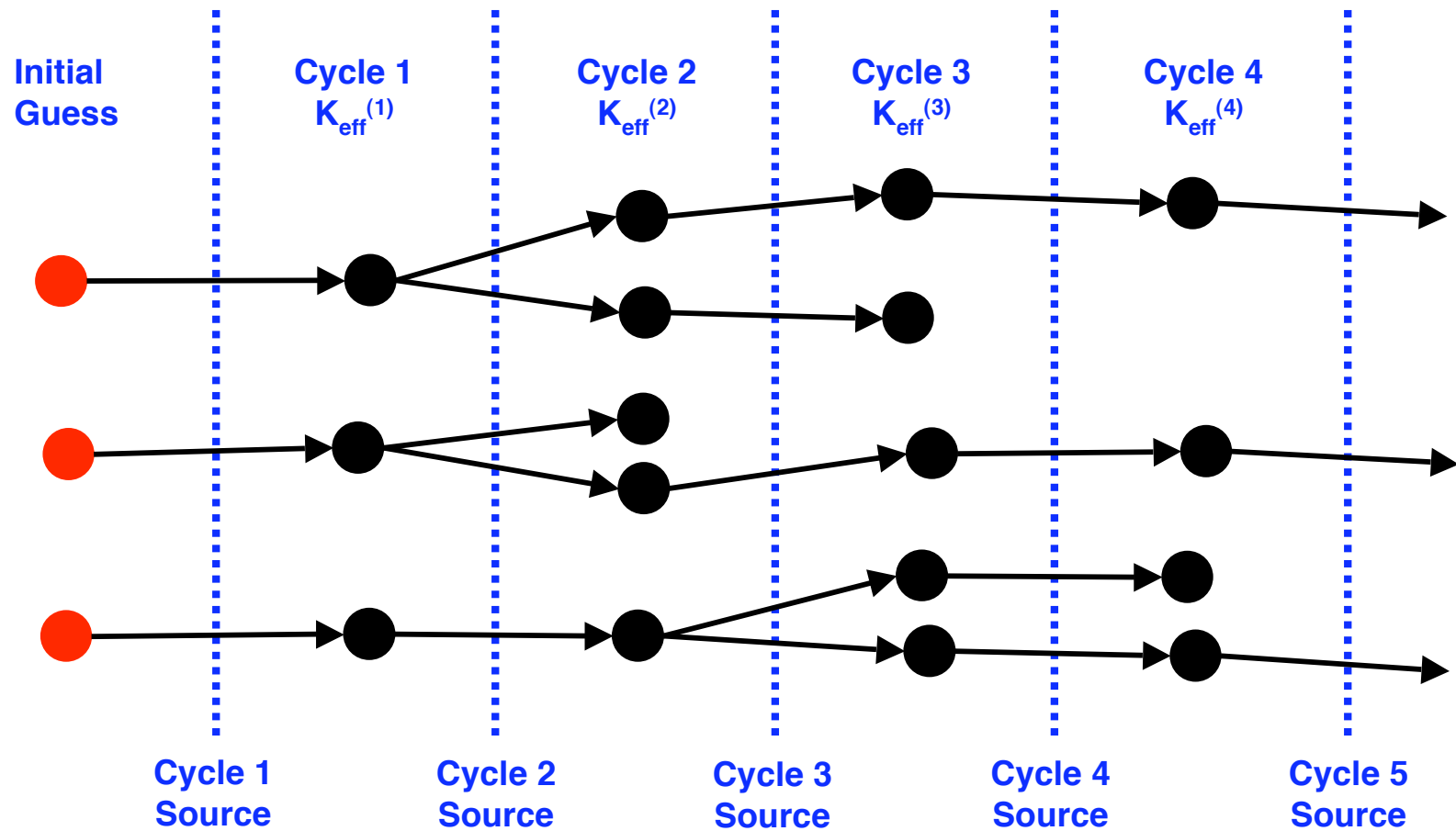
- **If converged → turn on tallies**

- **If statistics small enough → stop**

.....

Power Iteration for MC Criticality Calculations

cycle \equiv iteration \equiv batch \equiv generation

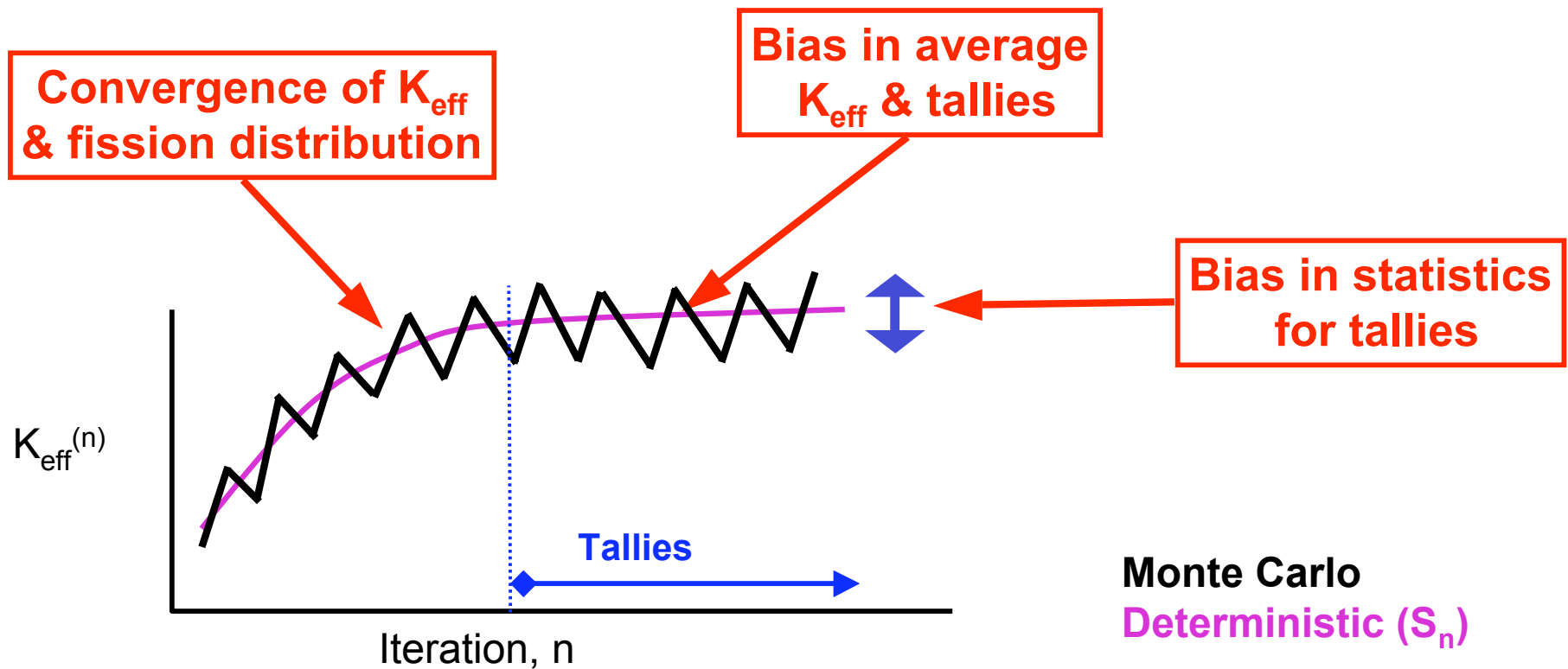


● Source particle generation

● Monte Carlo random walk

→ Neutron

Concerns



This talk:

- Brief description & explanation for each concern
- Illustrate magnitude using **realistic PWR quarter-core**
- Discuss practical approaches to avoid the problems

Bias in Keff & Tallies

Bias in K_{eff}

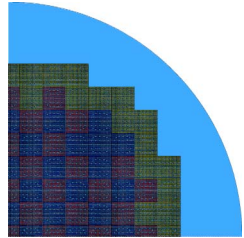
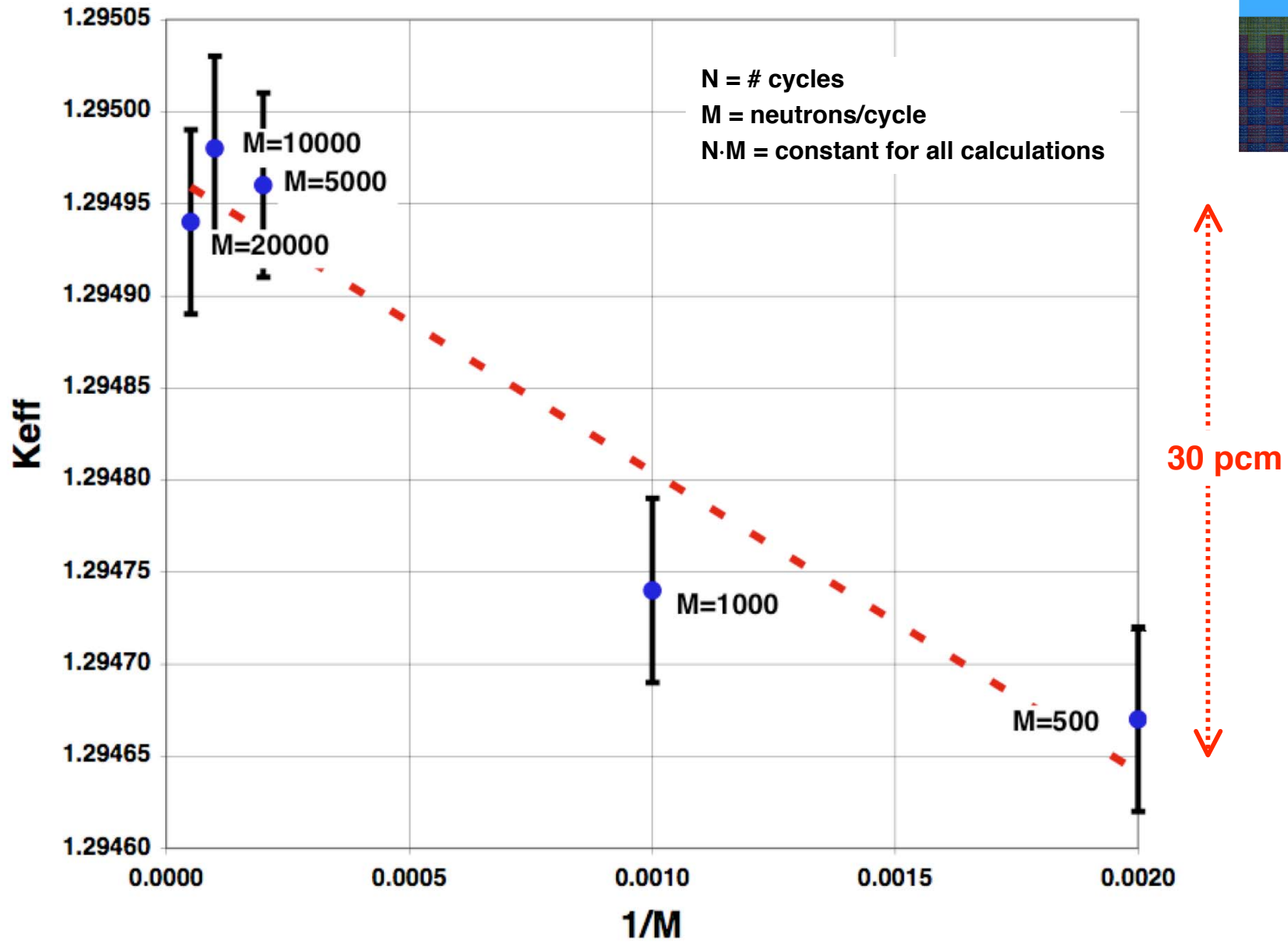
- Power iteration is used for Monte Carlo K_{eff} calculations
 - For one cycle (iteration):
 - M_0 neutrons start
 - M_1 neutrons produced, $E[M_1] = K_{eff} \cdot M_0$
 - At end of each cycle, must **renormalize** by factor M_0 / M_1
 - Dividing by stochastic quantity (M_1) introduces bias
- Bias in K_{eff}, due to renormalization

$$\text{bias in } K_{eff} = -\frac{\sigma_k^2}{K_{eff}} \cdot \left(\frac{\text{sum of lag-i correlation}}{\text{coeff's between batch K's}} \right) \propto \frac{1}{M_0}$$

Note: $\sigma_k^2 = \text{population variance}$; $\sigma_{keff}^2 = \sigma_k^2 / N$

- Run the reactor problem with different M (neutrons/cycle)
500, 1000, 5000, 10000, 20000

Reactor - Bias in Keff



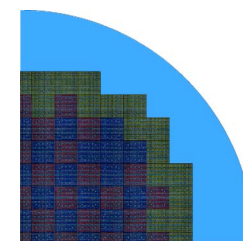
Reactor - Bias in Fission Tallies

| | | | | | | | | | | | | | | |
|------|------|------|------|------|------|------|------|-----|-----|-----|-----|-----|-----|-----|
| 0.0 | -0.5 | -0.6 | -0.2 | -0.3 | 0.5 | 0.8 | | | | | | | | |
| -0.2 | -0.7 | -0.8 | 0.1 | 0.3 | 0.7 | 0.6 | | | | | | | | |
| -0.5 | -0.7 | -0.7 | 0.0 | 0.3 | 0.7 | 1.0 | 1.3 | 1.2 | 1.6 | 2.0 | | | | |
| -0.1 | -0.7 | -0.8 | 0.2 | 0.3 | 0.8 | 1.1 | 1.2 | 1.2 | 1.3 | 2.4 | | | | |
| -0.4 | -0.6 | -0.5 | 0.0 | -0.1 | 0.2 | 0.7 | 0.6 | 1.4 | 2.0 | 1.9 | 2.7 | 3.2 | | |
| -0.7 | -0.9 | -0.8 | -0.4 | 0.2 | 0.5 | 0.4 | 1.0 | 1.2 | 1.6 | 2.0 | 1.6 | 2.6 | | |
| -0.6 | -0.3 | -0.7 | -0.6 | -0.6 | 0.3 | 0.8 | 1.1 | 1.2 | 1.5 | 1.1 | 1.7 | 1.8 | | |
| -0.5 | -0.8 | -1.0 | -0.8 | -0.5 | 0.2 | 0.8 | 0.9 | 1.2 | 1.2 | 1.4 | 1.3 | 1.9 | | |
| -0.5 | -0.9 | -0.8 | -1.0 | -0.6 | 0.2 | 0.2 | 0.6 | 0.9 | 1.1 | 0.8 | 0.7 | 1.1 | 0.9 | 1.5 |
| -0.9 | -0.9 | -1.1 | -1.0 | -0.9 | -0.1 | 0.2 | 0.6 | 0.8 | 0.6 | 0.6 | 0.6 | 1.3 | 1.2 | 1.1 |
| -1.2 | -1.3 | -1.2 | -1.0 | -0.6 | -0.5 | -0.3 | 0.2 | 0.9 | 0.7 | 1.1 | 0.9 | 1.3 | 1.2 | 1.1 |
| -1.3 | -1.5 | -1.0 | -0.9 | -0.7 | -0.5 | -0.6 | 0.3 | 0.4 | 0.5 | 1.3 | 1.4 | 2.1 | 1.9 | 1.6 |
| -1.7 | -1.5 | -1.1 | -1.1 | -0.6 | -0.5 | -0.2 | -0.1 | 0.3 | 0.6 | 1.0 | 1.7 | 2.0 | 2.1 | 1.9 |
| -1.5 | -1.5 | -1.4 | -1.0 | -1.1 | -0.8 | 0.0 | 0.1 | 0.3 | 0.4 | 1.0 | 1.0 | 1.5 | 3.1 | 2.3 |
| -1.6 | -1.6 | -1.2 | -1.2 | -0.6 | -0.7 | -0.4 | -0.2 | 0.1 | 0.2 | 0.5 | 1.6 | 2.1 | 2.4 | 2.3 |

**Percent errors in
 1/4-assembly fission rates
 using 500 neutrons/cycle**

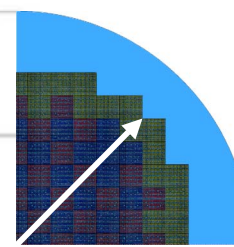
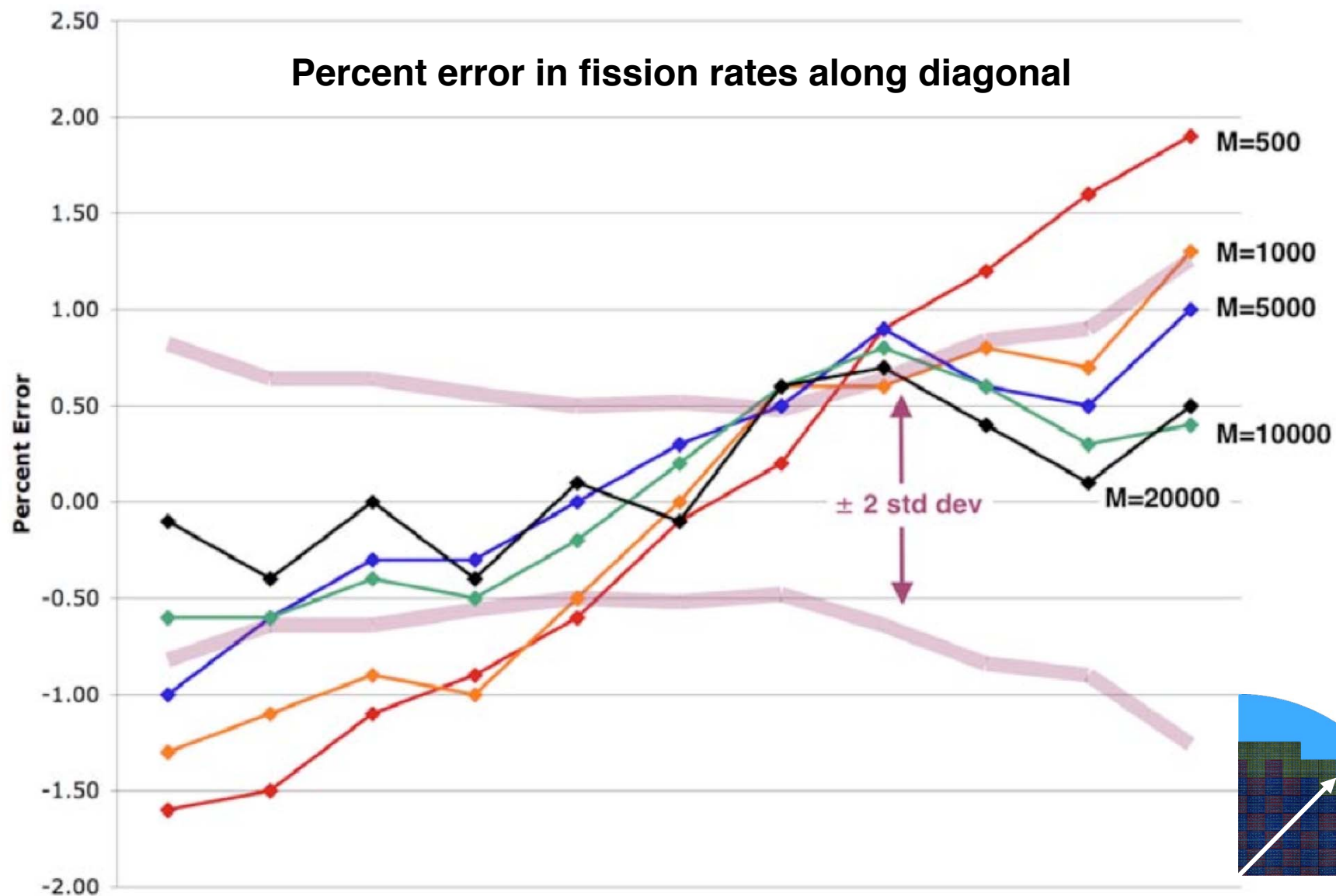
Errors of -1.7% to +3.2%

Statistics ~ .1% to .3%

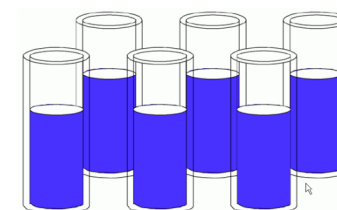
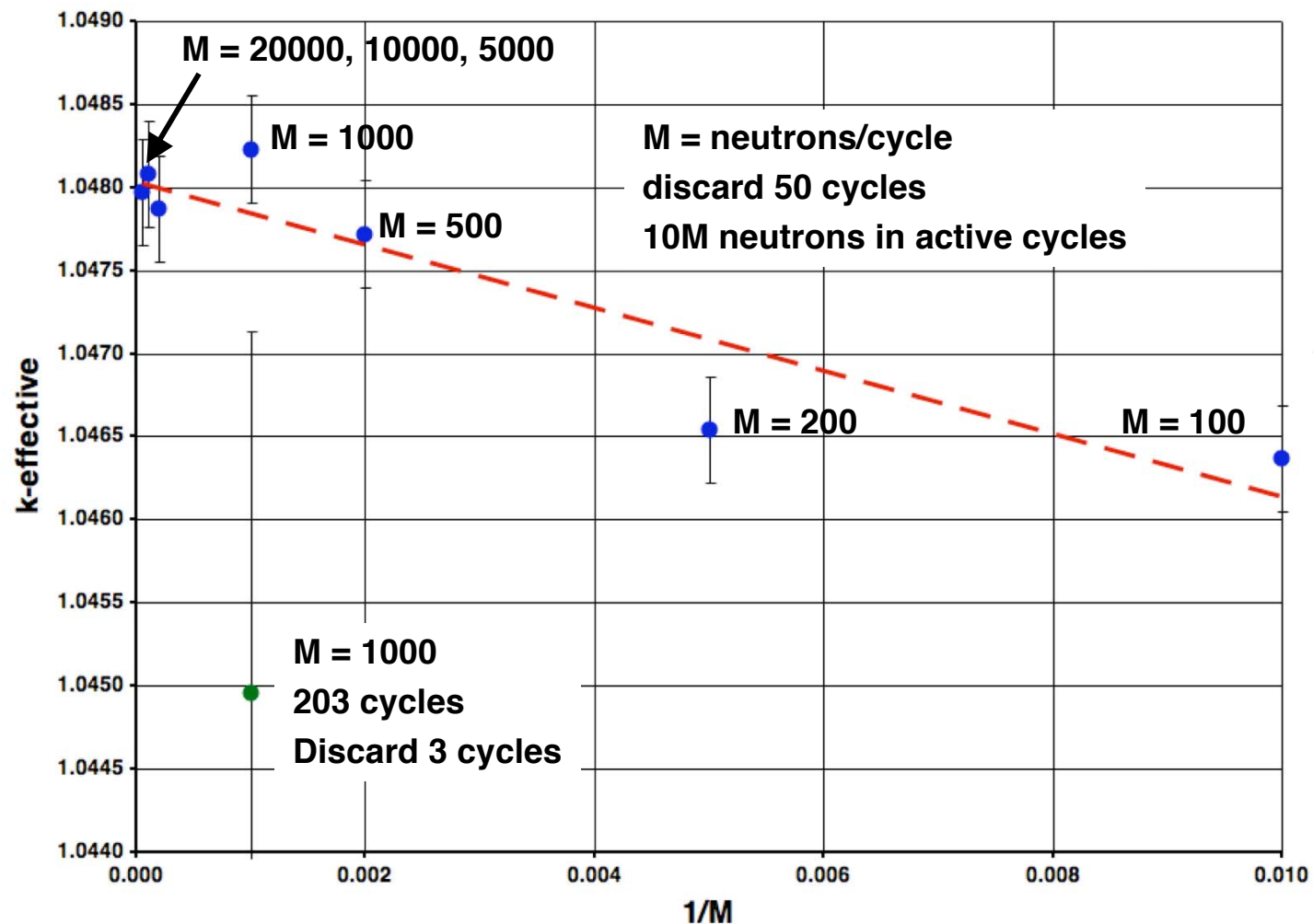


**Reference: ensemble-average of 25 independent calculations,
 with 25 M neutrons each & 20K neutrons/cycle**

Reactor - Bias in Fission Tallies



Criticality Safety - Bias in Keff



Note: Bias in green point is a convergence problem due to using Keno default - discard 3 cycles, 203 cycles total

Bias in Keff & Tallies

- **Past work - eliminating bias**

- **MacMillan**

- **Approach:** Weight the tallies for each cycle n by

$$W_n = \frac{\prod_{j=1}^{n-1} k_j}{K^{n-1}}, \quad \text{where } K = \left(\prod_{j=1}^N k_j \right)^{1/N}, \quad N = \text{number of active cycles}$$

- **Difficulty:** Must save all tallies for all cycles, combine at end of problem

- **Gast & Candelore**

- **Approach:** Increase M (neutrons/cycle) each cycle by 10 neutrons
 - **Difficulty:** For finite number of cycles, bias still exists

- **Practical solution - use large M (neutrons/cycle)**

- **Years ago**

- Slow computers, $M \sim 500 \Rightarrow$ bias could be a problem

- **Today**

- Fast computers, typically $M \sim 10K$ or $100K \rightarrow$ bias negligible
 - Large M gives more efficient parallel calculations

Bias in Keff & Tallies - Comments

- **For reactor problem with 500 neutrons/cycle**
 - Bias in Keff is ~ 30 pcm
 - Bias in the power distribution shows a significant tilt
 - Errors of -1.7% to $+3.2\%$ in power fractions
 - The bias is much larger than the MC uncertainties
- **Bias in Keff & the fission distribution is smaller with 1000 neutrons per cycle, and smaller still with 5,000 or 10,000 neutrons per cycle**
- **Practical solution - use large M (neutrons/cycle)**
 - For $M \sim 10K$ or more \Rightarrow bias negligible
 - Large M gives more efficient parallel calculations
- **Wielandt's method also reduces bias**
 - Reduces frequency of renormalizations, reduces correlation

Convergence of Source Distribution

Introduction

- Monte Carlo codes use power iteration to solve for K_{eff} & Ψ for eigenvalue problems
- Power iteration convergence is well-understood:

n = cycle number, k_0, u_0 - fundamental, k_1, u_1 - 1st higher mode

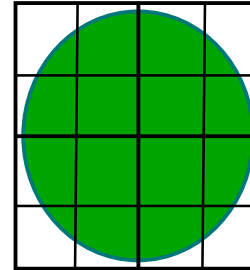
$$\Psi^{(n)}(\vec{r}) = \vec{u}_0(\vec{r}) + a_1 \cdot \rho^n \cdot \vec{u}_1(\vec{r}) + \dots$$

$$k_{\text{eff}}^{(n)} = k_0 \cdot \left[1 - \rho^{n-1} (1 - \rho) \cdot g_1 + \dots \right]$$

- First-harmonic source errors die out as ρ^n , $\rho = k_1 / k_0 < 1$
 - First-harmonic K_{eff} errors die out as $\rho^{n-1} (1 - \rho)$
 - Source converges slower than K_{eff}
- Most codes only provide tools for assessing K_{eff} convergence.
- ⇒ MCNP5 also looks at Shannon entropy of the source distribution, H_{src} .

K_{eff} Calculations - Convergence Diagnostics

- Divide the fissionable regions of the problem into N_s spatial bins



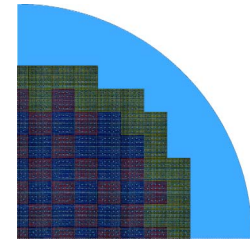
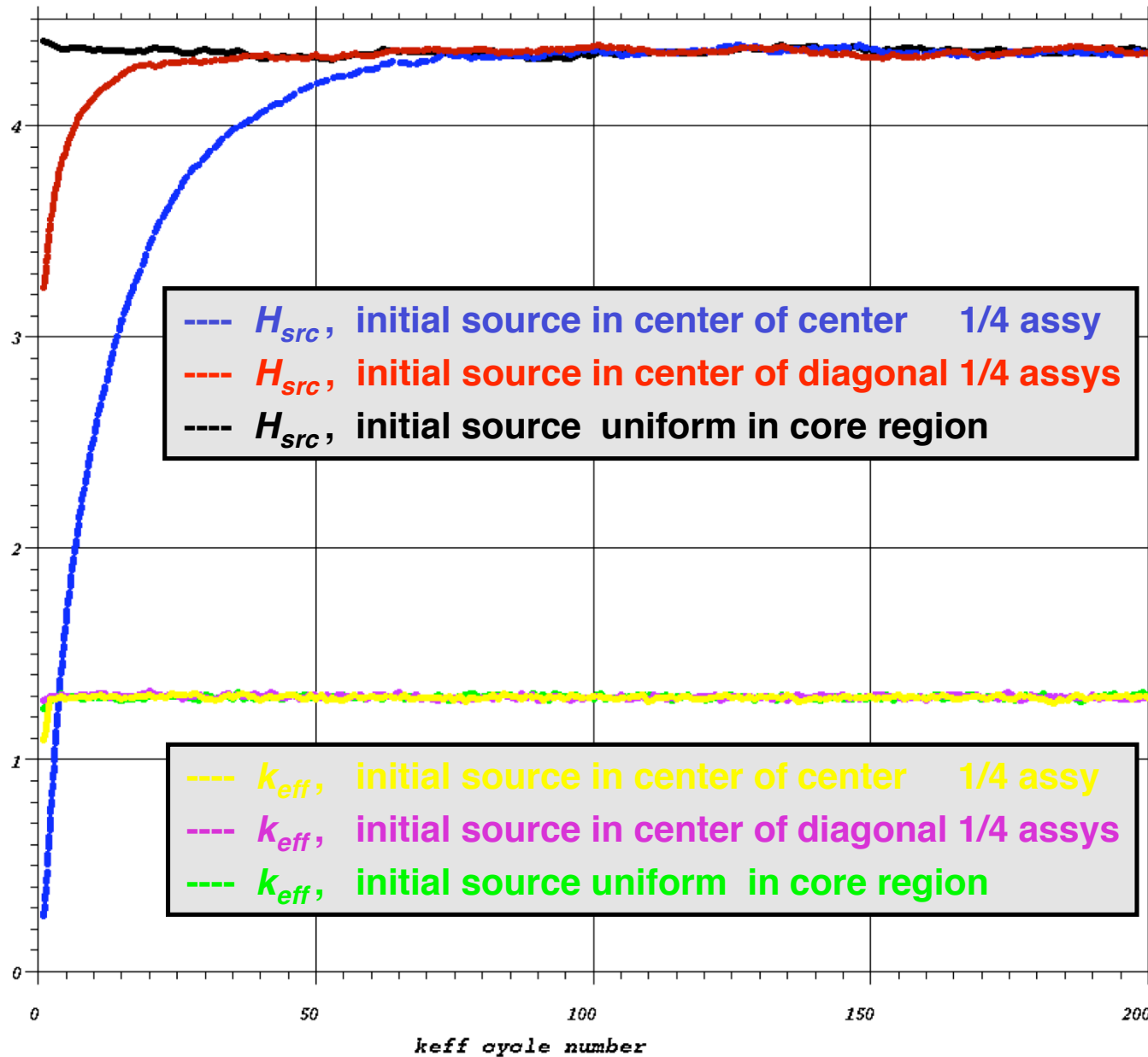
- Shannon entropy of the source distribution

$$H(S) = - \sum_{J=1}^{N_s} p_J \cdot \ln_2(p_J), \quad \text{where } p_J = \frac{(\# \text{ source particles in bin } J)}{(\text{total } \# \text{ source particles in all bins})}$$

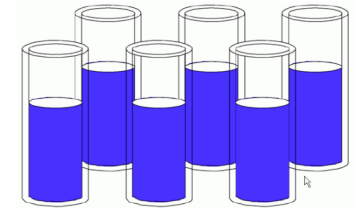
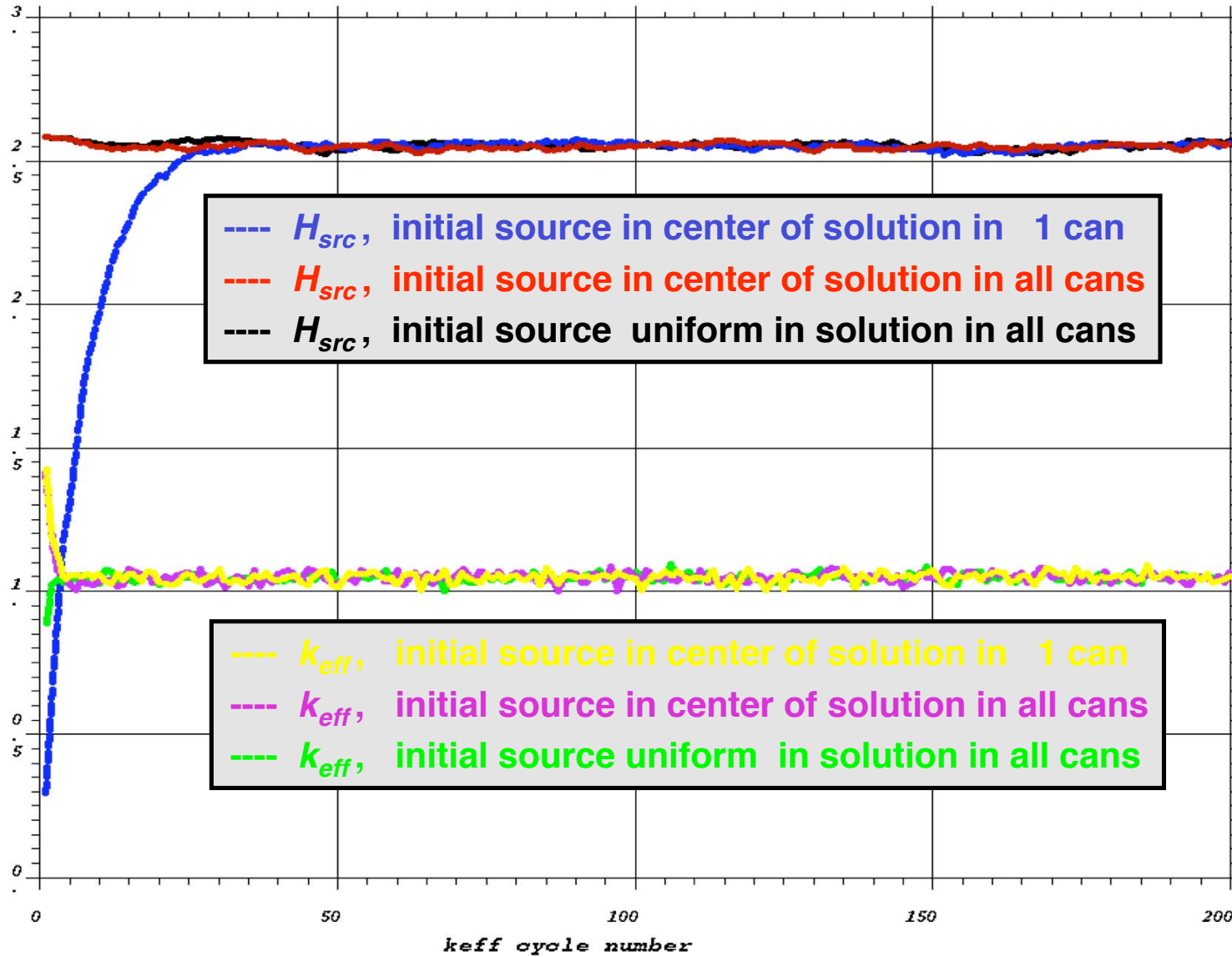
- For a uniform source distribution, $H(S) = \ln_2(N_s)$
- For a point source (in a single bin), $H(S) = 0$
- For any general source, $0 \leq H(S) \leq \ln_2(N_s)$

⇒ As the source distribution converges in 3D space,
a line plot of $H(S^{(n)})$ vs. n (the iteration number) converge

Reactor - Convergence for Different Source Guesses



Criticality Safety - Convergence for Different Source Guesses



Keff & Fission Source Convergence

- Use **K_{eff} vs cycle** & **H_{src} vs cycle** to assess convergence of both K_{eff} and the fission distribution
- The number of cycles to converge is determined by:
 - **Dominance ratio** $\rho = k_1 / k_0$
 - Closeness of **initial source guess** to converged distribution
- Note that convergence does not depend on the number of neutrons/cycle (M)

Keff & Fission Source Convergence

- **Dominance ratio determines the rate of convergence**

$\rho > .9 \Rightarrow$ many cycles to converge

- **To reduce the dominance ratio**

- Take advantage of problem symmetry & reflecting boundary, to eliminate some higher modes

| | | |
|----------------------|-----------|-----------------|
| PWR reactor example: | full core | $\rho \sim .98$ |
| | 1/2 core | $\rho \sim .97$ |
| | 1/4 core | $\rho \sim .96$ |
| | 1/8 core | $\rho \sim .94$ |

- Use Wielandt method (when available) to increase the average number of generations per cycle, L

| | | |
|-----------------------|--------|-----------------|
| PWR 1/4 core example: | L = 1 | $\rho \sim .96$ |
| | L = 5 | $\rho \sim .83$ |
| | L = 10 | $\rho \sim .72$ |
| | L = 20 | $\rho \sim .57$ |

- **Smaller dominance ratio \Rightarrow fewer cycles to converge**

Keff & Fission Source Convergence

- Better initial source guess \Rightarrow fewer cycles to converge
- Typical
 - Point at center - terrible guess
 - Reactor: uniform in core region - good guess
 - Criticality Safety: points in each fissionable region, or uniform in each fissionable region - good guess

Conclusions - Convergence

- If you are computing more than just K_{eff} (eg, local reaction rates, dose fields, fission distributions, heating distributions, etc.):

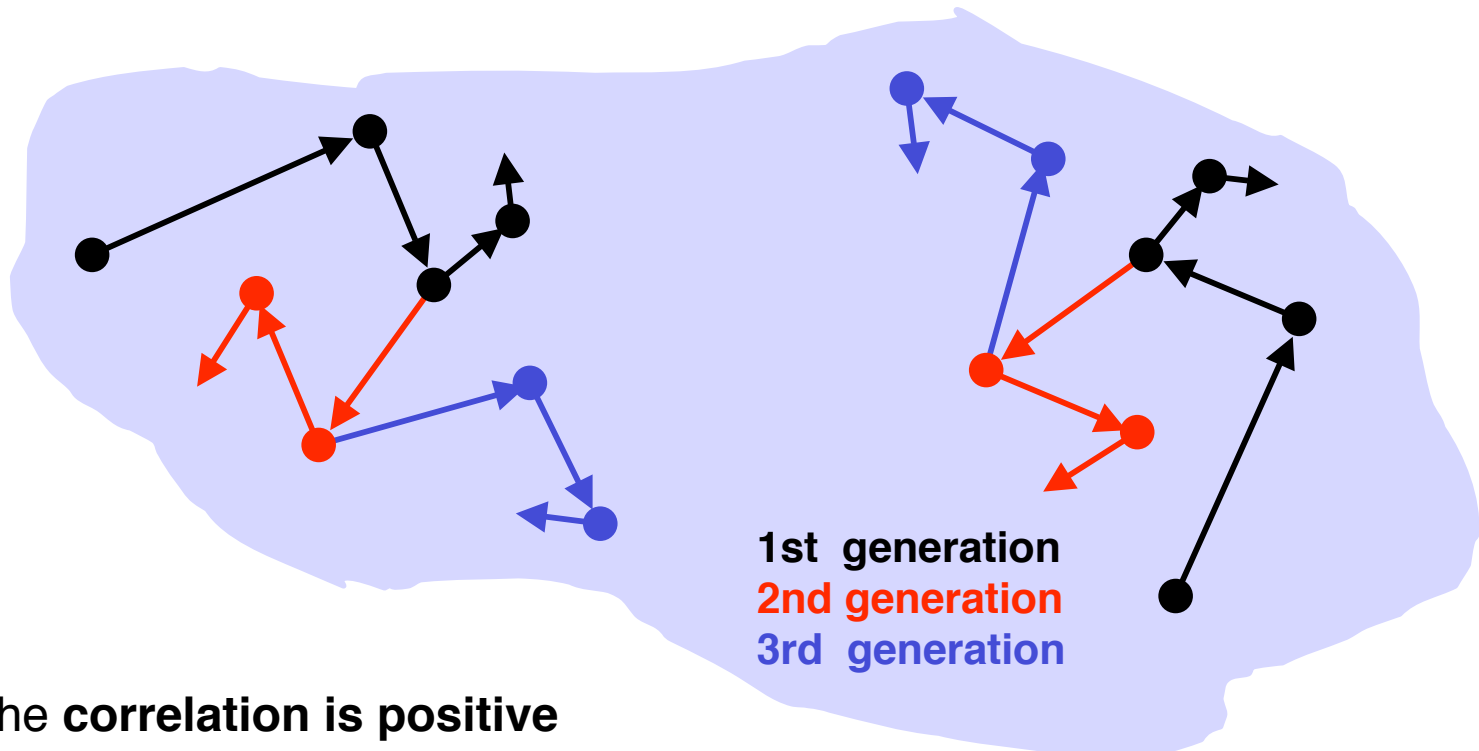
Should check both k_{eff} and H_{src} for convergence

- Use problem symmetry, if possible
- Use Wielandt method, when available
- Better initial source guess \Rightarrow fewer cycles to converge
 - Reactor: uniform in core region
 - Criticality Safety: points in each fissionable region, or uniform in each fissionable region

Underprediction Bias in Confidence Intervals in Monte Carlo Keff Calculations

Tallies & Correlation

- MC eigenvalue calculations are solved by power iteration
 - A **generation model** is used in following neutron histories
 - Tallies from one generation (including K) are **correlated** with tallies in successive generations



- The **correlation is positive**

Bias in σ^2

- For tally X , made N times

(for large N)

$$\bar{X} = \frac{\sum_{n=1}^N X_n}{N} = \text{mean value of } X$$

$$\tilde{\sigma}_{\bar{X}}^2 = \frac{1}{N} \cdot \left(\frac{\sum_{n=1}^N X_n^2}{N-1} - \bar{X}^2 \right) = \text{variance computed by codes, assuming independence of } X_n \text{'s}$$

$$\sigma_{\bar{X}}^2 \approx \tilde{\sigma}_{\bar{X}}^2 + \tilde{\sigma}_{\bar{X}}^2 \cdot 2 \cdot \sum_{i=1}^{\infty} r_i = \text{True variance, including correlations } r_i = \text{lag-}i \text{ correlation coef. between } X_n \text{'s}$$

- (True σ^2) > (computed σ^2), since correlations are positive

$$\frac{\text{True } \sigma_{\bar{X}}^2}{\text{Computed } \sigma_{\bar{X}}^2} = \frac{\sigma_{\bar{X}}^2}{\tilde{\sigma}_{\bar{X}}^2} \approx 1 + 2 \cdot \left(\begin{array}{l} \text{sum of lag-}i \text{ correlation} \\ \text{coeff's between tallies} \end{array} \right)$$

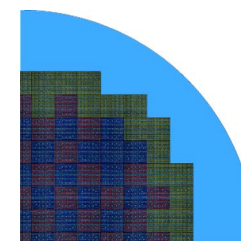
Variance underprediction bias is **independent of N and M**

Bias in Uncertainties

| | | | | | | | | | | | | | | |
|-----|-----|-----|-----|-----|-----|-----|-----|-----|-----|-----|-----|-----|-----|-----|
| 3.4 | 3.1 | 2.7 | 2.7 | 2.6 | 2.3 | 2.7 | | | | | | | | |
| 3.3 | 3.7 | 3.6 | 3.7 | 3.7 | 2.7 | 2.9 | | | | | | | | |
| 3.8 | 3.8 | 3.9 | 4.0 | 3.6 | 3.3 | 3.0 | 2.9 | 2.5 | 2.5 | 2.2 | | | | |
| 3.8 | 3.9 | 4.2 | 3.3 | 3.5 | 3.4 | 3.2 | 3.6 | 3.0 | 3.0 | 2.8 | | | | |
| 3.9 | 3.6 | 3.5 | 3.3 | 3.4 | 3.4 | 4.0 | 3.9 | 3.5 | 3.2 | 3.1 | 2.5 | 1.7 | | |
| 4.1 | 3.8 | 3.5 | 3.2 | 2.9 | 2.6 | 2.9 | 3.2 | 3.1 | 2.8 | 2.7 | 1.9 | 1.7 | | |
| 3.4 | 3.4 | 3.2 | 3.5 | 2.6 | 2.4 | 2.6 | 3.0 | 2.9 | 2.9 | 2.8 | 2.3 | 2.1 | | |
| 4.2 | 3.5 | 3.4 | 3.1 | 2.7 | 2.3 | 2.0 | 2.4 | 2.5 | 2.5 | 2.1 | 2.3 | 2.3 | | |
| 3.9 | 3.6 | 3.1 | 2.9 | 2.3 | 1.9 | 1.9 | 2.3 | 2.4 | 2.9 | 2.7 | 2.7 | 2.2 | 2.8 | 2.3 |
| 3.7 | 3.3 | 3.6 | 2.4 | 2.2 | 2.2 | 2.5 | 1.8 | 2.2 | 2.6 | 2.7 | 2.9 | 2.5 | 2.4 | 2.5 |
| 3.0 | 3.1 | 3.0 | 2.2 | 2.2 | 2.1 | 2.4 | 2.5 | 2.4 | 2.6 | 2.7 | 2.6 | 2.7 | 3.0 | 2.6 |
| 2.9 | 3.7 | 3.3 | 2.6 | 2.5 | 2.8 | 3.0 | 2.9 | 3.5 | 3.2 | 3.3 | 3.1 | 3.1 | 3.2 | 3.3 |
| 3.2 | 3.1 | 2.9 | 3.1 | 3.2 | 3.3 | 3.5 | 3.5 | 3.6 | 3.9 | 3.7 | 3.9 | 3.5 | 3.4 | 2.9 |
| 3.4 | 3.0 | 3.1 | 3.6 | 3.4 | 3.5 | 3.9 | 3.7 | 4.0 | 4.3 | 4.0 | 4.3 | 3.8 | 4.2 | 3.5 |
| 3.5 | 3.2 | 2.8 | 3.5 | 3.8 | 3.9 | 3.9 | 3.9 | 4.1 | 4.1 | 4.6 | 4.4 | 4.7 | 4.5 | 3.8 |

True relative errors in
1/4-assembly fission rates,
as multiples of calculated
relative errors, $\sigma_{\text{TRUE}} / \sigma_{\text{MCNP}}$

Calculated uncertainties
are 1.7 to 4.7 times smaller
than true uncertainties



Average factor = 3.1

Correlation vs Tallies

- MC codes ignore correlation in tallies when computing σ^2 's
- σ^2 's computed by MC codes are always too small

$$\frac{\text{True } \sigma_{\bar{X}}^2}{\text{Computed } \sigma_{\bar{X}}^2} = 1 + 2 \cdot \left(\frac{\text{sum of lag-i correlation}}{\text{coeff's between tallies}} \right)$$

- The size of underprediction bias in σ^2 's depends on how tallies are performed:

| | | |
|-------------------------------------|--|--|
| MCNP: | generation tallies for Keff, history tallies for everything else | <p style="text-align: center;">Larger</p> <p style="text-align: center;">↓</p> <p style="text-align: center;">Correlation & Bias</p> <p style="text-align: center;">↓</p> <p style="text-align: center;">None</p> |
| VIM, KENO, RACER, RCP,: | generation tallies | |
| MCNP+Wielandt, MONK: | several generations | |
| Repeated MC runs, averaged: | all generations from each run | |

Past Work - Bias in Uncertainties

$$\frac{\text{True } \sigma_{\bar{x}}^2}{\text{Computed } \sigma_{\bar{x}}^2} = 1 + 2 \cdot \sum_{k=1}^{\infty} r_k$$

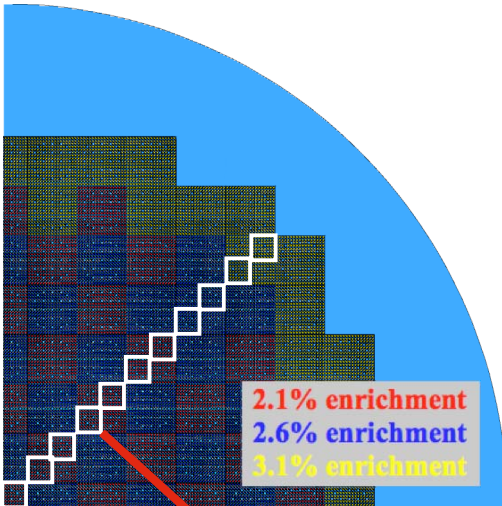
- **MacMillan (1973)** [similar approach by Gast in 1974]
 - **Calculate** r_1 for each tally (lag-1 inter-cycle correlation coefficient)
 - **Assume dominance ratio ρ is known**
 - **Assume** $r_k \leq r_1 \cdot \rho^k$ for $k=2,3,\dots$
 - Then,

$$\frac{\text{True } \sigma_{\bar{x}}^2}{\text{Computed } \sigma_{\bar{x}}^2} \leq 1 + \frac{2 \cdot r_1}{1 - \rho}$$
 - This factor can then be used to correct the computed σ for the tally
 - **Difficulties:**
 - Only gives a conservative upper bound
 - Useless if ρ near 1.0
 - Requires extra storage for each tally
 - **Notoriously sensitive to noise**
 - **Assumption for higher r_k 's may often be incorrect**
 - **Dominance ratio is usually not known**

Bias in Uncertainties - Comments

- Uncertainties computed by MC codes exhibit a bias due to inter-cycle correlation effects that are neglected in tallies
- Primarily affects local tally statistics, not K-effective statistics
- **Computed uncertainties are always smaller than the true uncertainties for a tally**
- **Running more cycles or more neutrons per cycle does not reduce the biases**
- **Wielandt's method can reduce or eliminate the underprediction bias in uncertainties (see next slide)**

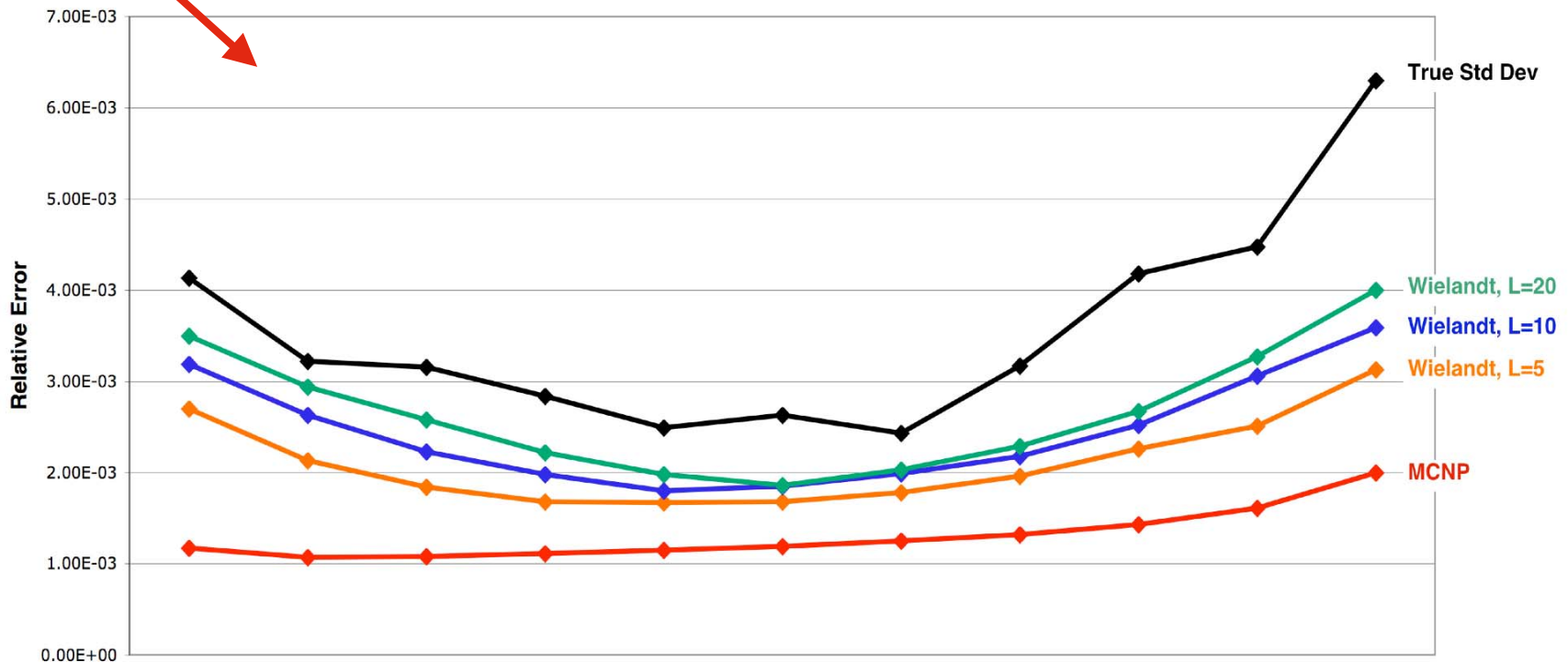
Reduced Uncertainty Bias, using Wielandt



Wielandt's method increases the fission chain-length in each cycle, and reduces inter-cycle correlations

Run the problem using different amounts of Wielandt acceleration (different shift parameters) to get average chain-lengths of 5, 10, 20 generations per cycle

Plot relative error in quarter-assemblies along diagonal



Best Practices - Summary

- To avoid bias in Keff & tally distributions, use 10K or more neutrons/cycle
- Always check convergence of both Keff & Hsrc
- Take advantage of problem symmetry, if possible
- Use a good initial source guess, uniform in fissionable regions
- Run at least a few hundred active cycles to allow codes adequate information to compute statistics
- Be aware that statistics on tallies from codes are underestimated, possibly make multiple independent runs

References

- **Monte Carlo Methods**
 - F. B. Brown, "Fundamentals of Monte Carlo Particle Transport," LA-UR-05-4983, available at <http://mcnp.lanl.gov/publications> (2005).
- **Monte Carlo k-effective Calculations**
 - J. Lieberoth, "A Monte Carlo Technique to Solve the Static Eigenvalue Problem of the Boltzmann Transport Equation," Nukleonik 11,213 (1968).
 - M. R. Mendelson, "Monte Carlo Criticality Calculations for Thermal Reactors," Nucl. Sci Eng. 32, 319-331 (1968).
 - H. Rief and H. Kschwendt, "Reactor Analysis by Monte Carlo," Nucl. Sci. Eng., 30, 395 (1967).
 - W. Goad and R. Johnston, "A Monte Carlo Method for Criticality Problems," Nucl. Sci. Eng. 5, 371-375 (1959).
 - J Yang & Y. Naito, "The Sandwich Method for Determining Source Convergence in Monte Carlo Calculations", Proc. 7th Int. Conf. Nuclear Criticality Safety, ICNC2003, Tokai-mura, Iburaki, Japan, Oct 20-24, 2003, JAERI-Conf 2003-019, 352 (2003).
- **Superhistory Method**
 - R.J. Brissenden and A.R. Garlick, "Biases in the Estimation of Keff and Its Error by Monte Carlo Methods," Ann. Nucl. Energy, Vol 13, No. 2, 63-83 (1986).
- **Wielandt Method**
 - F.B. Brown, "Wielandt Acceleration for MCNP5 Monte Carlo Eigenvalue Calculations", M&C+SNA-2007, LA-UR-07-1194 (2007)
 - T Yamamoto & Y Miyoshi, "Reliable Method for Fission Source Convergence of Monte Carlo Criticality Calculation with Wielandt's Method", J. Nuc. Sci. Tech., 41, No. 2, 99-107 (Feb 2004).
 - S Nakamura, Computational Methods in Engineering and Science, R. E. Krieger Pub. Company, Malabar, FL (1986).
- **Shannon entropy & convergence**
 - T. Ueki & F.B. Brown, "Stationarity and Source Convergence in Monte Carlo Criticality Calculations", ANS Topical Meeting on Mathematics & Computation, Gatlinburg, TN April 6-11, (2003).
 - T. Ueki & F.B. Brown, "Stationarity Modeling and Informatics-Based Diagnostics in Monte Carlo Criticality Calculations", Nucl. Sci. Eng. 149, 38-50 (2005)
 - F.B. Brown, "On the Use of Shannon Entropy of the Fission Distribution for Assessing Convergence of Monte Carlo Criticality Calculations", proceedings PHYSOR-2006, Vancouver, British Columbia, Canada (Sept 2006).

References

- **Bias, correlation, & statistics**

- E.M. Gelbard and R.E. Prael, "Monte carlo Work at Argonne National Laboratory", in Proc. NEACRP Meeting of a Monte Carlo Study Group, ANL-75-2, Argonne National Laboratory, Argonne, IL (1974).
- R. C. Gast and N. R. Candelore, "Monte Carlo Eigenfunction Strategies and Uncertainties," in Proc. NEACRP Meeting of a Monte Carlo Study Group, ANL-75-2, Argonne National Laboratory, Argonne, IL (1974).
- R. J. Brissenden & A. R. Garlick, "Biases in the Estimation of Keff and Its Error by Monte Carlo Methods," Ann. Nucl. Energy, 13, 2, 63-83 (1986)
- D. B. MacMillan, "Monte Carlo Confidence Limits for Iterated-Source Calculations," Nucl. Sci. Eng., 50, 73 (1973).
- E. M. Gelbard and R. E. Prael, "Computation of Standard Deviations in Eigenvalue Calculations," Prog. Nucl. Energy, 24, 237 (1990).
- T Ueki, "Intergenerational Correlation in Monte Carlo K-Eigenvalue Calculations", Nucl. Sci. Eng. 141, 101-110 (2002)
- L.V. Maiorov, "Estimates of the Bias in the Results of Monte Carlo Calculations of Reactors and Storage Sites for Nuclear Fuel", Atomic Energy, Vol 99, No 4, 681-693 (2005).
- T Ueki, "Intergenerational Correlation in Monte Carlo K-Eigenvalue Calculations", Nucl. Sci. Eng. 141, 101-110 (2002)
- T. Ueki and F. B. Brown, "Autoregressive Fitting for Monte Carlo K-effective Confidence Intervals," Trans. Am. Nucl. Soc., 86, 210 (2002).
- T. Ueki, "Time Series Modeling and MacMillan's Formula for Monte Carlo Iterated-Source Methods," Trans. Am. Nucl. Soc., 90, 449 (2004).
- T. Ueki & B. R. Nease, "Times Series Analysis of Monte Carlo Fission Sources - II: Confidence Interval Estimation", Nucl. Sci. Eng., 153, 184-191 (2006).
- O. Jacquet et al., "Eigenvalue Uncertainty Evaluation in MC Calculation, Using Time Series Methodologies," Proc. Int. Conf. Advanced Monte Carlo for Radiation Physics, Particle Transport Simulation and Applications (Monte Carlo 2000), Lisbon, Portugal, October 23–26, 2000. A. KLING et al., Eds., Springer-Verlag, Berlin, Heidelberg (2001).

Adjoint-Weighting in Continuous Energy Monte Carlo Criticality Calculations

The Adjoint Flux

- The k-eigenvalue Boltzmann equation has an adjoint equation

$$\mathbf{H}\psi = \frac{1}{k}\mathbf{F}\psi$$

$$\mathbf{H}^\dagger\psi^\dagger = \frac{1}{k}\mathbf{F}^\dagger\psi^\dagger$$

- The eigenfunction solutions are the modes of the adjoint flux.
- The fundamental mode is the describes the steady-state importance of neutrons to the overall chain reaction.

Iterated Fission Probability Interpretation

- Developed by H. Hurwitz Jr. at KAPL.
- Quantity proportional to the adjoint flux.
- Defined as follows:

Consider a neutron introduced into a critical system at a location in phase space. The expected steady state neutron population resulting from that original progenitor neutron is defined as the iterated fission probability.

- Can be demonstrated mathematically (Bell & Glasstone)

Iterated Fission Probability Interpretation

- **Another interpretation of the adjoint flux: Radiation going backwards from a detector to a source.**
- **Fixed source MC calculations use this methodology.**
 - Works well for multigroup, but has problems with continuous energy scattering physics
- **The iterated fission probability interpretation requires only a forward calculation.**
 - No issues with continuous energy scattering

The Adjoint Flux in Reactor Physics

- Many quantities in reactor physics are derived in the form of inner products of the adjoint and the flux.

- Point Reactor Kinetics Parameters:

- Neutron Generation Time:

$$\Lambda = \frac{\langle \psi^\dagger \frac{1}{v} \psi \rangle}{\langle \psi^\dagger \mathbf{F} \psi \rangle}$$

- Effective Delayed Neutron Fraction:

$$\beta_{\text{eff}} = \frac{\langle \psi^\dagger \mathbf{B} \psi \rangle}{\langle \psi^\dagger \mathbf{F} \psi \rangle}$$

- Rossi-Alpha

$$\alpha = -\frac{\langle \psi^\dagger \mathbf{B} \psi \rangle}{\langle \psi^\dagger \frac{1}{v} \psi \rangle}$$

The Adjoint Flux in Reactor Physics

- Many quantities in reactor physics are derived in the form of inner products of the adjoint and the flux.

- Linear Perturbation Theory:

$$\Delta\rho = -\frac{\langle \psi^\dagger \mathbf{P} \psi \rangle}{\langle \psi^\dagger \mathbf{F} \psi \rangle}$$

$$\mathbf{P} = \Delta\Sigma_t - \Delta\mathbf{S} - \frac{1}{k} \Delta\mathbf{F}$$

- Sensitivity and Data Uncertainty Analysis

The Adjoint Flux in Monte Carlo

- **Current capabilities and research**
 - Fixed source adjoint fluxes (multigroup and continuous energy)
 - Criticality adjoint fluxes (multigroup)
 - KENO Eigenvalue Contribution estimator
 - MCNIC scripts

The Adjoint Flux in Monte Carlo

- Current effort at LANL:

Develop a framework within a production Monte Carlo code (MCNP) to perform continuous energy adjoint-weighted tallies for k-eigenvalue problems with very little additional CPU cost and minimal impact on the source code.

- Features:

- Framework is an inter-generational accounting scheme.
- Uses only existing random walks.
- Efficient memory storage of extra information.
- Modular design should be extendable to other MC codes.

Adjoint Tallies: Heuristic Development

- Consider a reactor in a critical configuration.
- Introduce neutrons at a specific point in phase space.
- Define a tally to find the average asymptotic population caused by those neutrons:

$$T = \frac{1}{N} (\pi_1 + \pi_2 + \dots + \pi_N)$$

- Want to know the physical meaning of this tally.

Adjoint Tallies: Heuristic Development

- Thought Experiment: Bare slab reactor with two point sources.
- Sources A and B have relative intensities p and $q = 1 - p$.
- Two tallies: A and B. If neutron emitted in source, tally the resulting asymptotic population in respective bin.



Adjoint Tallies: Heuristic Development

- Two tallies: A and B. If neutron emitted in source, tally the resulting asymptotic population in respective bin.

$$T_A = \frac{1}{N} \sum_{i \in A} \pi_i$$

$$T_B = \frac{1}{N} \sum_{i \in B} \pi_i$$



Adjoint Tallies: Heuristic Development

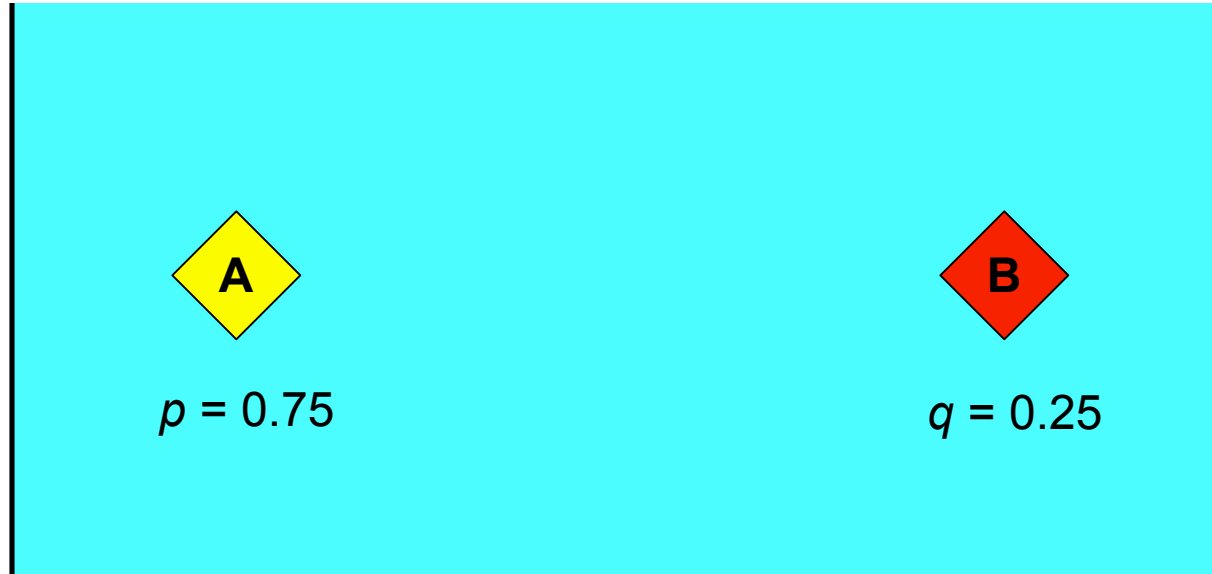
- Case 1: A and B symmetric ($p = q$)



- Tallies A and B will tend to the same value.

Adjoint Tallies: Heuristic Development

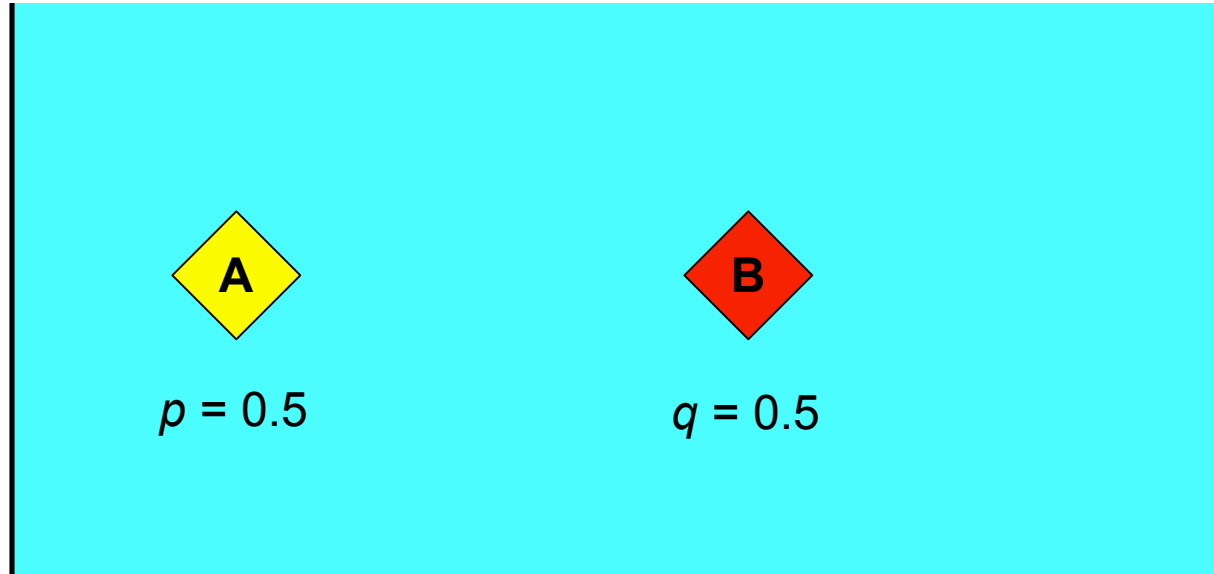
- Case 2: A and B symmetric ($p > q$)



- **Tallies A will be higher.**
 - Source A has a higher intensity and will get more contributions.

Adjoint Tallies: Heuristic Development

- Case 3: A and B asymmetric ($p = q$)



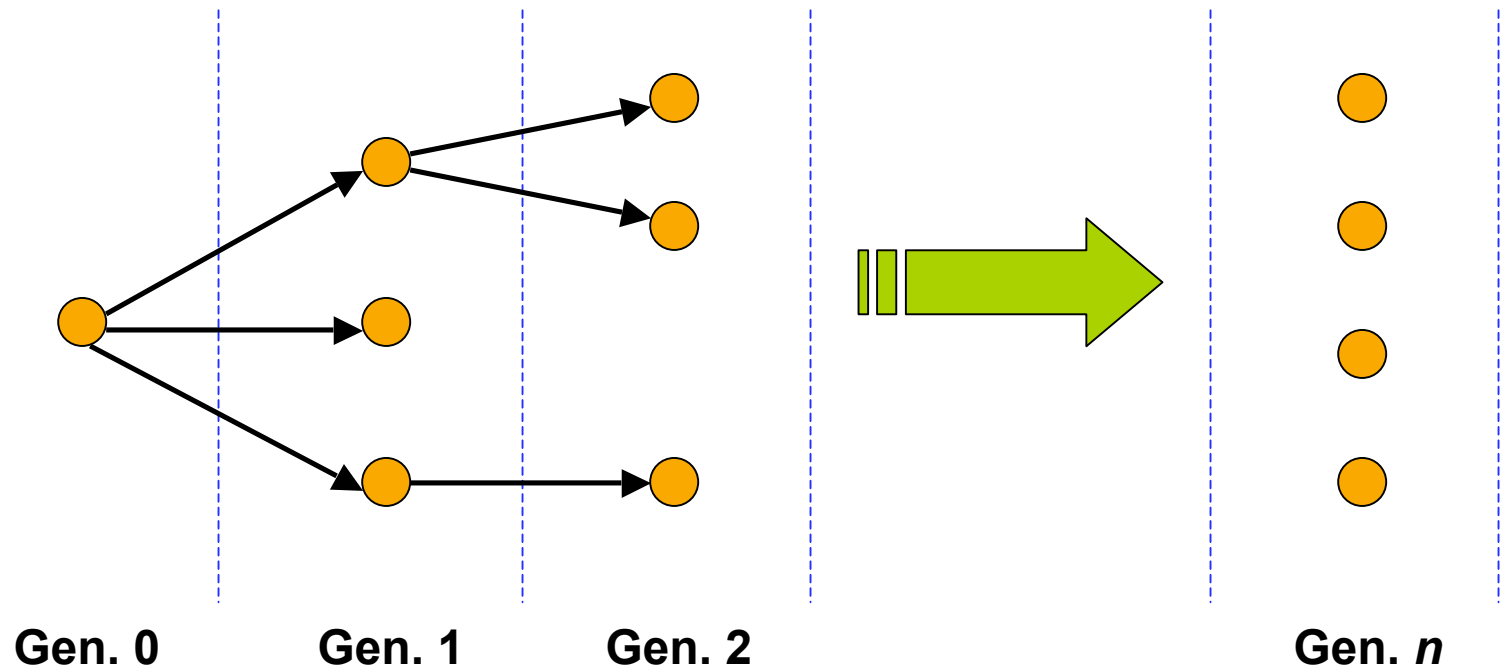
- **Tally B will be higher.**
 - Neutrons from A are more likely to leak.

Adjoint Tallies: Heuristic Development

- **Conclusion: This tally is proportional to the two things:**
 - Intensity of the source in the location.
 - Ability of neutrons to produce more fission neutrons (importance).
- **Result is the importance (or adjoint) weighted source.**
- **Can generalize to an arbitrary “source”:**
 - Fission source
 - Scattering source
 - Flux distribution
- **More rigorous development is possible.**

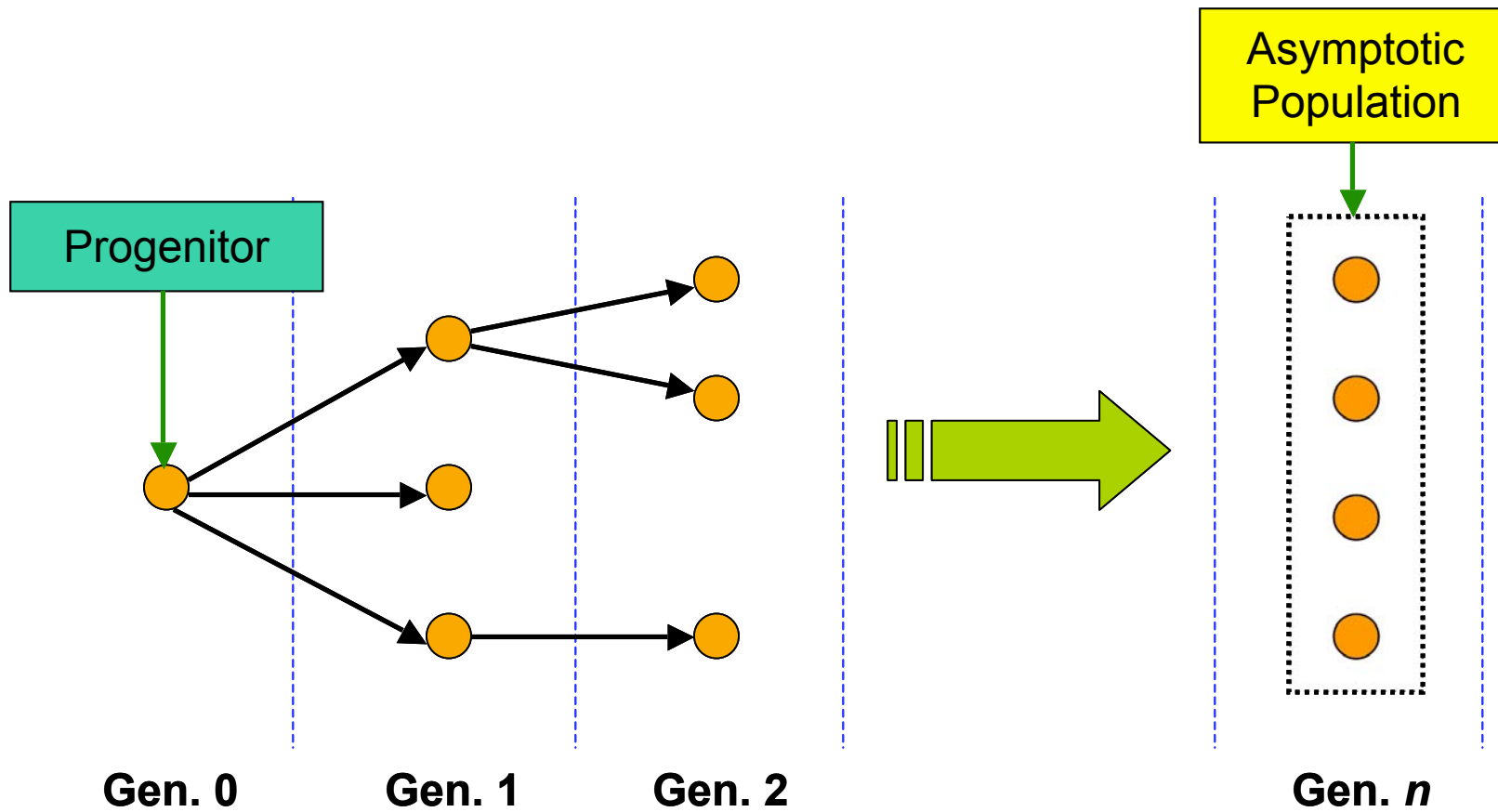
Method Terminology

- Track neutron lineage through many generations.



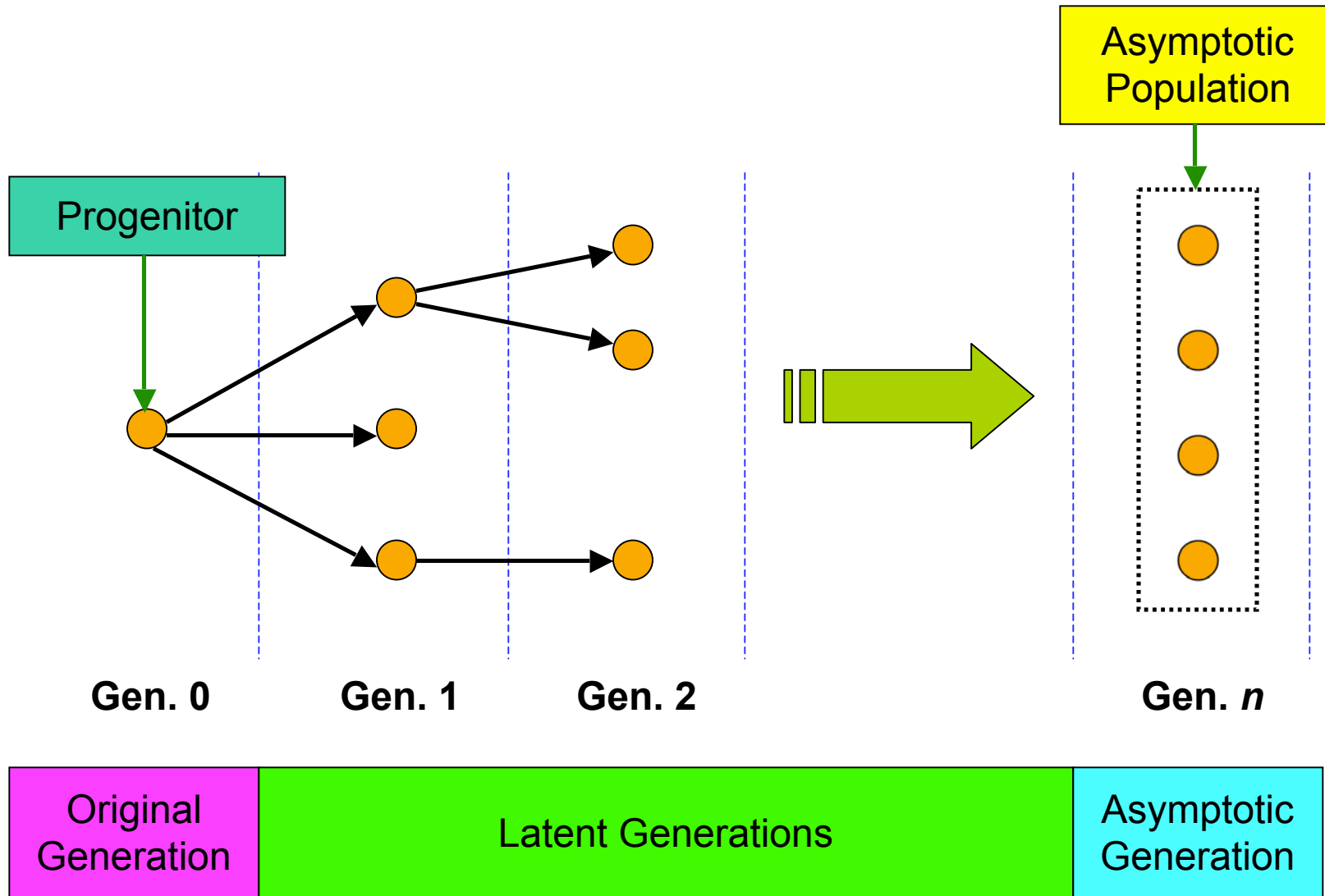
Method Terminology

- Track neutron lineage through many generations.



Method Terminology

- Track neutron lineage through many generations.



Example: Adjoint-Weighted Fission Source

- Want to know the adjoint-weighted fission source integrated over all of phase space.
- Each cycle, neutrons born from fission source.
- Follow each neutron and sum asymptotic population times the source weight.

$$\left\langle \psi^\dagger \frac{1}{k} \mathbf{F} \psi \right\rangle = \frac{1}{W} \sum_p \pi_p w_{0,p}$$

- Index p denotes all progeny of this source neutron.
- Factor of $1/k$ comes from fission source renormalization.

Example: Adjoint-Weighted Flux

- Want to know the adjoint-weighted flux integrated over all of phase space.
- Track length tallies sample the flux PDF.

$$\langle \psi^\dagger \psi \rangle = \frac{1}{W} \sum_p \pi_p \sum_{\tau \in p} w_{0,p} d_\tau$$

- Index τ denotes the tracks.
- Source weight used because each progenitor must be launched identically.
- Easy to add any tally multiplier (ex. $1/v$)

Reactor Kinetics Tallies

- **Adjoint-weighted neutron density:**

$$\left\langle \psi^\dagger \frac{1}{\nu} \psi \right\rangle = \frac{1}{W} \sum_p \pi_p \sum_{\tau \in p} \frac{1}{\nu_\tau} w_{0,p} d_\tau$$

- **Adjoint-weighted fission source:**

$$\left\langle \psi^\dagger \mathbf{F} \psi \right\rangle = \frac{1}{W} k \sum_p \pi_p w_{0,p}$$

- **Adjoint-weighted delayed fission source:**

$$\left\langle \psi^\dagger \mathbf{B} \psi \right\rangle = \frac{1}{W} k \sum_{p \in \beta} \pi_p w_{0,p}$$

- **Kinetics parameters obtained from taking ratios.**
 - Accurate error analysis requires correlations.

Perturbation Tallies

- Still under development (only analog multigroup tested)
- Each term summed together:

$$\langle \psi^\dagger \mathbf{P} \psi \rangle = \left\langle \psi^\dagger \left(\Delta \Sigma_t - \Delta \mathbf{S} - \frac{1}{k} \Delta \mathbf{F} \right) \psi \right\rangle$$

$$\langle \psi^\dagger \mathbf{P} \psi \rangle = \frac{1}{W} \sum_p \pi_p \left[\sum_{\tau \in p} \Delta \Sigma_t w_{0,p} d_\tau - \sum_{s \in p} \frac{\Delta \Sigma_s}{\Sigma_s} w_{0,p} - \sum_{f \in p} \frac{\Delta v \Sigma_f}{v \Sigma_f} w_{0,p} \right]$$

- For scatter and fission, xs taken at incident energy.

Perturbation Tallies

- Still under development (only analog multigroup tested)
- Each term summed together:

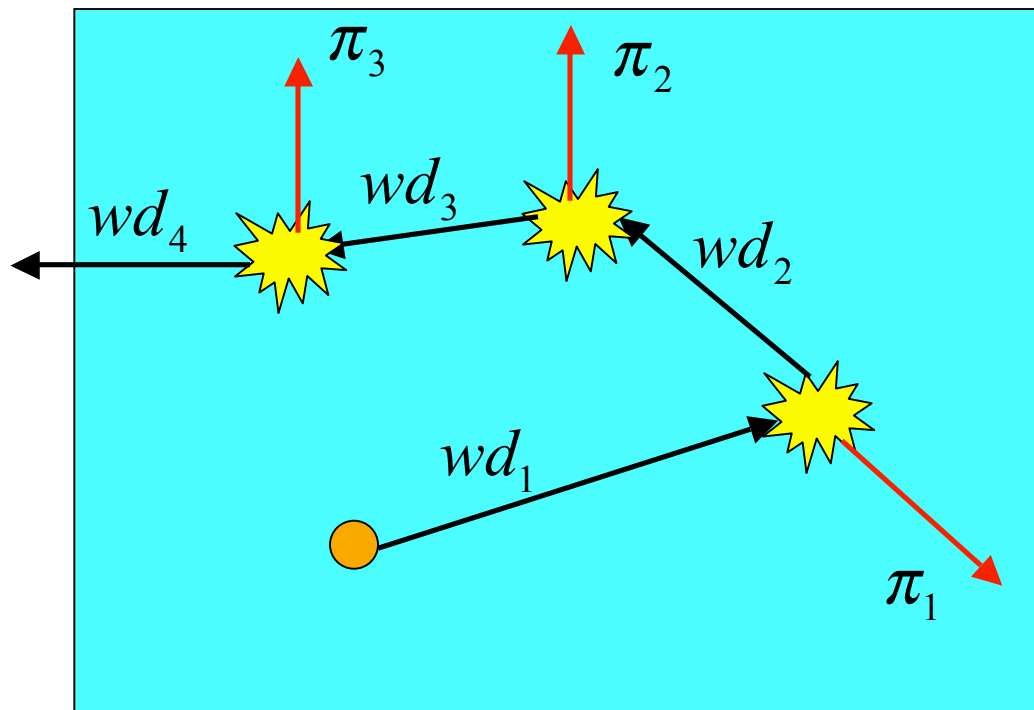
$$\langle \psi^\dagger \mathbf{P} \psi \rangle = \left\langle \psi^\dagger \left(\Delta \Sigma_t - \Delta \mathbf{S} - \frac{1}{k} \Delta \mathbf{F} \right) \psi \right\rangle$$

$$\langle \psi^\dagger \mathbf{P} \psi \rangle = \frac{1}{W} \sum_p \pi_p \left[\sum_{\tau \in p} \Delta \Sigma_t w_{0,p} d_\tau - \sum_{s \in p} \frac{\Delta \Sigma_s}{\Sigma_s} w_{0,p} - \sum_{f \in p} \frac{\Delta v \Sigma_f}{v \Sigma_f} w_{0,p} \right]$$

- For scatter and fission, xs taken at incident energy.
- Divide by adjoint-weighted fission source tally to get reactivity change.

Issue: Branching and Causality

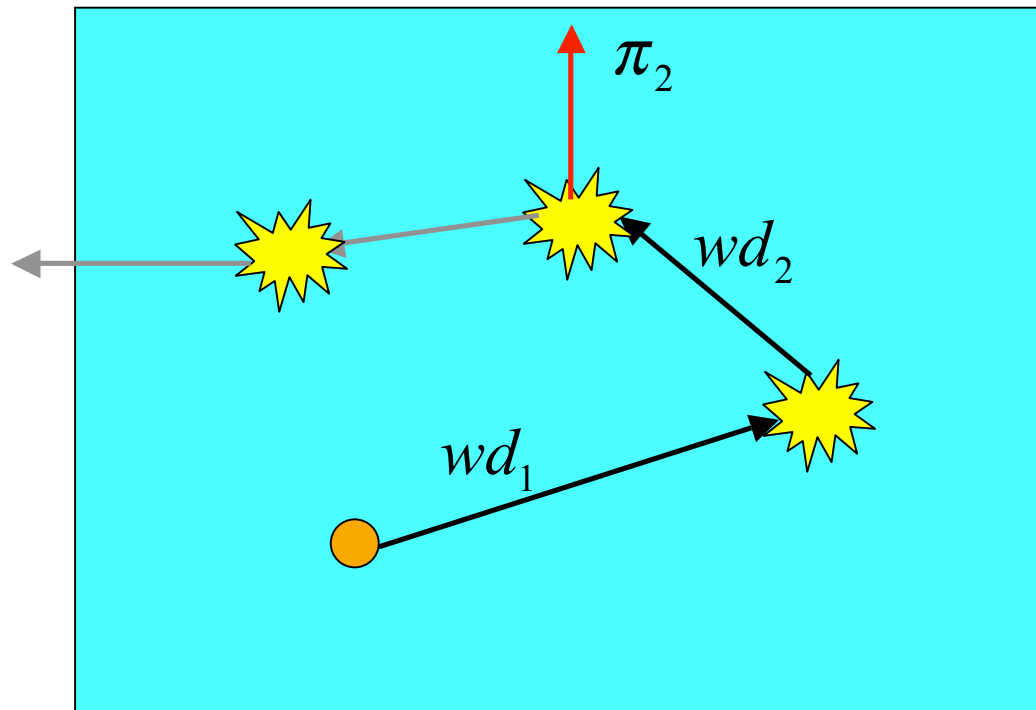
- **Implicit capture causes branching**
 - Fission source neutrons generated at multiple different locations from same progenitor neutron.



- **Must tally in a way to preserve causality.**

Issue: Branching and Causality

- Only tally pervious tracks for each branch:

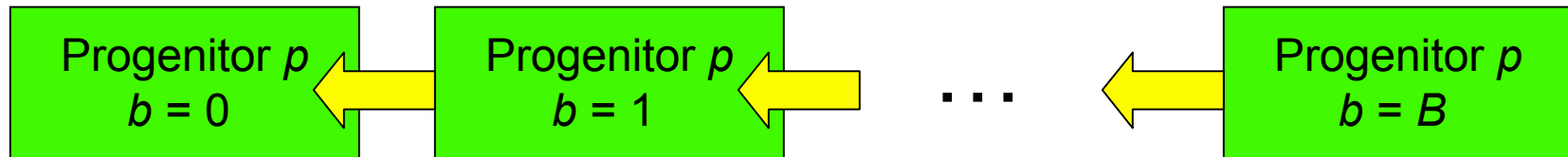


$$\langle \psi^\dagger, \psi \rangle_{p,b=2} = \pi_{p,2} (wd_1 + wd_2)$$

- Sum over all branches for the progenitor.

Issue: Branching and Causality

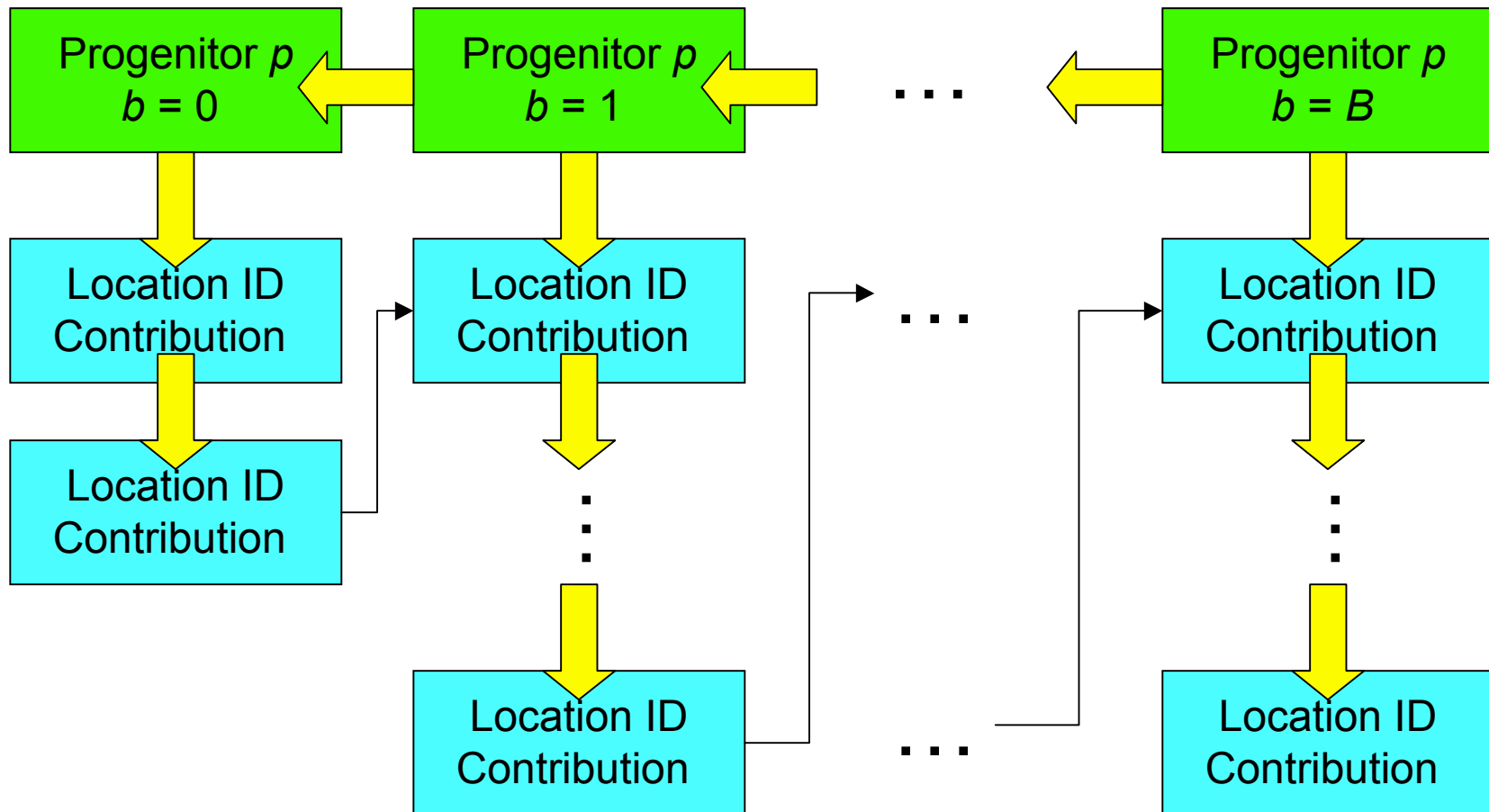
- Data type needs to remember branches.



- Pointer associations connect branches.

Issue: Storage for Local Quantities

- Local adjoint-weighting poses storage challenges.



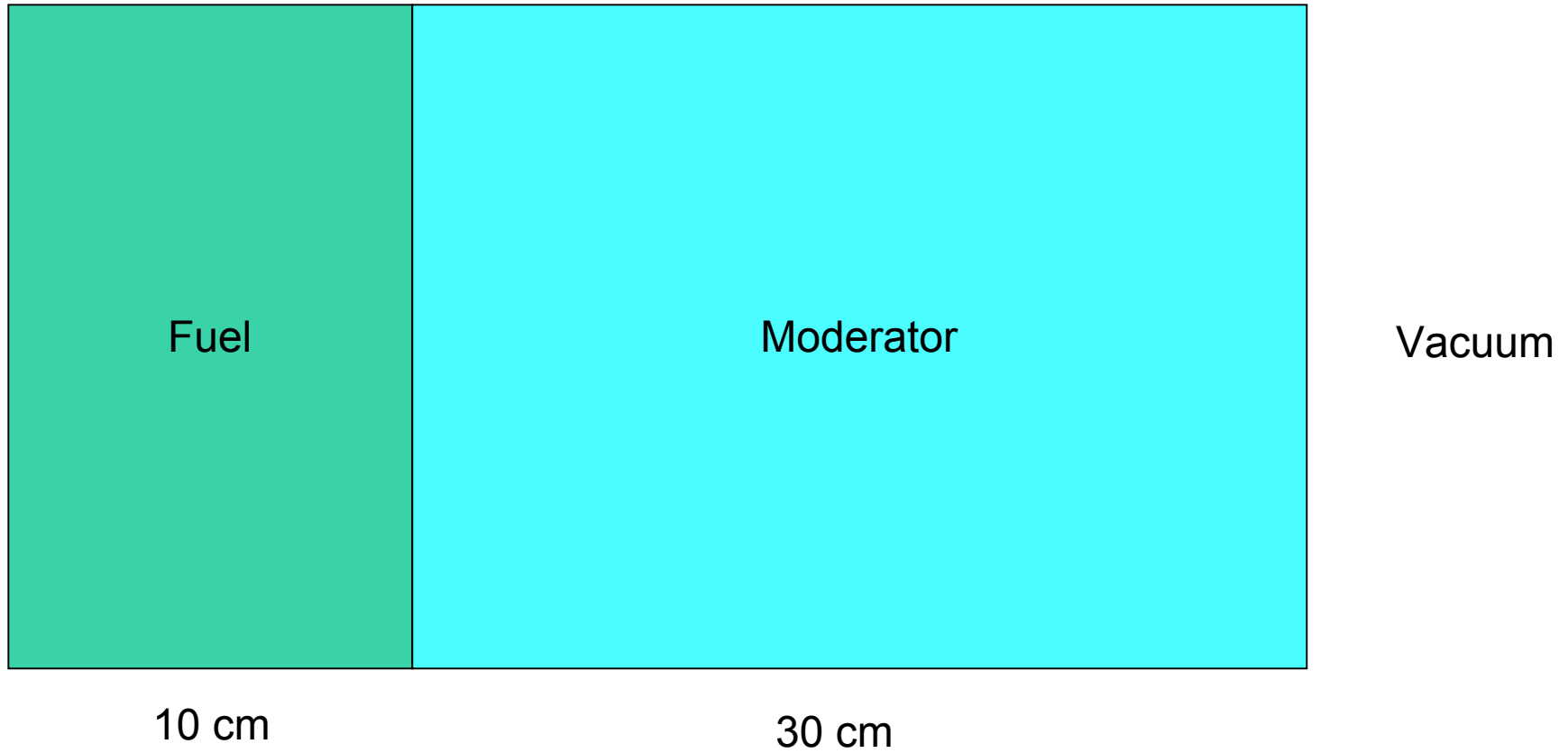
Validation and Verification

- **Comparison with 1D discrete ordinates results (PARTISN)**
 - Localized adjoint-weighted fluxes
 - Reactor kinetics parameters
 - Perturbation results
- **Experimental comparisons**
 - Reactor kinetics parameters
- **Convergence studies**
 - How many generations need to be skipped?

V & V: Adjoint-Weighted Flux

- Measure localized adjoint-weighted flux.
- Shows effectiveness of an area upon the chain reaction.
- **Two problems:**
 - Multigroup reflected slab
 - Continuous energy reflected slab

V & V: Adjoint-Weighted Flux

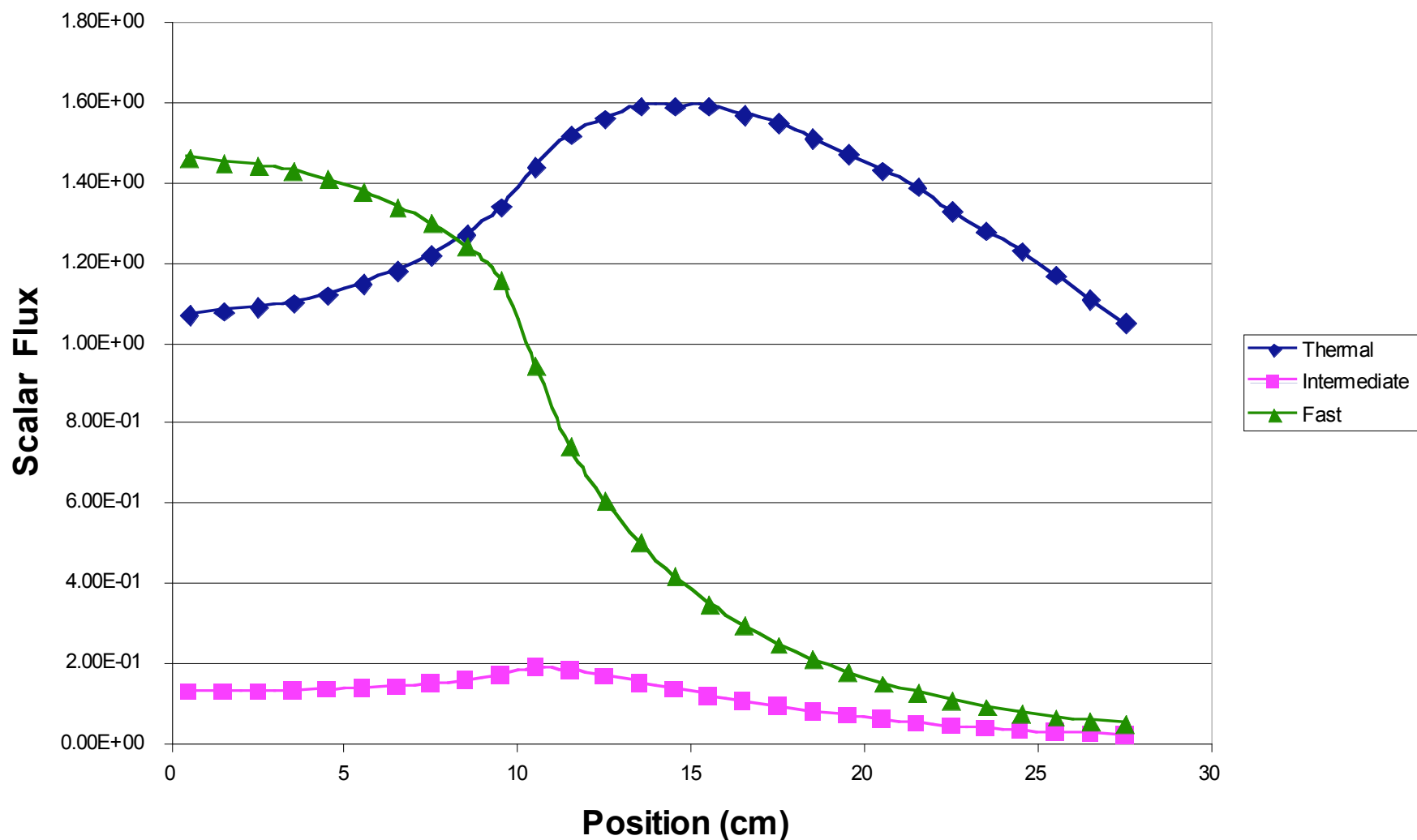


V & V: Adjoint-Weighted Flux

| | | | | | | | | |
|-------------|----------|------------|-------------|-----------------|--------|------------------|------------------|------------------|
| Fuel | g | Σ_t | $v\Sigma_f$ | Σ_γ | χ | $\Sigma_{s,g-1}$ | $\Sigma_{s,g-2}$ | $\Sigma_{s,g-3}$ |
| | 1 | 0.05 | 0 | 0 | 1 | 0.05 | 0 | 0 |
| | 2 | 0.15 | 0 | 0.01 | 0 | 0 | 0.14 | 0 |
| | 3 | 0.15 | 0.0238 | 0 | 0 | 0 | 0 | 0.14 |
| Mod | g | Σ_t | $v\Sigma_f$ | Σ_γ | χ | $\Sigma_{s,g-1}$ | $\Sigma_{s,g-2}$ | $\Sigma_{s,g-3}$ |
| | 1 | 0.2 | 0 | 0 | -- | 0.15 | 0.05 | 0 |
| | 2 | 0.2 | 0 | 0 | -- | 0 | 0.05 | 0.15 |
| | 3 | 0.2 | 0 | 0.001 | -- | 0 | 0 | 0.199 |

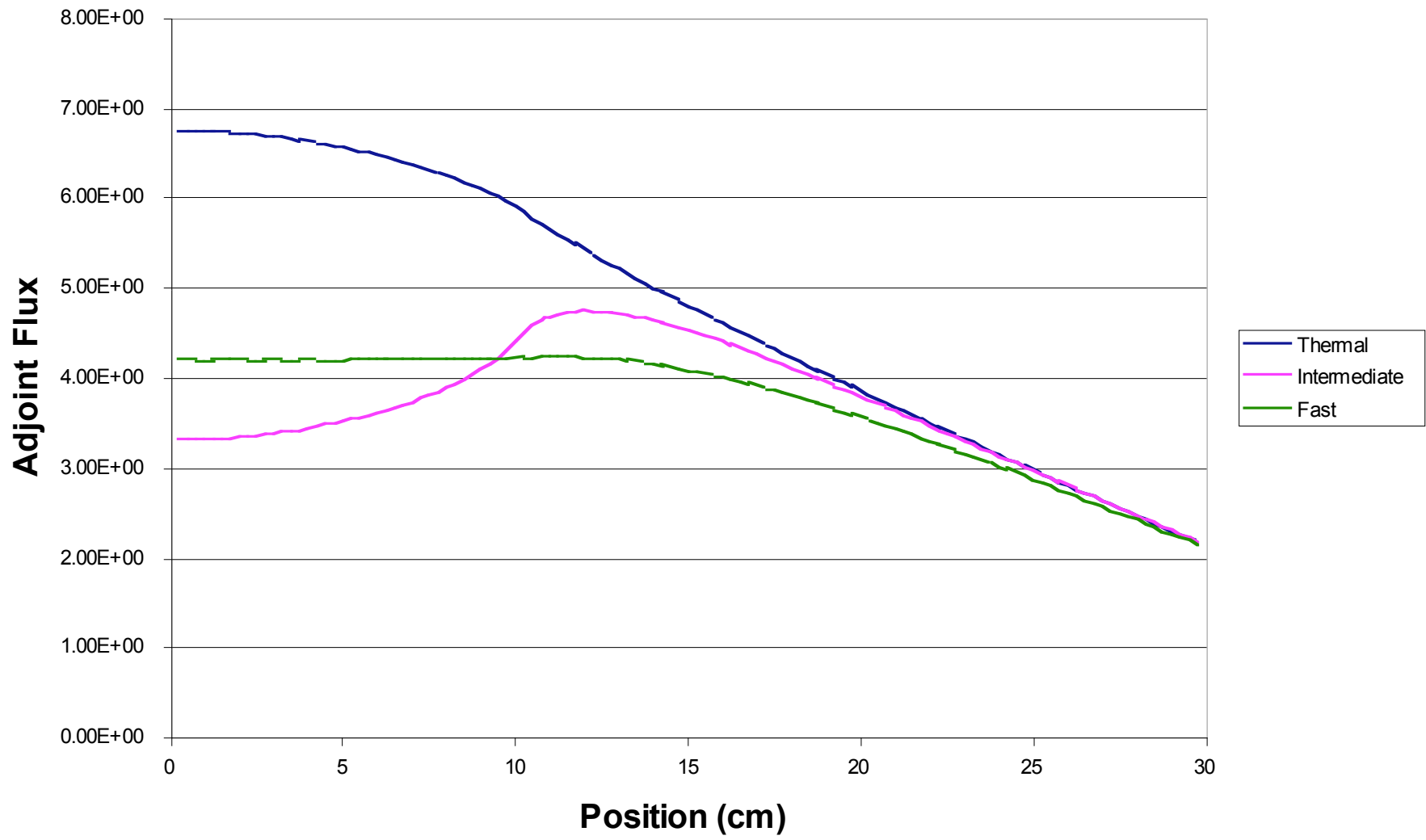
V & V: Adjoint-Weighted Flux (Multigroup)

MCNP Scalar Flux (3-group slab)



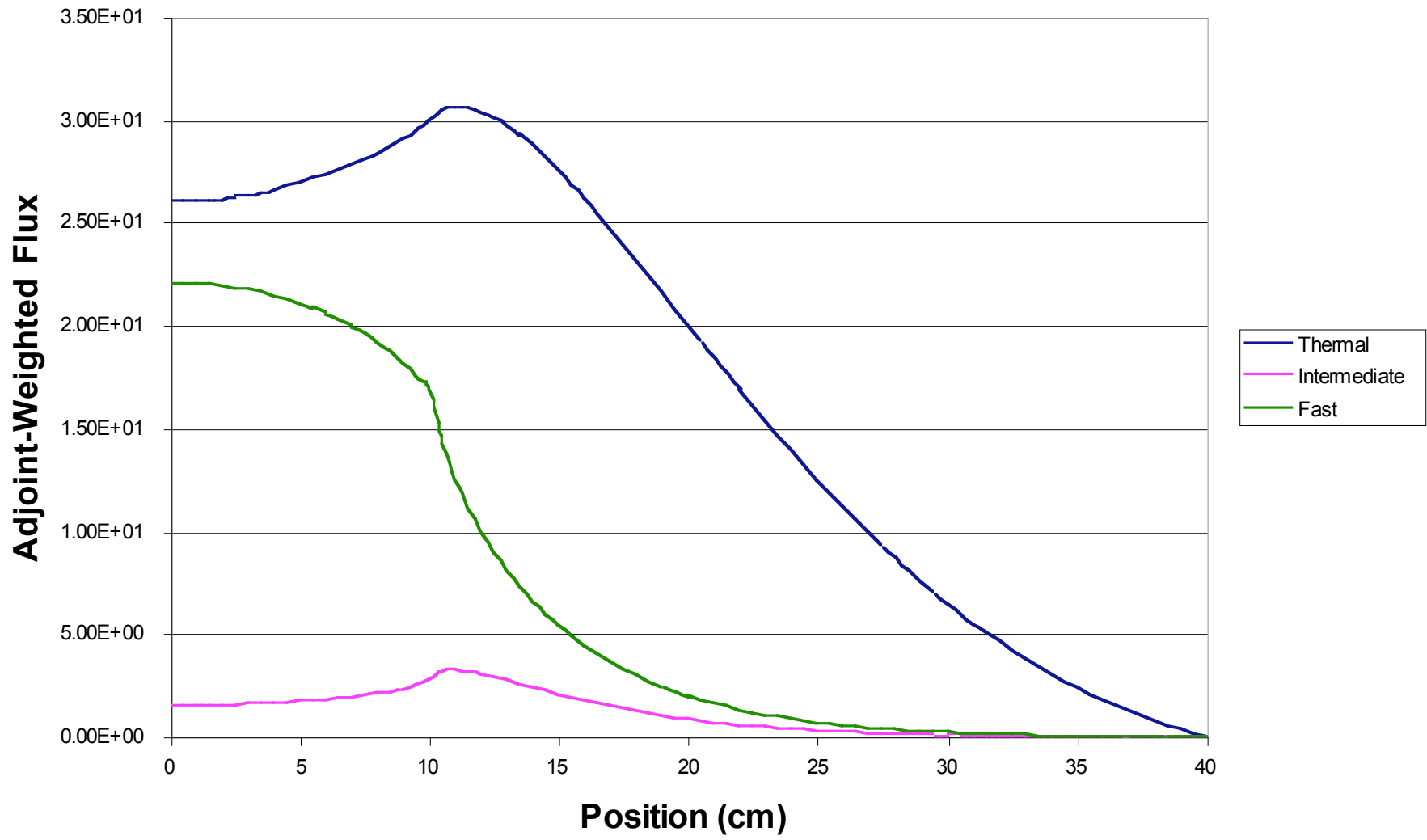
V & V: Adjoint-Weighted Flux (Multigroup)

Partisn Adjoint Flux (3-group slab)



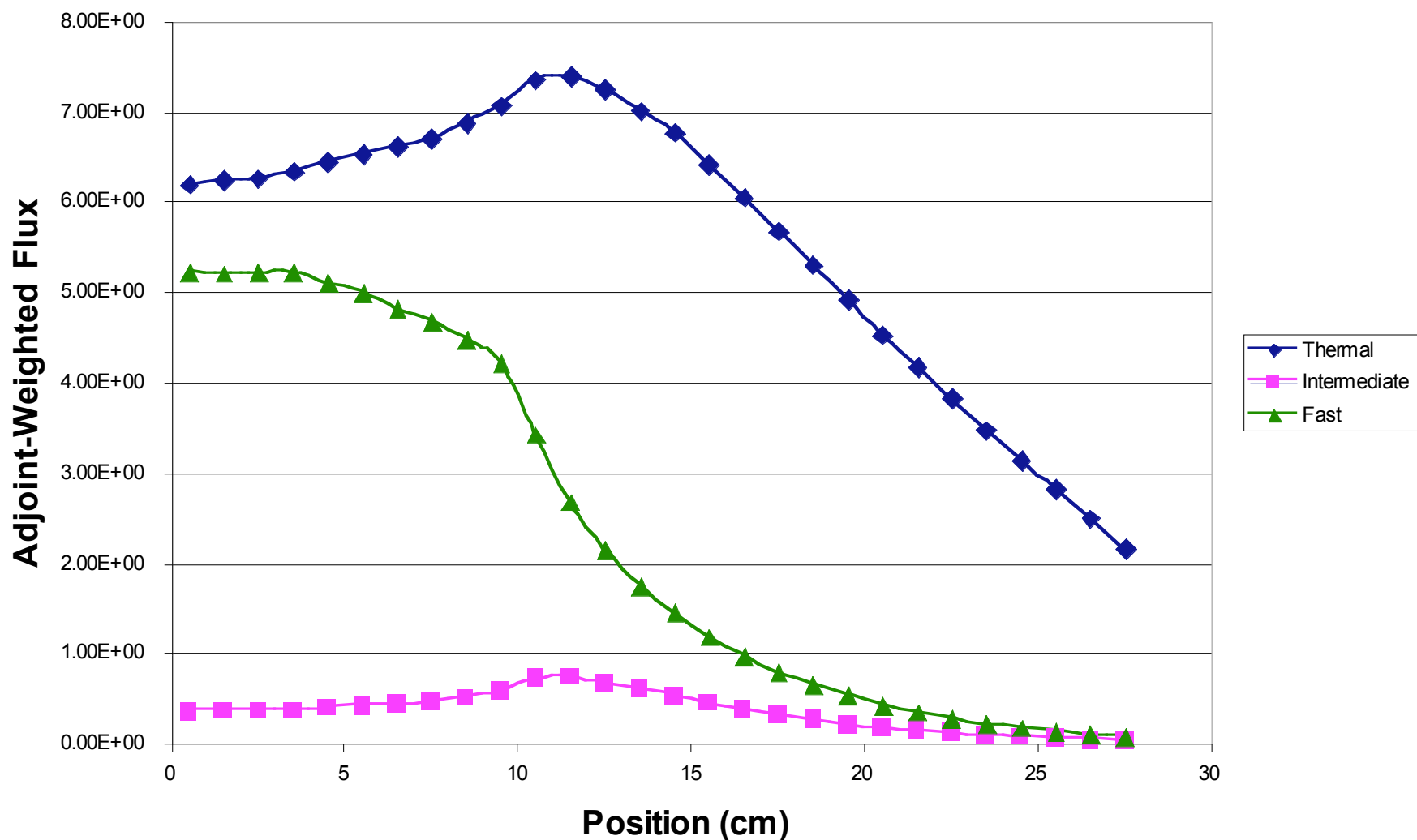
V & V: Adjoint-Weighted Flux (Multigroup)

Partisn Adjoint-Weighted Flux (3-group slab)



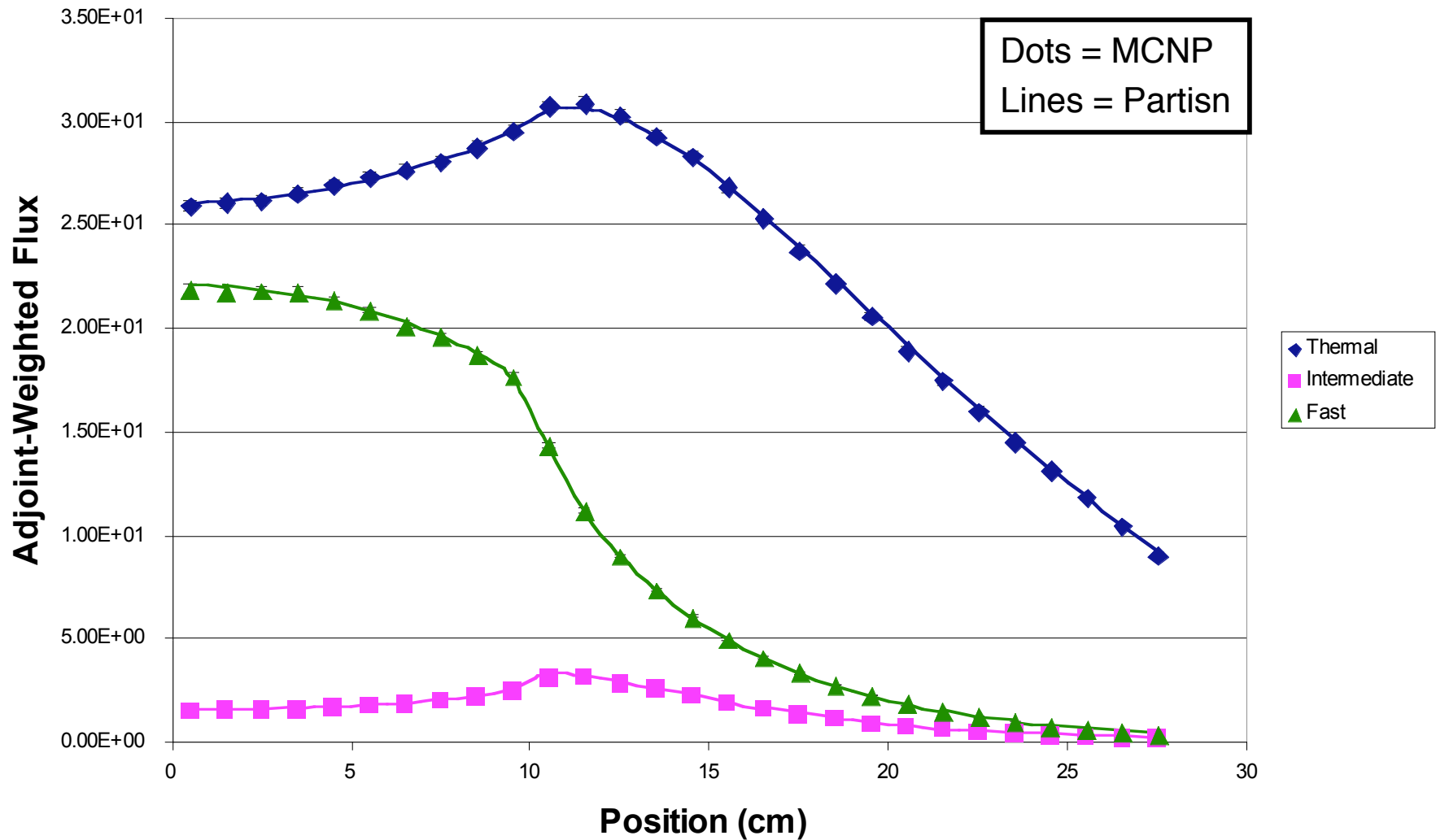
V & V: Adjoint-Weighted Flux (Multigroup)

MCNP Adjoint-Weighted Flux (3-group slab)

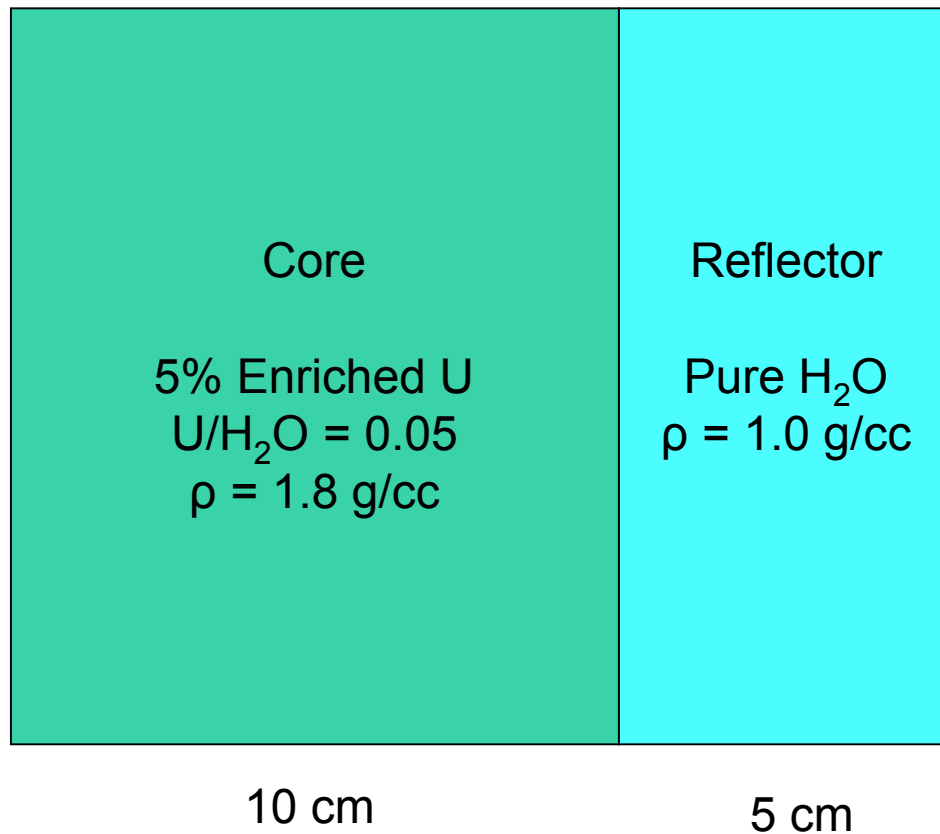


V & V: Adjoint-Weighted Flux (Multigroup)

MCNP/Partisn Comparison (3-group slab)



V & V: Adjoint-Weighted Flux (Continuous Energy)



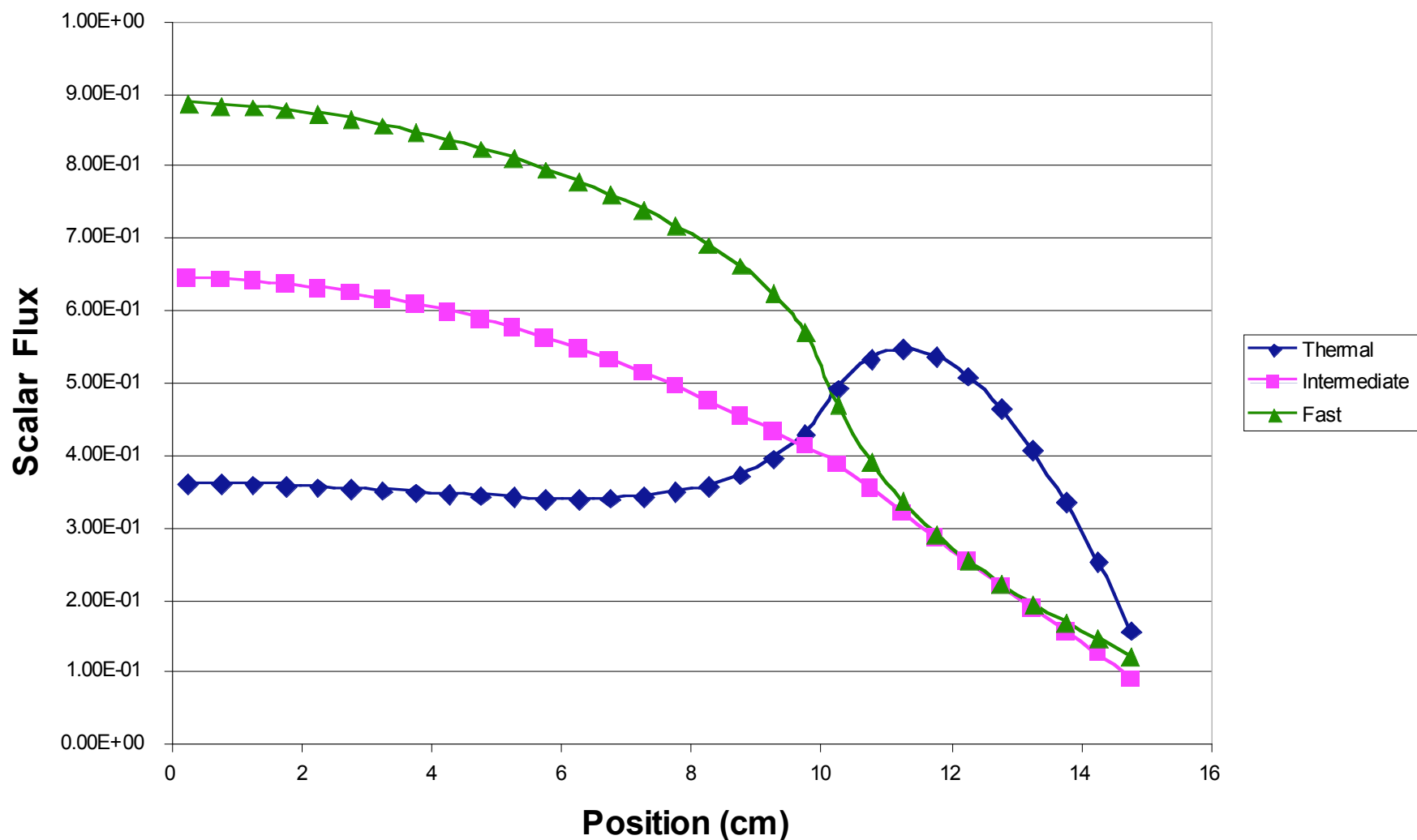
Vacuum

Fast: > 0.1 MeV
Thermal: < 0.625 eV

ENDF/B-VI.5 nuclear data

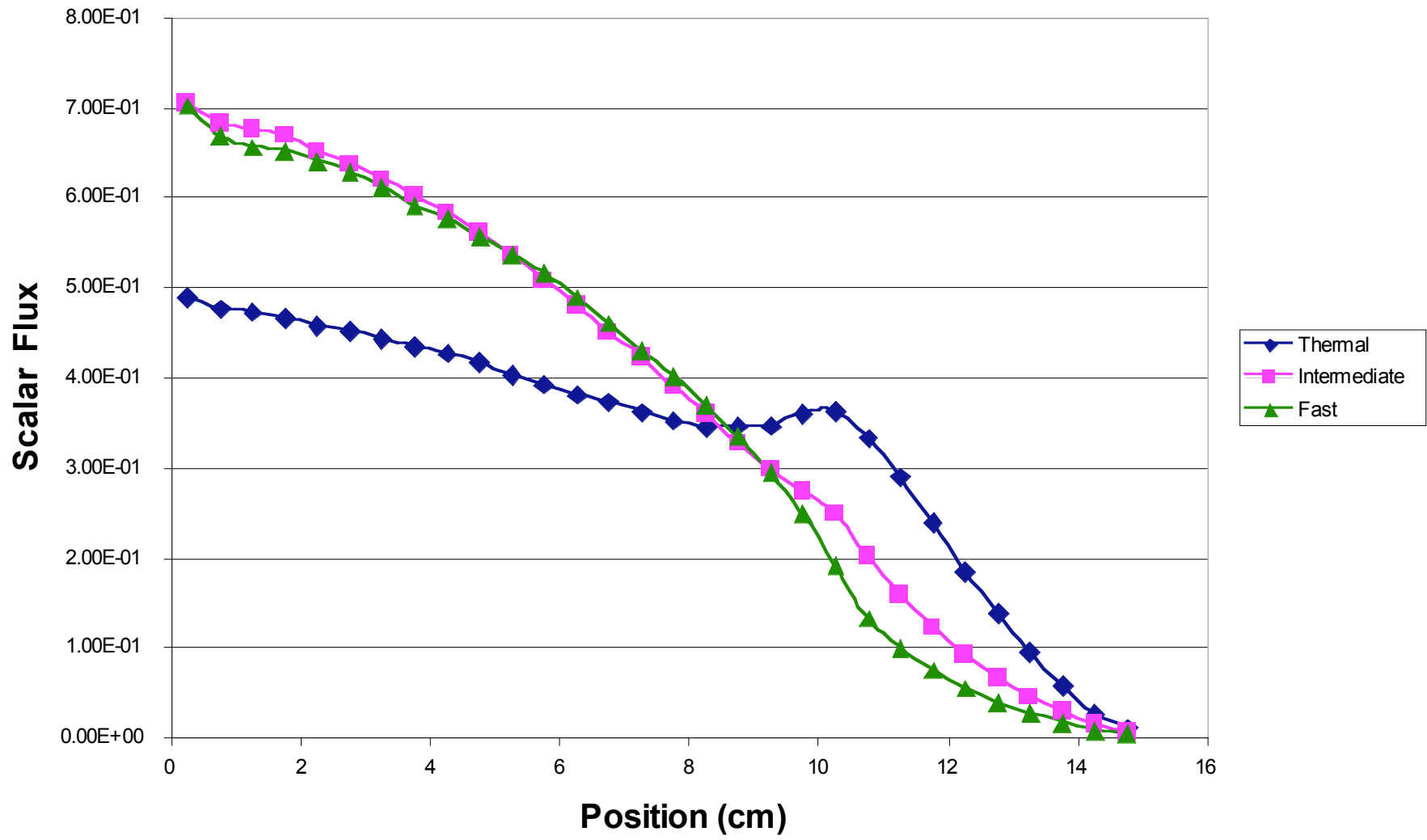
V & V: Adjoint-Weighted Flux (Continuous Energy)

MCNP Scalar Flux (Continuous Energy)



V & V: Adjoint-Weighted Flux (Continuous Energy)

MCNP Adjoint-Weighted Flux (Continuous Energy)



V & V: Kinetics Parameters (Multigroup)

Lifetime Comparisons

| # | G | Problem Description |
|----|---|---|
| 1 | 4 | Bare thermal slab, fuel/moderator mix |
| 2 | 4 | Reflected thermal slab, fuel + moderator |
| 3 | 4 | Bare fast slab |
| 4 | 4 | Reflected fast slab |
| 5 | 8 | Bare slab w/ intermediate spectrum |
| 6 | 4 | Bare fast sphere |
| 7 | 4 | Reflected fast sphere |
| 8 | 4 | Highly reflective slab |
| 9 | 4 | Subcritical bare fast slab ($k = 0.78$) |
| 10 | 4 | Supercritical bare fast slab ($k = 1.14$) |

V & V: Kinetics Parameters (Multigroup)

Lifetime Comparisons

| # | Partisn | MCNP |
|----|------------------|-----------------------------|
| 1 | 14.1323 μ s | 14.1025 +/- 0.0545 μ s |
| 2 | 135.2317 μ s | 135.0876 +/- 0.2081 μ s |
| 3 | 9.8100 ns | 9.8099 +/- 0.0010 ns |
| 4 | 43.4114 ns | 43.5719 +/- 0.0913 ns |
| 5 | 112.0523 ns | 112.5003 +/- 0.4341 ns |
| 6 | 1.7211 ns | 1.7185 +/- 0.0022 ns |
| 7 | 10.1982 ns | 10.1969 +/- 0.0158 ns |
| 8 | 6.1221 μ s | 6.1115 +/- 0.0073 μ s |
| 9 | 10.1715 ns | 10.1714 +/- 0.0138 ns |
| 10 | 9.6725 ns | 9.6752 +/- 0.0115 ns |

V & V: Kinetics Parameters (Continuous Energy)

| Experiment | Measured α (ms ⁻¹) | ACODE α (ms ⁻¹) | Progenitor α (ms ⁻¹) |
|------------|--|---------------------------------------|--|
| Godiva | -1110 +/- 20 | -1030 +/- 60 | -1136 +/- 12 |
| Jezebel | -640 +/- 10 | -510 +/- 120 | -643 +/- 13 |
| Flattop-23 | -267 +/- 5 | -252 +/- 30 | -296 +/- 5 |
| BIG TEN | -117 +/- 1 | -120 +/- 5 | -122 +/- 2.5 |
| STACY-29 | -0.122 +/- 0.004 | -- | -0.128 +/- 0.002 |
| WINCO-5 | -1.1093 +/- 0.0003 | -- | -1.153 +/- 0.037 |

V & V: Perturbations (Multigroup)

4-Group Bare Slab with modified cross sections

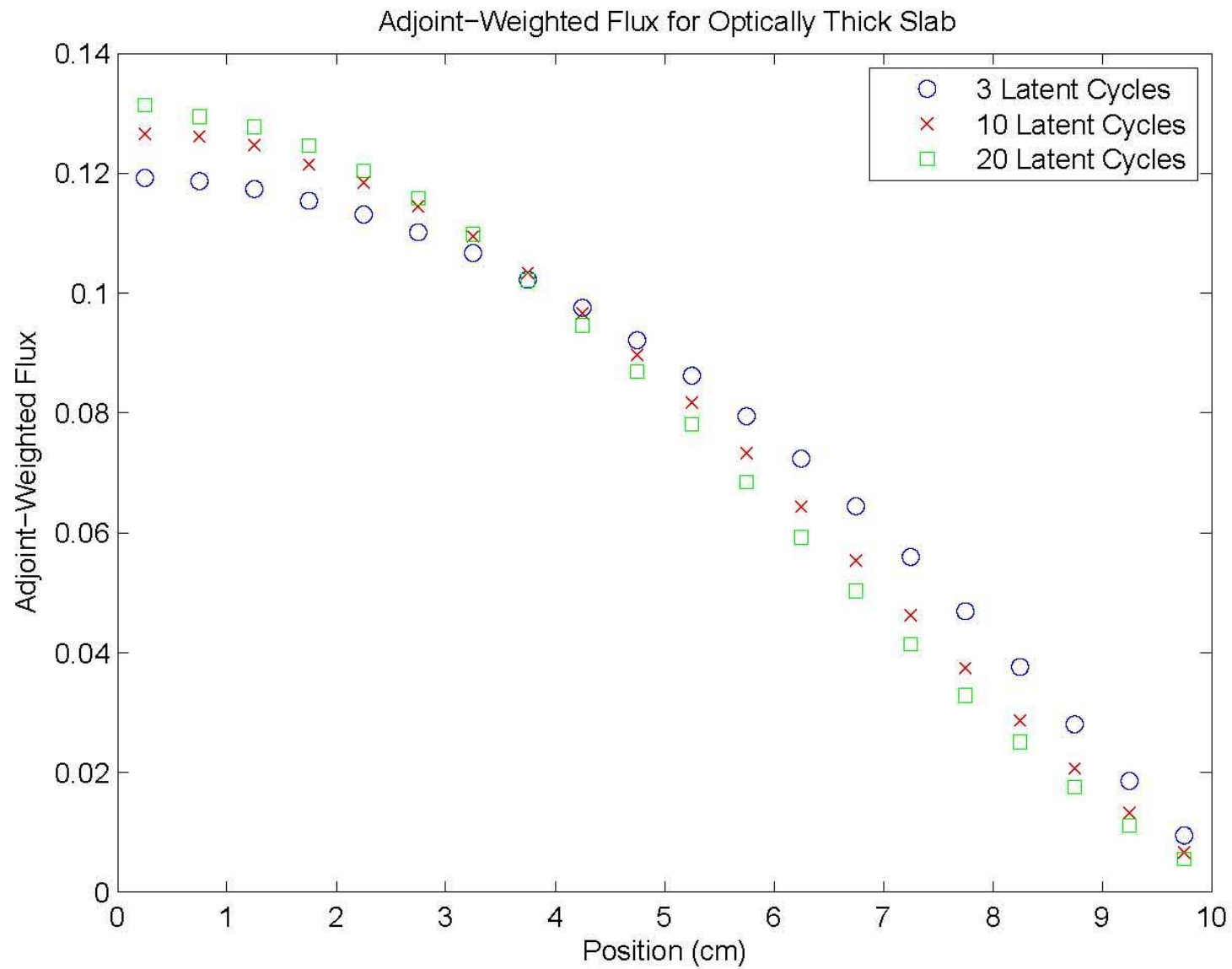
| # | $\Sigma_{\gamma,4}$ | $\Sigma_{f,4}$ | $\Sigma_{s,4-4}$ | V_4 |
|---|---------------------|----------------|------------------|-------|
| 1 | +0.05 b | | | |
| 2 | | +0.05 b | | |
| 3 | +0.05 b | +0.05 b | | |
| 4 | | | | +0.01 |
| 5 | +0.05 b | +0.05 b | | +0.01 |
| 6 | | | +0.05 b | |

V & V: Perturbations (Multigroup)

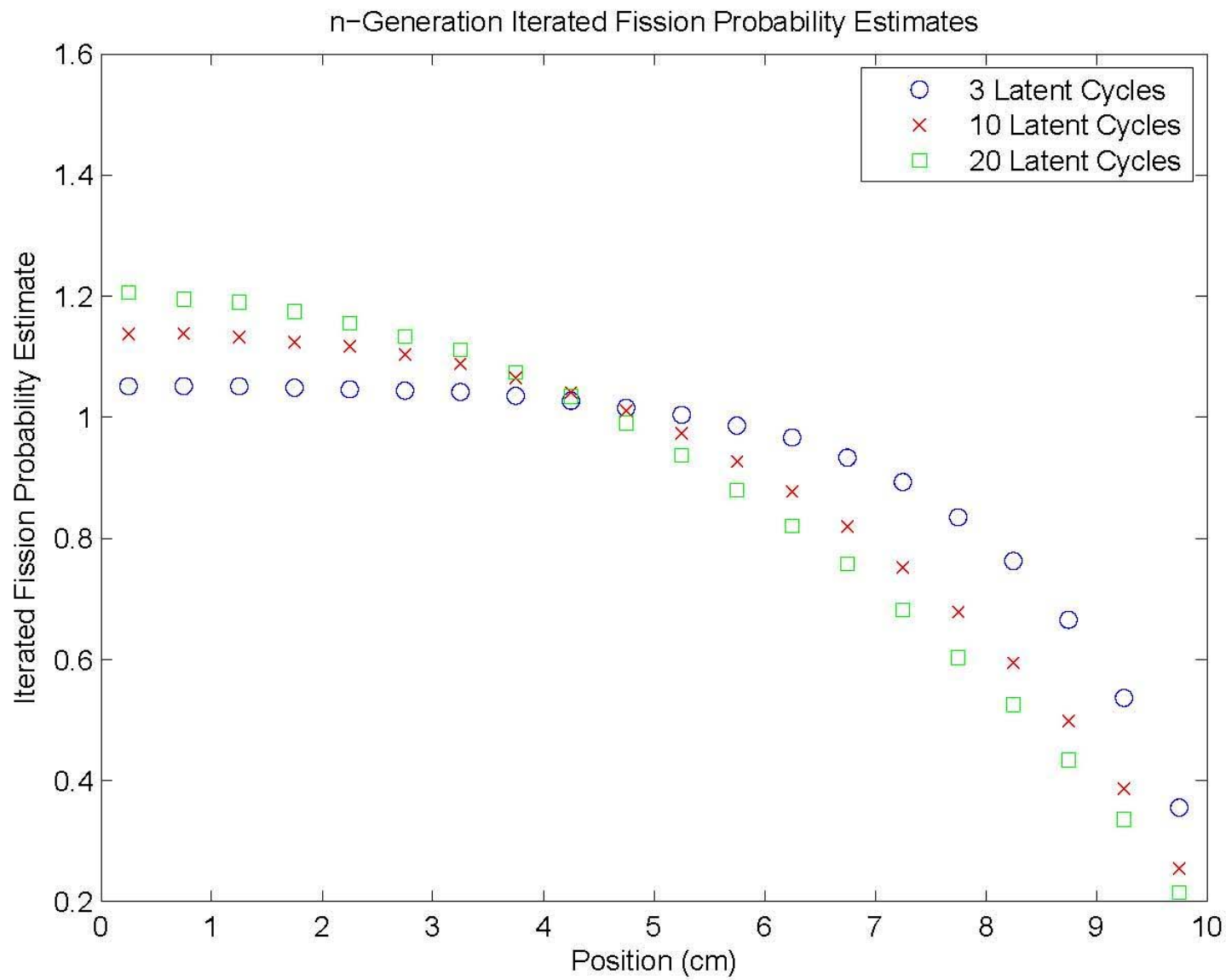
Changes in Reactivity

| # | Partisn (exact) | MCNP (1 st order) |
|---|-----------------|------------------------------|
| 1 | -0.00032839 | -0.00032748 +/- 0.00000152 |
| 2 | +0.00049517 | +0.00049465 +/- 0.00000308 |
| 3 | +0.00016644 | +0.00016744 +/- 0.00000405 |
| 4 | +0.00033068 | +0.00032891 +/- 0.00000107 |
| 5 | +0.00049767 | +0.00049931 +/- 0.00000483 |
| 6 | +0.00002166 | +0.00002192 +/- 0.00000283 |

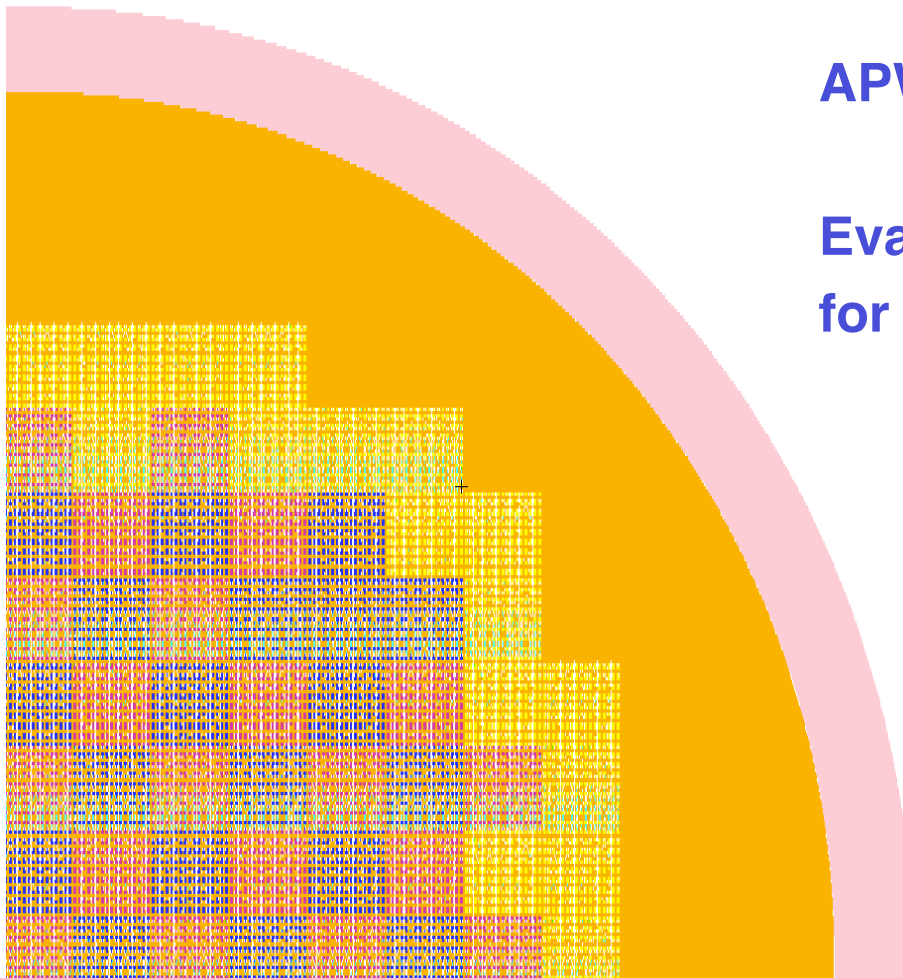
V & V: Convergence



V & V: Convergence



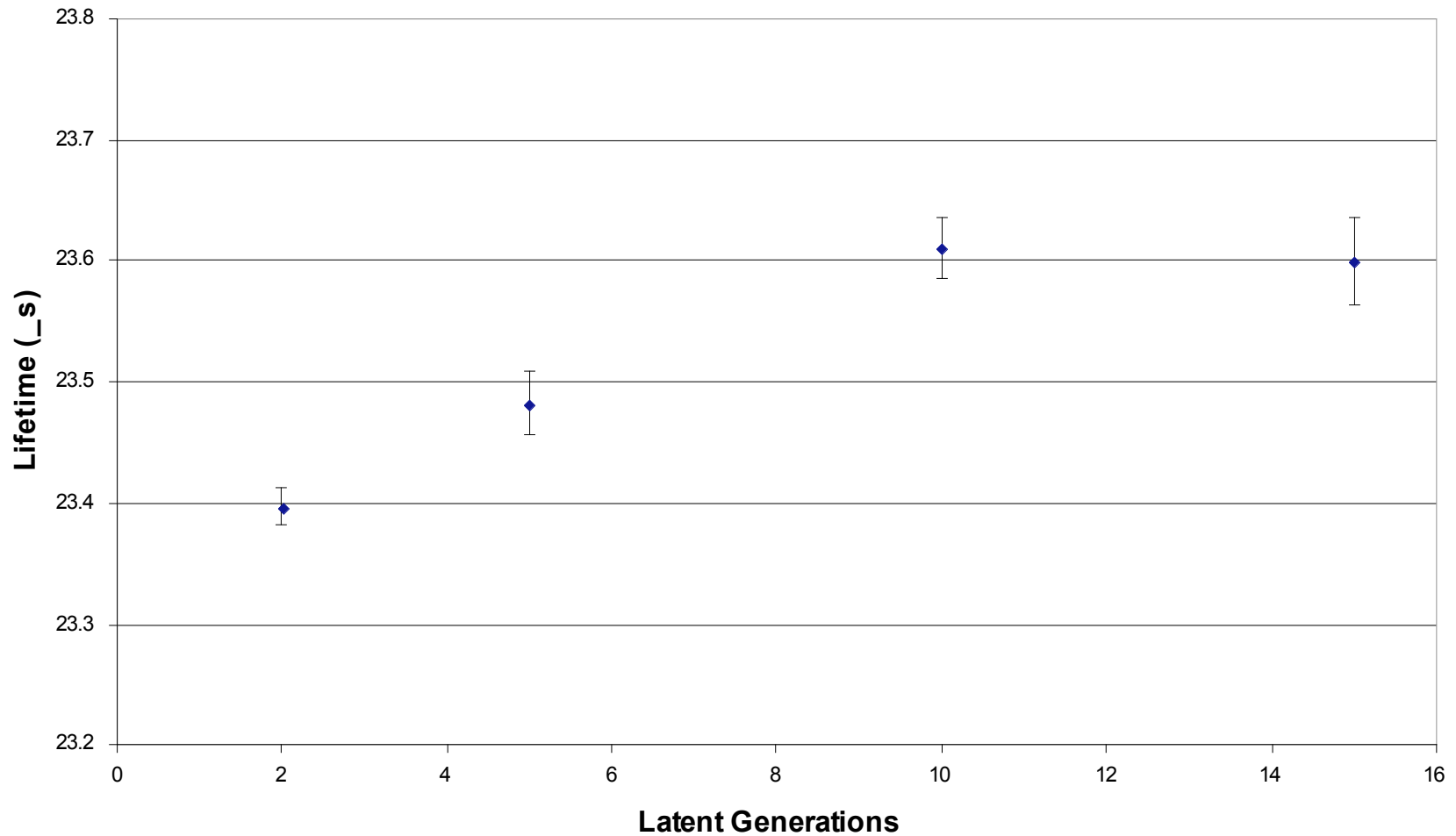
V & V: Convergence



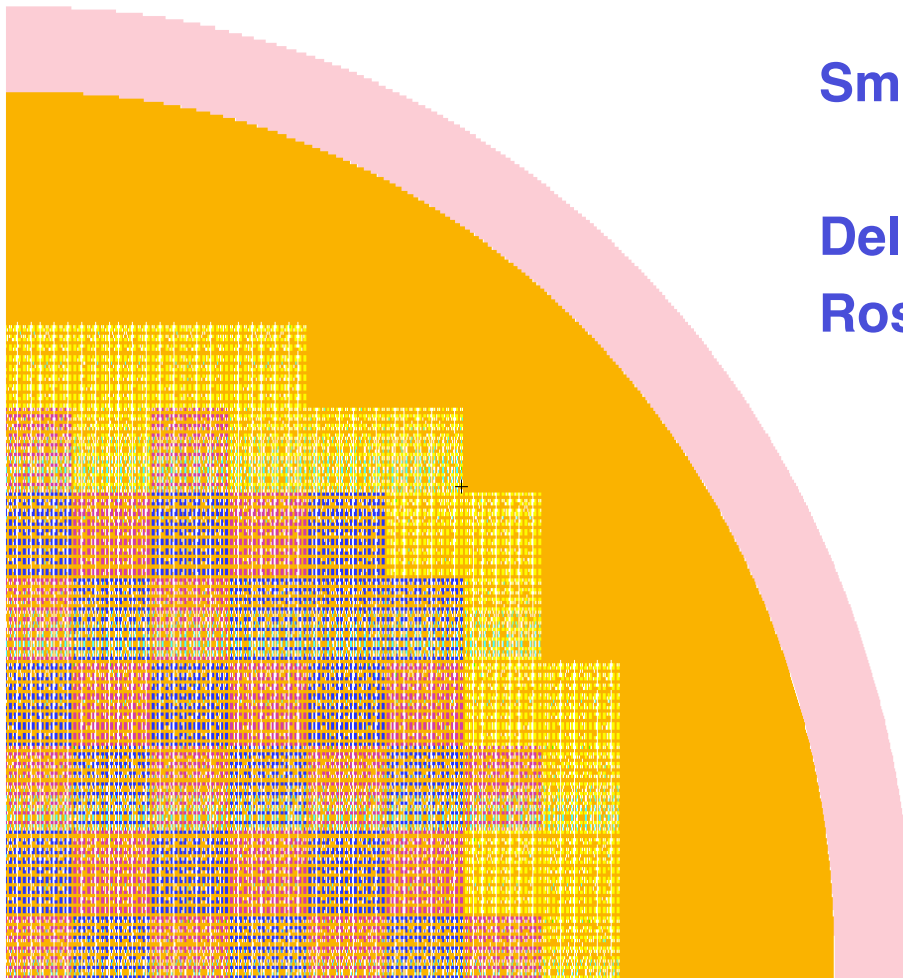
APWR quarter core 2D

Evaluate kinetics parameters
for various latent generations.

APWR Lifetime Convergence



V & V: Convergence



Small difference observed $< 1\%$.

Delayed neutron fraction and
Rossi- α are smaller still.

- **Adjoint-weighted tallies should be possible for Continuous Energy Monte Carlo criticality calculations.**
 - Iterated fission probability gives way to measure importance.
 - Minimal increase in CPU time.
- **Results show promise.**
 - Adjoint-weighted fluxes have correct shape.
 - Reactor kinetics parameters show good agreement with Partisn and experiment.
 - Perturbation results are encouraging, more work needed.
- **Adjoint-weighting applicable to other areas of reactor analysis.**

Advances in Monte Carlo Criticality Methods Workshop

M&C 2009
Saratoga Springs, NY
May 7, 2009

Bill Martin

Nuclear Engineering and Radiological Sciences

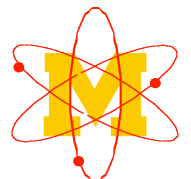
University of Michigan

wrm@umich.edu



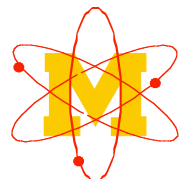
Outline of Session

- **Summary of approaches to handle temperature effects in Monte Carlo simulation**
- **On-the-fly Doppler broadening (Gokhan Yesilyurt)**



Treating Temperature Dependence

- **Generate NJOY libraries during NTH iterations**
- **Generate NJOY libraries prior to the NTH iterations**
- **Pseudo-materials approach**
- **On-the-fly Doppler broadening (Gokhan Yesilyurt)**



Acknowledgements

- ❑ Results for the STAR-CD/MCNP coupling were provided by Professor Tom Downar at the University of Michigan (UM). Also contributing to this work were Drs. Yunlin Xu and Volkan Seker, who are now at the UM.
- ❑ The following faculty and students at the UM contributed to the work on pseudo-materials and RELAP5/MCNP coupling:
 - John C. Lee, Professor
 - Wei Ji, former PhD candidate (now Professor at RPI)
 - Gokhan Yesilyurt, PhD candidate
 - Jeremy Conlin, PhD candidate
 - Kaushik Banerjee, PhD candidate
 - Etienne de Villèle, former exchange student at UM



Temperature effects on Monte Carlo calculations

- ❑ Consequences of temperature effects
 - Thermal expansion: changes in dimensions and densities
 - Changes to cross-section data:
 - Doppler broadening
 - $S(\alpha, \beta)$ thermal scattering kernel
- ❑ For most Monte Carlo codes, temperature effects must be handled explicitly by the code users
 - Input changes to account for dimension & density changes
 - Cross-section data generated at the correct problem temperatures
 - **MCNP automatically Doppler broadens elastic scattering cross-sections. MCNP does NOT adjust:**
 - resolved resonance data
 - unresolved resonance data
 - thermal scattering kernels



Accounting for Temperature Effects in MCNP

Approaches to account for temperature changes:

- **A. Generate explicit temperature – dependent cross section libraries (NJOY)**
- **B. Modify existing libraries (MAKXSF)**
- **C. Approximate approach using pseudo-materials**
- **D. On-the-fly Doppler broadening – the primary focus of this session (Gokhan Yesilyurt)**



A. Generate explicit temp-dep datasets (NJOY)

- ❑ Use NJOY (or similar cross-section processing code) to generate nuclear cross-section datasets
- ❑ Must generate a separate dataset for each nuclide at each region temperature
- ❑ NJOY routines take care of Doppler broadening (resolved & unresolved) & thermal scattering kernels
- ❑ Two approaches:
 - **Iterative NJOY updates**: run NJOY during the neutronic-thermal/hydraulic (NTH) iterations for each temperature needed for the current T/H calculation.
 - **Pregenerated NJOY libraries**: run NJOY beforehand for a range of temperatures that adequately covers the temperatures expected for the NTH calculation, e.g., every 5K from 300K to 1200K for fuel nuclides.



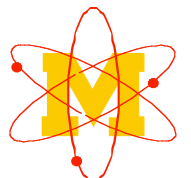
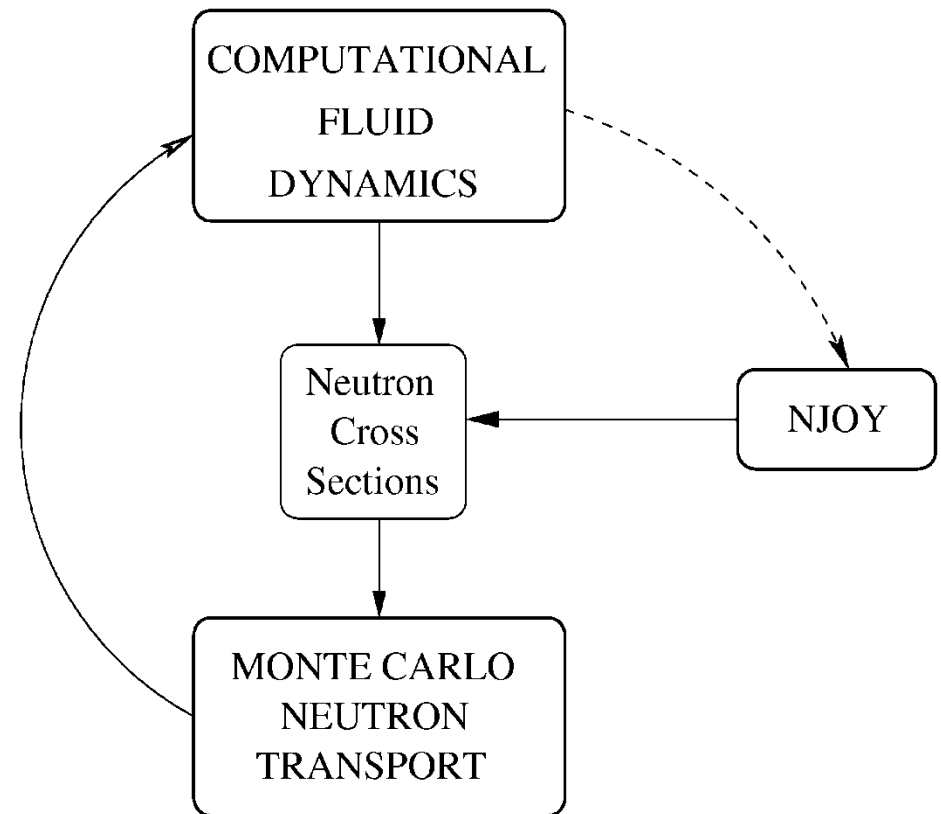
Computational results (Downar, Monterey 2007)

- Iterative NJOY updating is very time-consuming
 - 95 s to prepare U235 dataset on 3 Ghz Pentium P4.
 - Not practical for realistic reactor applications.
- Pregenerated NJOY libraries is a reasonable approach
 - Used to couple STAR-CD and MCNP
 - NJOY was run at 5K temperature increments over the temperature range. (Temperature increments of 1-2 K cause memory problems with MCNP.)
 - A Perl script was used to manage the NTH iterations.
 - The coupled code system (**McStar**) was applied to a 1/8 pin cell and a 3x3 array of pin cells.
 - Good agreement with DeCart/STAR-CD results



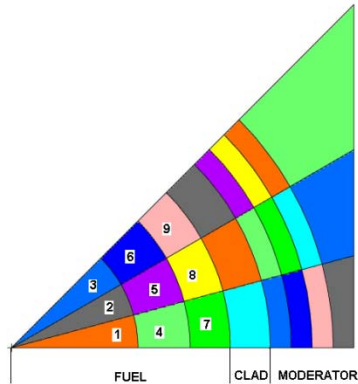
McSTAR

- ❑ Monte Carlo Neutron Transport : MCNP5
- ❑ Computational Fluid Dynamics : STAR-CD
- ❑ Cross Sections: NJOY

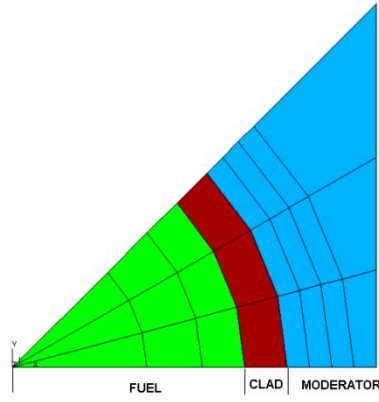


Results: coupled STAR-CD and MCNP results

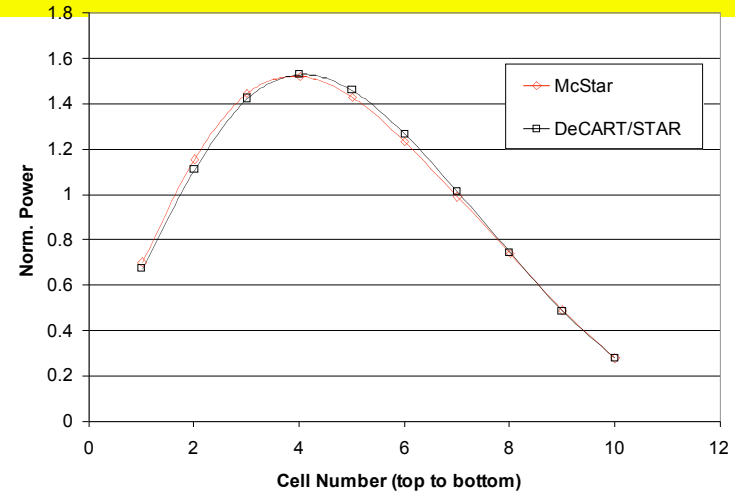
1/8 pin cell



MCNP MODEL

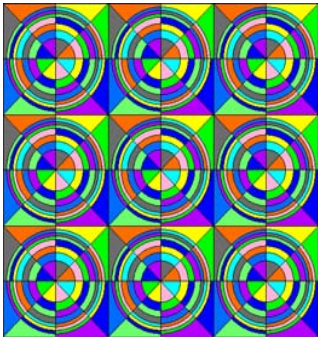


STAR-CD MODEL

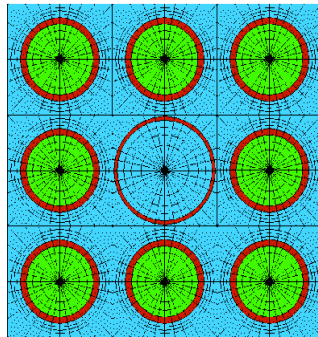


keff agrees within 52 pcm with DeCart/STAR-CD

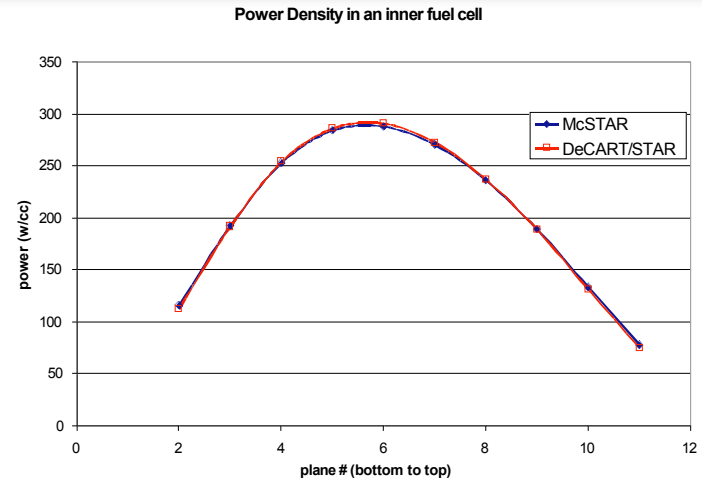
3x3 array of pin cells



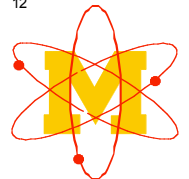
MCNP



STAR-CD



keff agrees within 66 pcm with DeCart/STAR-CD



Preliminary conclusions for McStar

- ❑ The preliminary results for two simple PWR test problems demonstrate the feasibility of coupling Monte Carlo to CFD for a potential audit tool.
- ❑ Validation of the cross section update methodology was performed to assess the accuracy of the 5K increment tables for these problems.
- ❑ McSTAR is now being applied to advanced BWR fuel assemblies with strong axial heterogeneities to verify the accuracy of the 2D/1D solution methods in DeCART



B. Modify existing MCNP library (MAKXSf)

- ❑ New version of MAKXSf
- ❑ Subset of NJOY routines, easy to use, part of MCNP5/1.50 distribution
- ❑ For ACE datasets (for MCNP), makxsf performs:
 - Doppler broadening of resolved resonance data (explicit profiles)
 - Interpolation of unresolved resonance data (probability tables) between ACE datasets at 2 different temperatures
 - Interpolation of thermal scattering kernels ($S(\alpha,\beta)$ data) between ACE datasets at 2 different temperatures
- ❑ For now, makxsf is run external to MCNP
- ❑ Long-term plan: put the makxsf routines in-line with the MCNP coding



C. Approximate method: pseudo-materials

- "Pseudo-materials" for temperature dependence
 - Equivalent to "**stochastic interpolation**"
 - To approximate the cross-sections for nuclide X at temperature T, use a **weighted combination of nuclide X at lower temperature T₁ and higher temperature T₂**
 - This weighted combination is input as an MCNP5 material with volume fractions given by the weights

$$w_2 = \frac{\sqrt{T} - \sqrt{T_1}}{\sqrt{T_2} - \sqrt{T_1}}, \quad w_1 = 1 - w_2$$

$$\Sigma_i = \Sigma(T_i)$$

$$\Sigma(T) = w_1 \cdot \Sigma_1 + w_2 \cdot \Sigma_2$$



Pseudo-materials example - MCNP input

Example: ^{235}U at 500 K

Existing datasets for MCNP:

(1) dataset for ^{235}U at **293.6** K: **92235.66c**

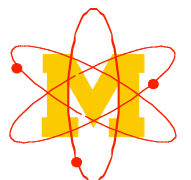
(2) dataset for ^{235}U at **3000.1** K: **92235.65c**

Weight the datasets using $T^{1/2}$ interpolation

$$w_2 = \frac{\sqrt{500} - \sqrt{293.6}}{\sqrt{3000.1} - \sqrt{293.6}} = .1389, \quad w_1 = .8611$$

MCNP input:

m1 92235.66c .8611 92235.65c .1389



Application: VHTR geometry*

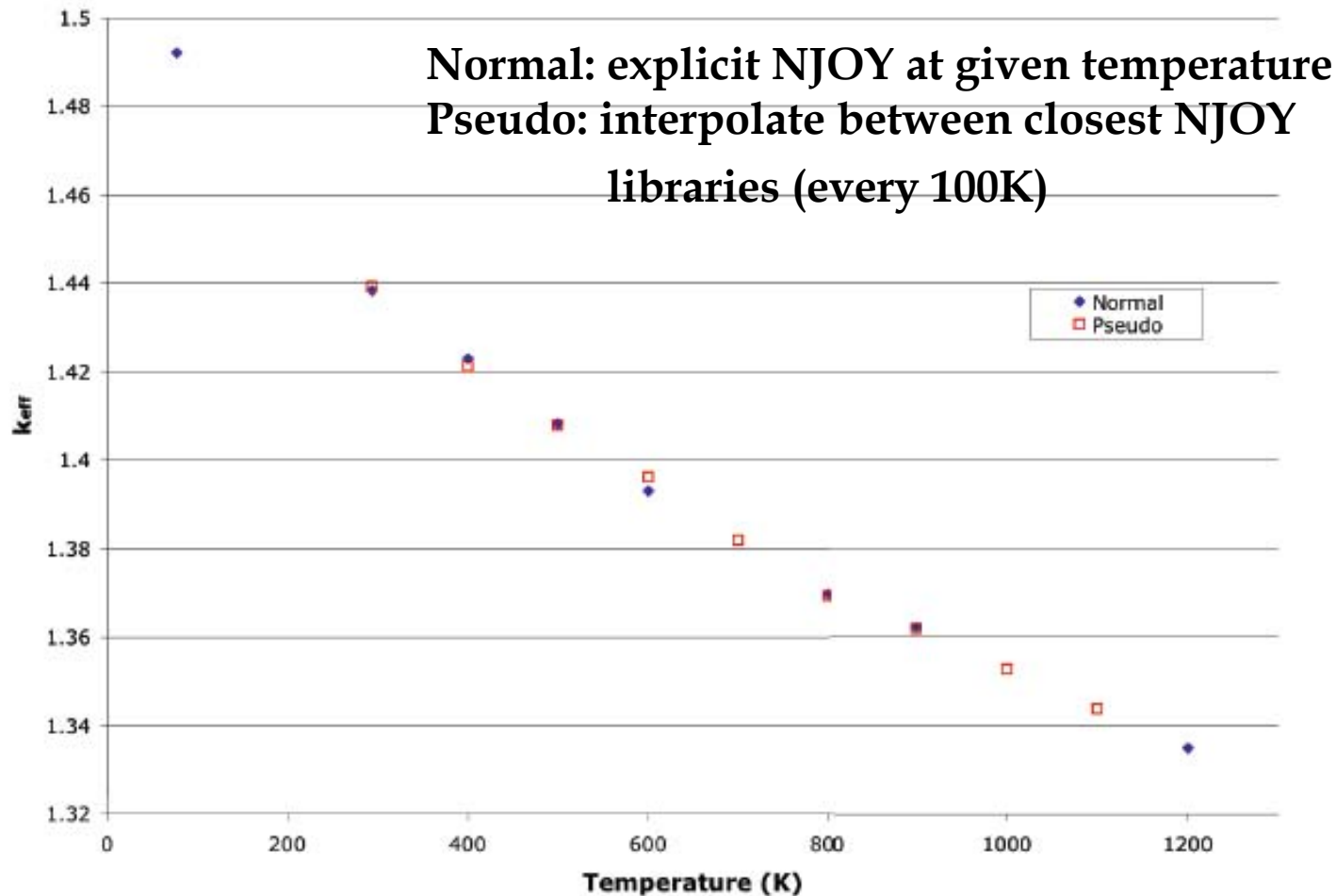
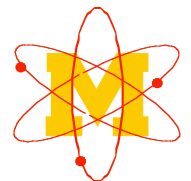


Figure 1. Comparison of k_{eff} between normal and pseudo materials with the VHTR geometry.

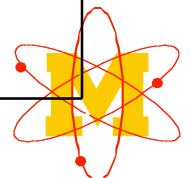
*JL Conlin, W Ji, JC Lee, WR Martin, "Pseudo-Material Construct for Coupled Neutronic-Thermal-Hydraulic Analysis of VHTR", Trans. ANS 91 (2005)



Application – LWR configuration

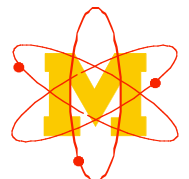
Results for LWR configuration with NJOY cross sections at 325K compared to pseudo-material approach using cross sections at 300K and 350K. Most deviations within statistics. (Downar, 2007 Monterey M&C)

| | 325 K (NJOY) | 325 K Interpolated | Deviation |
|-------------------|--|--|------------------|
| k_{eff} | 1.40974 (± 0.00043) | 1.41008 (± 0.00044) | 34 pcm |
| ϕ in Fuel | 1.37933 (± 0.0003) | 1.37929 (± 0.0003) | 0.00003 |
| $\sigma_{aF}\phi$ | 3.67362e-03 (± 0.0006) | 3.67648E-03 (± 0.0006) | 0.0008 |
| $\sigma_f\phi$ | 5.62964e-03 (± 0.0007) | 5.63817E-03 (± 0.0007) | 0.0010 |
| $\nu\sigma_f\phi$ | 1.38341e-02 (± 0.0007) | 1.38548e-02 (± 0.0007) | 0.0010 |



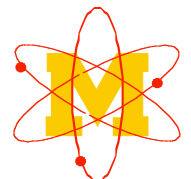
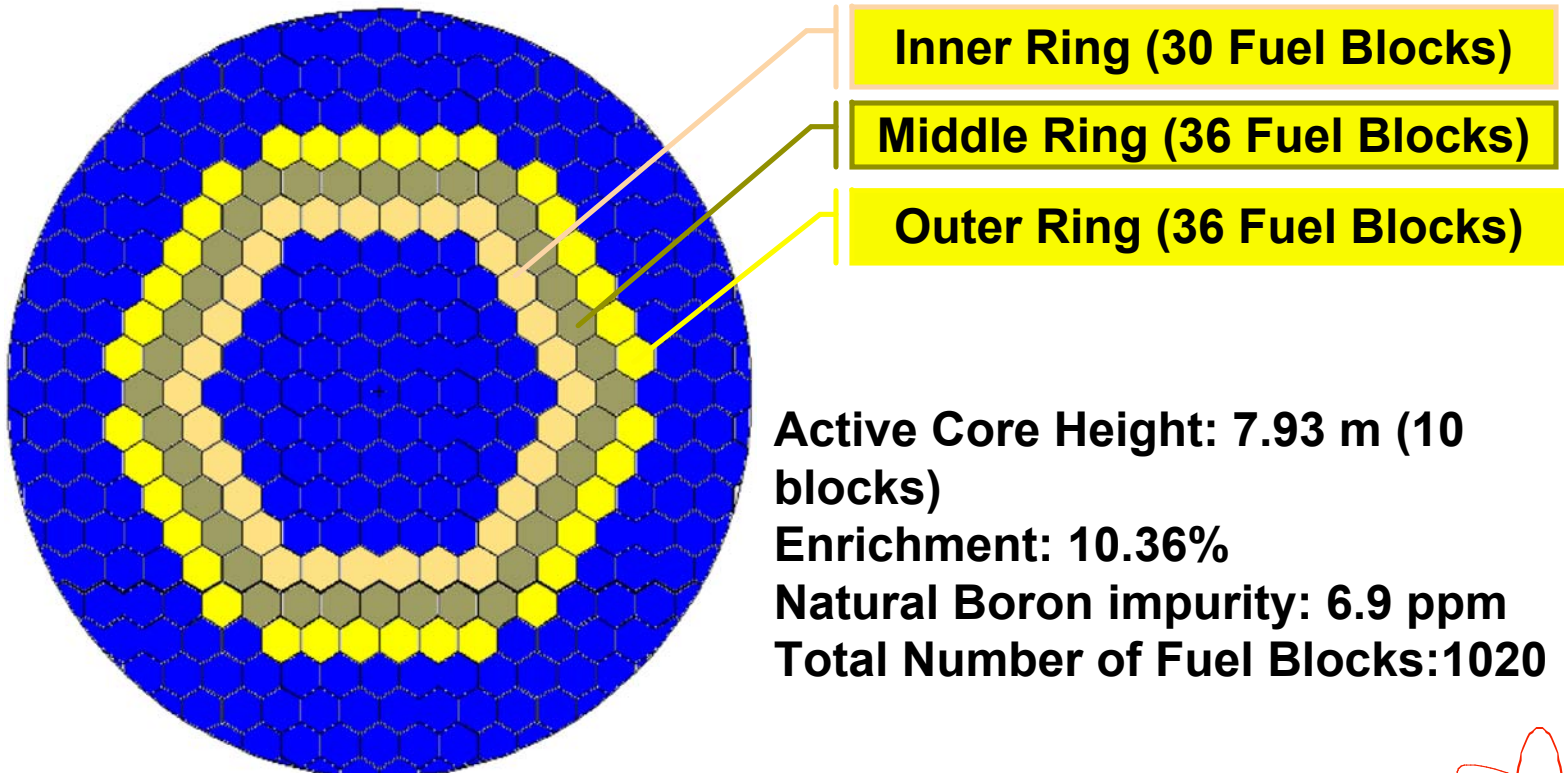
Application – full core VHTR with T/H feedback

- ❑ MCNP5 code was coupled with the RELAP5-3D/ATHENA code to analyze full core VHTR with temperature feedback (pseudo-materials) including explicit TRISO fuel
- ❑ Utilized a master process supervising independent computing platforms to automate coupled Nuclear-Thermal-Hydraulic (NTH) calculations.
- ❑ Axial power fractions determined for 10 axial zones for each of three rings by MCNP5 are input to RELAP5 to determine assembly-average temperature distributions.
- ❑ Updated RELAP5 temperature distributions are used for the next MCNP simulation to obtain updated power fractions. MCNP5 and RELAP5 iterations were performed in a cyclic fashion until convergence in temperature and power distributions were obtained.
- ❑ Totally automated with a Perl script that reads output files and generates input files.

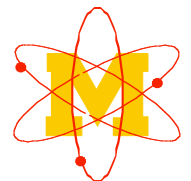
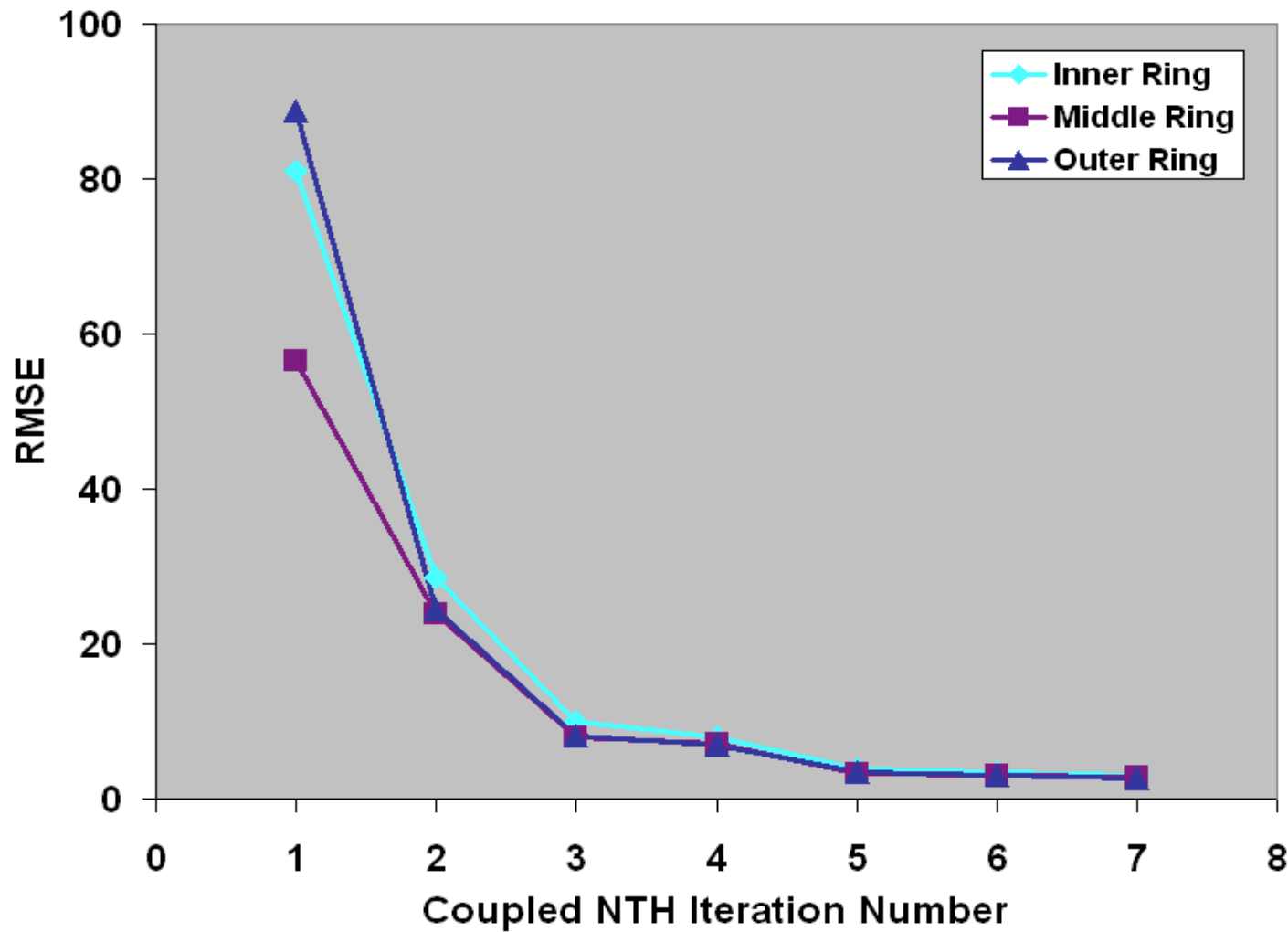


Description of VHTR reactor

- MCNP5 input decks were set up to represent the VHTR full core with homogeneous and heterogeneous fuel assemblies. Each ring has 10 axial fuel segments and 30, 36, and 36 fuel assemblies, respectively, for the inner, middle, and outer core rings.



RMS Error in Temperature vs. NTH Iteration



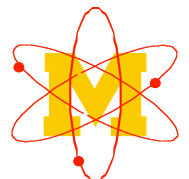
Pseudo-materials – advantages/disadvantages

□ Advantages

- **Libraries needed at fewer temperatures**
- **Can interpolate to any temperature bounded by the library temperatures**
- **No data preprocessing required**

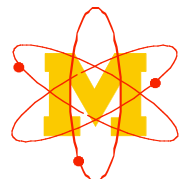
□ Disadvantages

- **Approximate interpolation** - **stochastic interpolation not functional interpolation**: one of the two datasets is chosen randomly during the random walk
- **Finite error due to interpolation – seems to be small**
- **Cannot be used for $S(\alpha, \beta)$ thermal scattering kernels**
 - **MCNP limitation**: does not allow mixture of $S(\alpha, \beta)$ materials
 - Need to pick $S(\alpha, \beta)$ dataset at nearest temperature



D. On-the-fly Doppler Broadening

- ❑ Gokhan Yesilyurt – PhD candidate at the UM.
- ❑ Monte Carlo code based on 0K cross sections
- ❑ When a neutron at energy E enters a region at temperature T , the cross sections for each material in that region are generated at that time.
- ❑ The cross sections are discarded when no longer needed.
- ❑ Any temperature in the range 77K-3200K can be accommodated. (this can be changed)
- ❑ Details are given in the next talk.





On-the-Fly Doppler Broadening for Monte Carlo Codes

Advances in Monte Carlo Criticality Methods Workshop
M&C 2009
Saratoga Springs, NY
May 7, 2009

Gokhan Yesilyurt
Department of Nuclear Engineering
and Radiological Sciences
University of Michigan

Outline

- Acknowledgements
- Overall Goal and Methodology
- Background
- Literature Survey
- The Need for On-The-Fly Doppler Broadening
- Theory
- Construction of Union Grid
- Alternative Doppler Code (ADC)
- Results
- Conclusions

Acknowledgments

- Forrest Brown (LANL)
- William R. Martin (UM Faculty)
- Financial support provided by DOE grant DE-FC07-06ID14745 (NERI).

Overall Goal and Methodology (1)

Goal: perform Doppler broadening of the cross sections on-the-fly during the random walk of neutrons in a Monte Carlo (MC) code.

❑ For realistic, detailed reactor calculations, Monte Carlo codes are part of a multiphysics simulation involving thermal-hydraulic feedback to adjust temperatures and densities. This process can result in 10000s of material temperatures for which broadened cross sections are needed.

❑ Existing codes (eg, MCNP) were not designed to accommodate this need.

Overall Goal and Methodology (2)

- ❑ Therefore, a regression model was developed based on the Adler-Adler multi-level resonance model for the cross sections as a function of temperature.
- ❑ New regression model allows on-the-fly Doppler broadening of the cross sections, letting an unlimited number of temperatures for only a modest computing cost, at the same time accounting for the interference effects between the closely spaced resonances in keV range.

Overall Goal and Methodology (3)

- ❑ The ultimate regression model must cover a very wide range of temperatures, including the all fields of study.

| Temperature Range (K) | Field of Study |
|------------------------------|----------------------------------|
| 77 - 293.6 | Cold Neutron Physics |
| 293.6 - 550 | Benchmarking Calculations |
| 550 - 1600 | Reactor Operation |
| 1600 - 3200 | Accident Conditions |

Background

- ❑ As the temperature increases, a wider spectrum of relative energy is generated due to the increase in the motion of the target nuclides.
- ❑ Cross sections at the peak of a given resonance decrease while cross sections on the wings increase.
- ❑ Summed over all resonance energies, the overall effect of the increased Doppler broadening at higher temperatures is to increase the total resonance absorption in the fuel region.

Literature Survey (1)

- ❑ T.H. Trumbull, from KAPL, interpolated nuclear data files generated by NJOY at various temperatures, using different interpolation schemes.
 - ❑ 0.1% accuracy - (1H,10B,16O) - $\Delta T=111K$
 - ❑ $>0.1\%$ accuracy - (235U,238U) - $\Delta T=28K$
- ❑ The pseudo material approach: developed at UM to perform interpolations of cross section libraries based on the fractional number densities.
- ❑ Different series approximations were used for different T intervals by J.H.Marable from ORNL in 1960s. The method was based on the single level resonance parameters.

Literature Survey (2)

❑ In NJOY, there are two ways to perform Doppler broadening of cross sections.

❑ Exact Doppler broadening kernel developed by Cullen

$$\sigma(y, T_2) = \frac{1}{y^2} \left(\frac{1}{\pi} \right)^{\frac{1}{2}} \int_0^{\infty} [\sigma(x, T_1)] x^2 \left\{ \exp[-(x-y)^2] - \exp[-(x+y)^2] \right\} dx$$

❑ Based on resonance parameters, $(\Gamma_t, \Gamma_n, \Gamma_\gamma, \Gamma_f, \sigma_{mr})$

❑ Single level (psi-chi)

$$\sigma^{cap, fis}(E, T) = \left(\frac{2}{\Gamma_T} \right) \left(\frac{E_R}{E} \right)^{1/2} A \psi(x, \xi_R)$$

❑ Multi level Adler-Adler

$$\sigma^{cap, fis}(E, \xi_R) = \frac{\pi \sqrt{E}}{k^2} \left\{ \sum_R \frac{1}{v_R} [(G_R \psi(x, \xi_R) + H_R \chi(x, \xi_R))] \right. \\ \left. + A_1 + \frac{A_2}{E} + \frac{A_3}{E^2} + \frac{A_4}{E^3} + B_1 E + B_2 E^2 \right\}$$

Literature Survey (3)

- Exact Doppler broadening equation:
 - Very expensive to compute on-the-fly.

- Psi-chi:
 - Not as accurate as exact Doppler broadening method.
 - Terms important for energies less than about $16kT / A$ are neglected.
 - Limited in application: All currently available evaluations do not represent cross sections as a series of single-level Breit-Wigner resonances.

- Adler-Adler:
 - More accurate than psi-chi and accounts for resonance interference in kev region.

The Need for On-the-fly Doppler Broadening (1)

- CPM3 was used to determine the list of resonance absorber nuclides for the Uranium based fuel.

Total Burnup: 100 GWd/MT-HM

List of resonance absorbers including FPs for U based fuel

| | | | | | | | | | |
|-------|-------|-------|-------|-------|-------|-------|-------|-------|--------|
| U234 | U235 | U236 | U238 | NP237 | PU238 | PU239 | PU240 | PU241 | PU242 |
| AM241 | AM242 | AM243 | CM242 | CM244 | KR83 | ZR93 | MO95 | MO97 | TC99 |
| RU101 | RH103 | RH105 | PD105 | PD108 | AG109 | CD113 | IN115 | XE131 | XE135 |
| CS133 | CS134 | CS135 | CE141 | PR141 | ND143 | ND145 | PM147 | PM148 | PM148m |
| SM147 | SM149 | SM150 | SM151 | SM152 | EU153 | EU154 | EU155 | | |

| | $T_{f,ave}$ | Total Size of 48 NDFs / Road (MB) |
|-------------|-------------|-----------------------------------|
| PWR | 1100 | 132 |
| VHTR | 1300 | 129 |

The Need for On-the-fly Doppler Broadening (2)

- ❑ Physical memory requirement to perform a Monte Carlo transport calculation with exact Doppler broadening.

Point-wise temperature dependent data files

| | Size of NDFs/Road (MB) | # of Assemblies | Fuel Roads / Assembly | Sym | # of Terms in Regression Model | Total size (MB) |
|-------------|------------------------|-----------------|-----------------------|------|--------------------------------|-----------------|
| PWR | 132 | 193 | 264 | 1/8 | - | 840,708 |
| VHTR | 129 | 1020 | 222 | 1/12 | - | 2,434,230 |

Regression Model

| | Size of NDFs/Road (MB) | # of Assemblies | Fuel Roads / Assembly | Sym | # of Terms in Regression Model | Total size (MB) |
|-------------|------------------------|-----------------|-----------------------|-----|--------------------------------|-----------------|
| PWR | 185 | - | - | - | 13 | 2,405 |
| VHTR | 185 | - | - | - | 13 | 2,405 |

Theory – Regression Model (1)

□ ψ and χ are the only temperature dependent functions in multi-level Adler-Adler resonance representation.

□ Resonance parameters can be held constant for a given neutron energy and nuclide.

$$\psi_R(T) = \sum_i a_{R,i} f_i(T)$$

$$\chi_R(T) = \sum_i b_{R,i} h_i(T)$$

□ a_R and b_R depend on the corresponding resonance parameters.

Theory – Regression Model (2)

□ Adler-Adler:

$$\sigma_R^x(T) = A_R + \sum_{R'} \left[B_{R'} \psi(T) + C_{R'} \chi(T) \right]$$

$$\sigma_R^x(T) = A_R + \sum_{R'} \left[B_{R'} \sum_i a_{R',i} f_i(T) + C_{R'} \sum_i b_{R',i} h_i(T) \right]$$

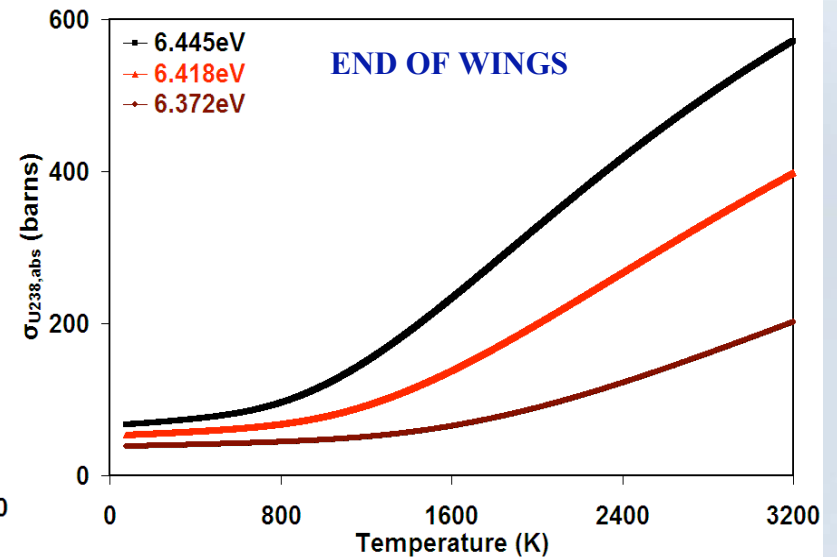
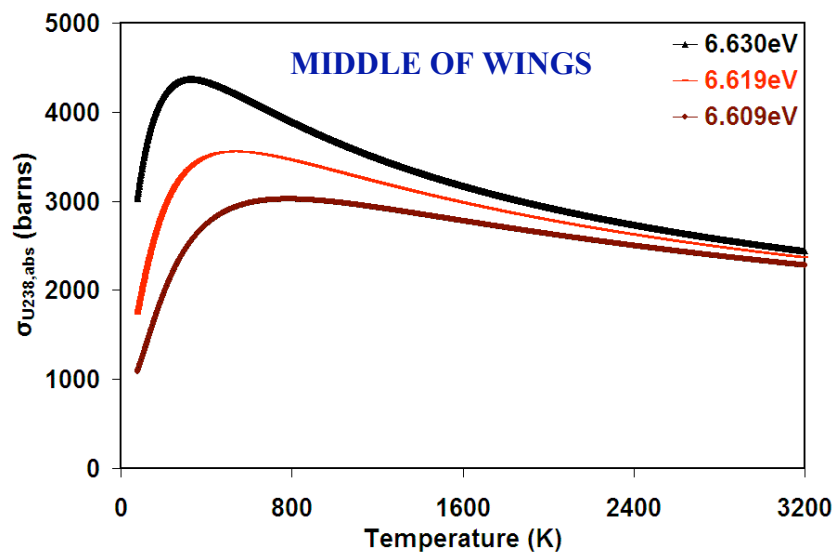
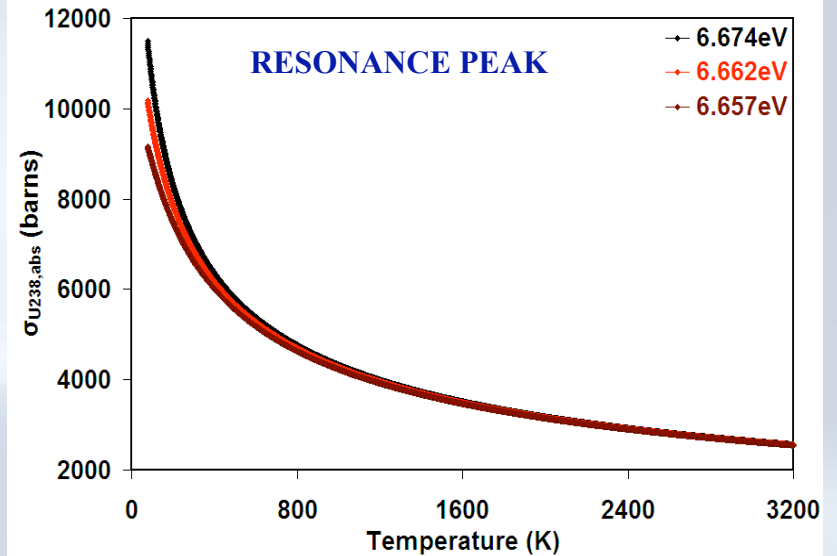
$$\sigma_R^x(T) = A_R + \sum_i f_i(T) \sum_{R'} a'_{R',i} + \sum_i h_i(T) \sum_{R'} b'_{R',i}$$

$$\sigma_R^x(T) = A_R + \sum_i f_i(T) a''_i + \sum_i h_i(T) b''_i$$

□ Once the temperature dependence of f_i and h_i is found, the constants in the above regression models can easily be adjusted by applying the real Doppler broadened cross sections for a given range of temperature.

Theory – Regression Model (3)

□ The temperature dependence of the cross sections must be investigated by dividing a given resonance region into multiple sub-regions.



Theory – Regression Model (4)

□ Around the peak of a resonance region:

$$\psi_R(z) = \frac{\xi_R}{2\sqrt{\pi}} \operatorname{Re} \left\{ \exp(z^2) \operatorname{erfc}(-z) \right\} \quad \chi_R(z) = \frac{\xi_R}{2\sqrt{\pi}} \operatorname{Im} \left\{ \exp(z^2) \operatorname{erfc}(-z) \right\}$$

where $z = i \frac{(x+i)}{2} \xi_R$. Taylor series expansions:

$$\exp(z^2) = \sum_{n=0}^{\infty} \frac{z^{2n}}{n!} \quad \operatorname{erfc}(-z) = 1 + \frac{2}{\sqrt{\pi}} \sum_{n=0}^{\infty} \frac{(-1)^n z^{2n+1}}{n!(2n+1)}$$

Since $\xi_R = \Gamma_T \left(\frac{A}{4kE_R T} \right)^{1/2}$, $z = \frac{a+bi}{\sqrt{T}}$

$$\psi_R(T) = \frac{c}{\sqrt{T}} \operatorname{Re} \left\{ \exp \left[\left(\frac{a+bi}{\sqrt{T}} \right)^2 \right] \operatorname{erfc} \left(-\frac{a+bi}{\sqrt{T}} \right) \right\} = \sum_{i=1}^{\infty} \frac{a_{R,i}}{T^{i/2}}$$

$$\chi_R(T) = \frac{c}{\sqrt{T}} \operatorname{Im} \left\{ \exp \left[\left(\frac{a+bi}{\sqrt{T}} \right)^2 \right] \operatorname{erfc} \left(-\frac{a+bi}{\sqrt{T}} \right) \right\} = \sum_{i=1}^{\infty} \frac{b_{R,i}}{T^{i/2}} \quad \sigma_{Adler-Adler}^x(T) = \sum_{i=0}^{\infty} \frac{e_i}{T^{i/2}}$$

Theory – Regression Model (5)

□ Around the end of a resonance wing:

$$\psi_R(z) = \frac{\xi_R}{2\sqrt{\pi}} \operatorname{Re} \left\{ \exp(z^2) \operatorname{erfc}(-z) \right\} \quad \chi_R(z) = \frac{\xi_R}{2\sqrt{\pi}} \operatorname{Im} \left\{ \exp(z^2) \operatorname{erfc}(-z) \right\}$$

where $z = i \frac{(x+i)}{2} \xi_R$. Asymptotic expansion:

$$\exp(z^2) \operatorname{erfc}(-z) = -\frac{1}{z\sqrt{\pi}} \sum_{n=0}^{\infty} \frac{(-1)^n (2n)!}{n! (2z)^{2n}}$$

Since $\xi_R = \Gamma_T \left(\frac{A}{4kE_R T} \right)^{1/2}$, $z = \frac{a+bi}{\sqrt{T}}$

$$\psi_R(T) = \frac{c}{\sqrt{T}} \operatorname{Re} \left\{ \exp \left[\left(\frac{a+bi}{\sqrt{T}} \right)^2 \right] \operatorname{erfc} \left(-\frac{a+bi}{\sqrt{T}} \right) \right\} = \sum_{i=0}^{\infty} a_{R,i} T^i$$

$$\chi_R(T) = \frac{c}{\sqrt{T}} \operatorname{Im} \left\{ \exp \left[\left(\frac{a+bi}{\sqrt{T}} \right)^2 \right] \operatorname{erfc} \left(-\frac{a+bi}{\sqrt{T}} \right) \right\} = \sum_{i=0}^{\infty} b_{R,i} T^i \quad \sigma_{Adler-Adler}^x(T) = \sum_{i=0}^{\infty} e_i T^i$$

Theory – Regression Model (6)

□ Around the middle of a resonance wing:

| | 6.630eV | | 6.619eV | | 6.609eV | |
|-------------------------------------|-----------------|-----------------|-----------------|-----------------|-----------------|-----------------|
| | SSE | RMSE | SSE | RMSE | SSE | RMSE |
| $\sum_{n=0}^{12} a_n (T)^n$ | 1.23E+04 | 1.99E+00 | 8.98E+03 | 1.70E+00 | 1.72E+04 | 2.35E+00 |
| $\sum_{n=0}^{12} a_n (T)^{n/2}$ | 2.94E+00 | 3.07E-02 | 2.66E+01 | 9.25E-02 | 2.68E+01 | 9.29E-02 |
| $\sum_{n=0}^{12} a_n (\ln T)^n$ | 3.13E+08 | 3.17E+02 | 4.12E+08 | 3.64E+02 | 4.36E+08 | 3.75E+02 |
| $\sum_{n=0}^{12} a_n (\ln T)^{n/2}$ | 2.94E+08 | 3.07E+02 | 4.07E+08 | 3.62E+02 | 3.70E+08 | 3.45E+02 |

$$\sigma^x(T) = \sum_{i=0}^{\infty} f_i T^{i/2}$$

Theory – Regression Model (7)

□ Combined Model:

A final numerical study was performed to find a single regression model by combining three different series solutions so that cross sections over all regions, including high, moderate and low portions of resonance wings, can be calculated accurately with a modest computing cost.

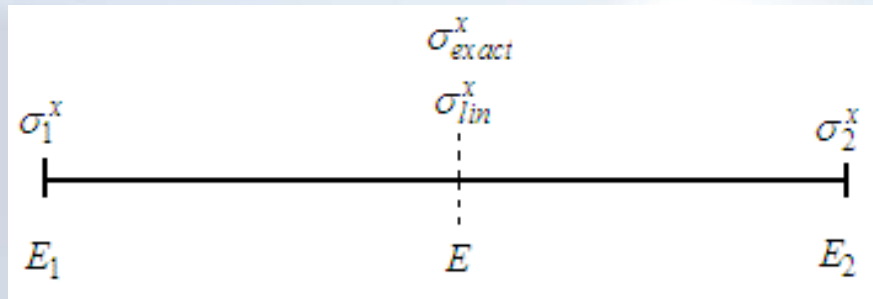
$$\sigma^x(T) = \sum_{n=1}^6 \frac{f_n}{T^{n/2}} + c + \sum_{n=1}^6 g_n T^{n/2}$$

□ Constants must be adjusted by using the Doppler broadened cross sections at a every fine T interval for every energy grid point and nuclide.



Construction of Union Energy Grid (1)

❑ **Fractional Tolerance (FT):** The relative difference in cross sections between the values of actual and linearly interpolated cross sections at mid-point of the successive energy grid points.



$$E = (E_1 + E_2) / 2 \quad \sigma_{lin}^x = (\sigma_1^x + \sigma_2^x) / 2$$

$$\text{If } FT \leq \frac{\sigma_{exact}^x - \sigma_{lin}^x}{\sigma_{exact}^x}, \text{ add point E.}$$

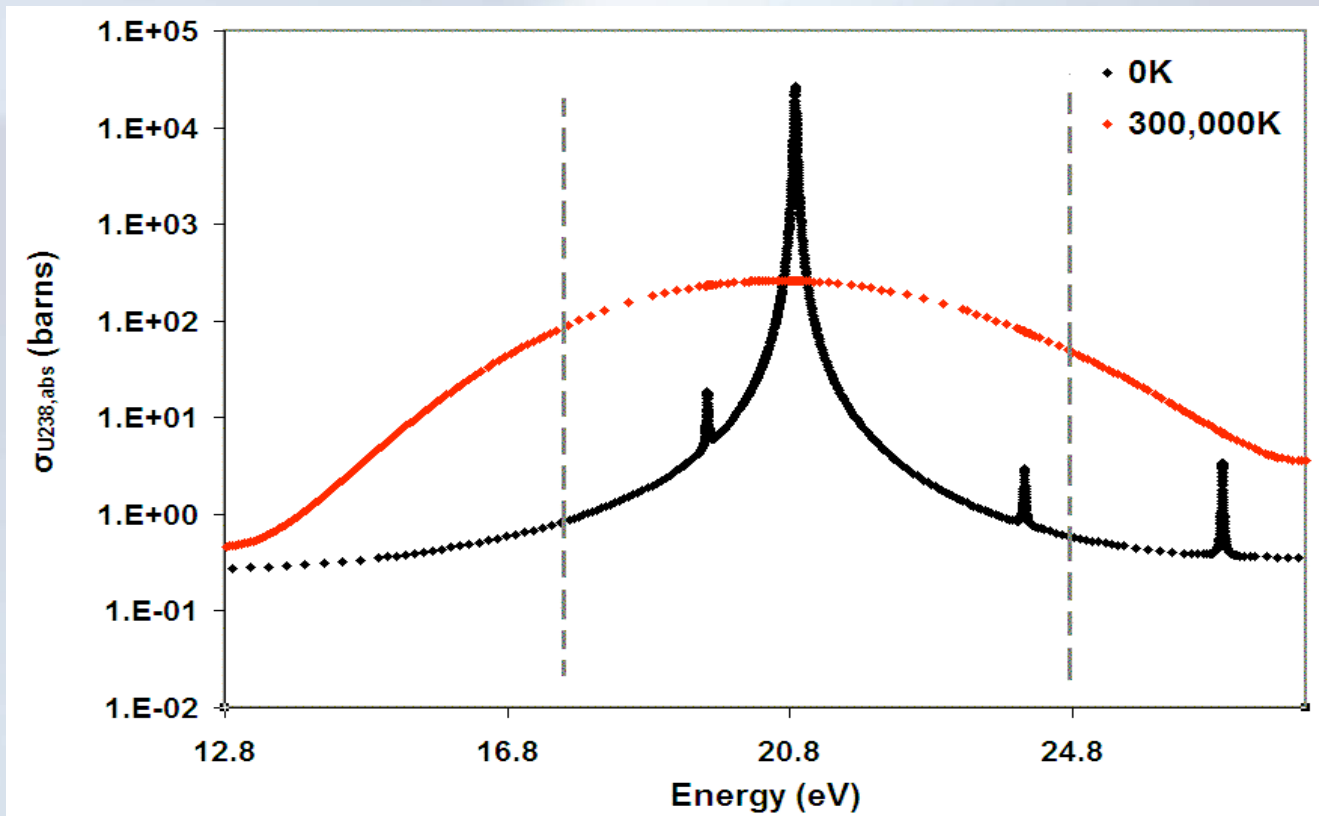
❑ **As the temperature increases:**

- ❑ **Around the resonance peak:** # of energy grids points decrease to satisfy a given FT.
- ❑ **On the resonance wings:** # of energy grids points increase to satisfy a given FT.



Construction of Union Energy Grid (2)

- At the bottom line, the energy grid structure at different elevated temperatures for a given nuclide differs from each other to satisfy a given FT.



Construction of Union Energy Grid (3)

| | Fractional Tolerance in NJOY | | | | | | | |
|-------|---|--------|--------|-------|-------|-------|-------|-------|
| | 0.1% | 0.3% | 0.5% | 1.0% | 2.0% | 3.0% | 4.0% | 5.0% |
| T (K) | Number of Energy Grid Points in Nuclear Data Files for U238 | | | | | | | |
| 0 | 193131 | 122935 | 100646 | 76856 | 57347 | 49659 | 44955 | 41676 |
| 77 | 103600 | 70240 | 59900 | 50049 | 43716 | 41408 | 40250 | 39514 |
| 293.6 | 85247 | 60192 | 52352 | 44810 | 39965 | 38089 | 37104 | 36494 |
| 500 | 77676 | 55786 | 49097 | 42506 | 38188 | 36509 | 35565 | 35006 |
| 1000 | 67437 | 50226 | 44773 | 39625 | 35957 | 34593 | 33810 | 33282 |
| 1500 | 62302 | 47227 | 42557 | 38000 | 34881 | 33616 | 32956 | 32490 |
| 2000 | 58735 | 45153 | 41098 | 36957 | 34109 | 32999 | 32384 | 31918 |
| 2500 | 56248 | 43774 | 39933 | 36177 | 33586 | 32543 | 31948 | 31560 |
| 3000 | 54282 | 42707 | 39051 | 35557 | 33208 | 32192 | 31661 | 31314 |

Construction of Union Energy Grid (4)

- ❑ However, the union energy grid, described above, can not be generated by NDP codes such as NJOY.
- ❑ Therefore, a c++ code was implemented to find a union energy grid for any temperature range of interest and nuclide.
- ❑ An Auxiliary Doppler Code (ADC) was implemented to perform the required task.
- ❑ ADC processes the OK cross section data for the temperature range of interest to construct a union energy grid and the corresponding cross sections for a given nuclide.

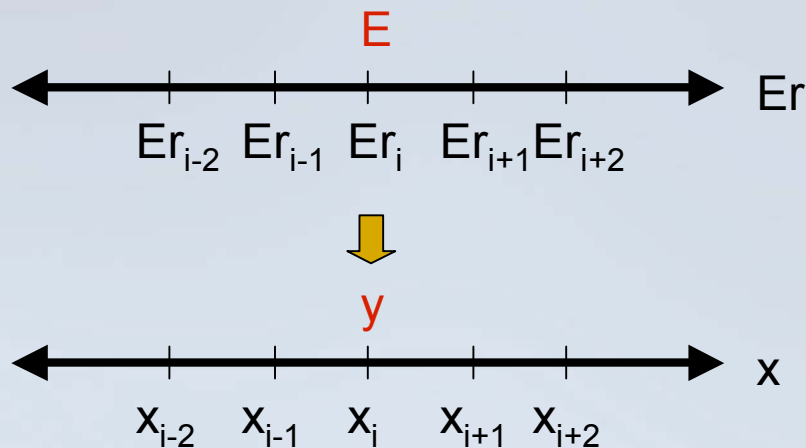
Alternative Doppler Code (ADC) (1)

The well-known Doppler broadening kernel developed by Cullen:

$$\sigma(y, T_2) = \frac{1}{y^2} \left(\frac{1}{\pi} \right)^{\frac{1}{2}} \int_0^{\infty} \sigma(x, T_1) x^2 \left[e^{-(x-y)^2} - e^{-(x+y)^2} \right] dx$$

$$y^2 = \alpha E = \beta V^2 \quad \Leftrightarrow \quad \alpha = \frac{A}{k(T_2 - T_1)} \quad \beta = \frac{M}{2k(T_2 - T_1)}$$

$$x^2 = \alpha E_r = \beta V_r^2$$



Alternative Doppler Code (ADC) (2)

To simplify the Doppler broadening kernel :

$$\sigma(y, T_2) = \sigma^*(y, T_2) - \sigma^*(-y, T_2)$$

$$\sigma^*(y, T_2) = \frac{1}{y^2} \frac{1}{\sqrt{\pi}} \int_0^{\infty} x^2 \sigma(x, T_1) e^{-(x-y)^2} dx$$

Zero (or room) temperature cross sections were tabulated as a function of energy with linear-linear interpolation in E in nuclear data files. So $\sigma(x, T_1)$ can be written in a discretized form as follows;

$$\sigma(x, T_1) = \sigma_i(T_1) + s_i(x^2 - x_i^2) \quad s_i = \frac{\sigma_{i+1}(T_1) - \sigma_i(T_1)}{x_{i+1}^2 - x_i^2}$$

Letting $z=x-y$ and inserting above equation into $\sigma^*(x, T_2)$, we have;

$$\sigma^*(y, T_2) = \sum_{i=0}^N \left\{ \left[\sigma_i(T_1) - s_i x_i^2 \right] A_i + s_i B_i \right\}$$

Alternative Doppler Code (ADC) (3)

where A_i and B_i are defined as follows;

$$A_i = \frac{1}{y^2} \frac{1}{\sqrt{\pi}} \int_{x_i-y}^{x_{i+1}-y} (z+y)^2 e^{-z^2} dz \quad B_i = \frac{1}{y^2} \frac{1}{\sqrt{\pi}} \int_{x_i-y}^{x_{i+1}-y} (z+y)^4 e^{-z^2} dz$$

Letting $H_n(x_i - y, x_{i+1} - y) = H_n(a, b) = \frac{1}{\sqrt{\pi}} \int_a^b z^n e^{-z^2} dz$

$$A_i = \frac{1}{y^2} [H_2(a, b) + 2yH_1(a, b) + y^2H_0(a, b)]$$

$$B_i = \frac{1}{y^2} [H_4(a, b) + 4yH_3(a, b) + 6y^2H_2(a, b) + 4y^3H_1(a, b) + y^4H_0(a, b)]$$

where $H_n(a, b) = F_n(a) - F_n(b)$ is calculated based on F-functions;

$$F_n(a) = \frac{1}{\sqrt{\pi}} \int_a^{\infty} z^n e^{-z^2} dz \quad F_0(a) = \frac{1}{2} \operatorname{erfc}(a) \quad F_1(a) = \frac{1}{2\sqrt{\pi}} e^{-a^2}$$

$$F_n(a) = \frac{n-1}{2} F_{n-2}(a) + a^{n-1} F_1(a)$$

Alternative Doppler Code (ADC) (4)

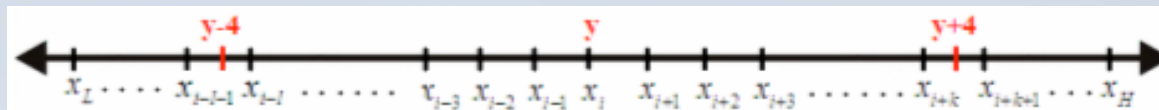
Extra attention must be paid when $(a-b)$ gets small. In such cases, since $H_n(a,b)$ loses its significance, $H_n(a,b)$ must be calculated by Taylor series expansion.

$$H_n(a,b) = \frac{b-a}{1!} G'_n(a) + \dots + \frac{(b-a)^m}{m!} G_n^m(a) + \dots$$

$$G_n^m(x) = \frac{d^{m-1}}{dx^{m-1}} [x^n e^{-x^2}] = e^{-x^2} P_n^m(x) \quad P_n^m = \frac{d}{dx} P_n^{m-1}(x) - 2x P_n^{m-1}(x) \quad P_n^1 = x^n$$

For $\sigma^*(y, T2)$ and $\sigma^*(-y, T2)$, the exponential function in broadening kernel limits the significant part of the integral to the range:

$$\sigma^*(y, T2): \quad y-4 < x < y+4, \quad -4 < z < 4$$

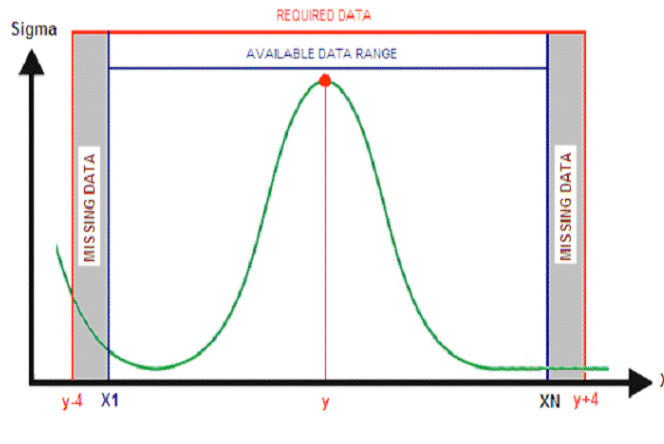


$$\sigma^*(-y, T2): \quad 0 \leq x < 4, \quad -y \leq z < 4-y$$



Alternative Doppler Code (ADC) (5)

One needs to pay extra attention when broadening the cross sections close to end points of the energy grid. As shown below, cross sections may end before $y-4$ or $y+4$. Therefore the cross sections in the missing data region must be approximated.



1. Low Energy Approximation ($1/v$)

$$\sigma(x, T_1) = \frac{C}{x}$$

$$\sigma^*(y, T_2) = \frac{1}{y^2} \frac{1}{\sqrt{\pi}} \int_{-y}^{x_1-y} [(z+y)C] e^{-z^2} dz$$

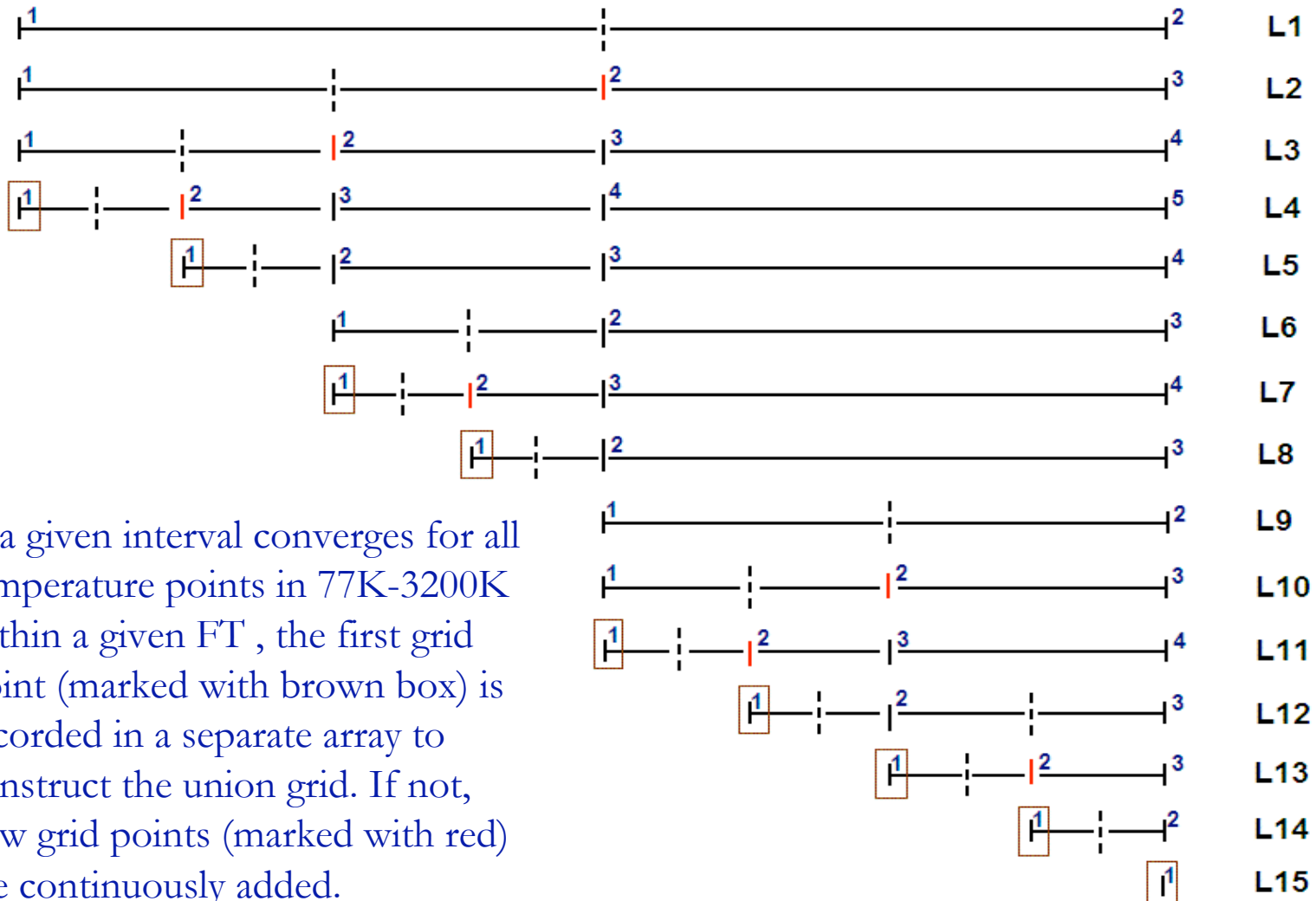
$$\sigma^*(y, T_2) = \frac{C}{y^2} [H_1(-y, x_1-y) + yH_0(-y, x_1-y)]$$

2. High Energy Approximation (Constant)

$$\sigma(x_{N+1}, T_1) = C \quad \sigma^*(y, T_2) = \frac{1}{y^2} \frac{1}{\sqrt{\pi}} \int_{x_N-y}^{\infty} [(z+y)^2 C] e^{-z^2} dz$$

$$\sigma^*(y, T_2) = \frac{C}{y^2} [F_2(x_N - y) + 2yF_1(x_N - y) + y^2F_3(x_N - y)]$$

Alternative Doppler Code (ADC) (6)



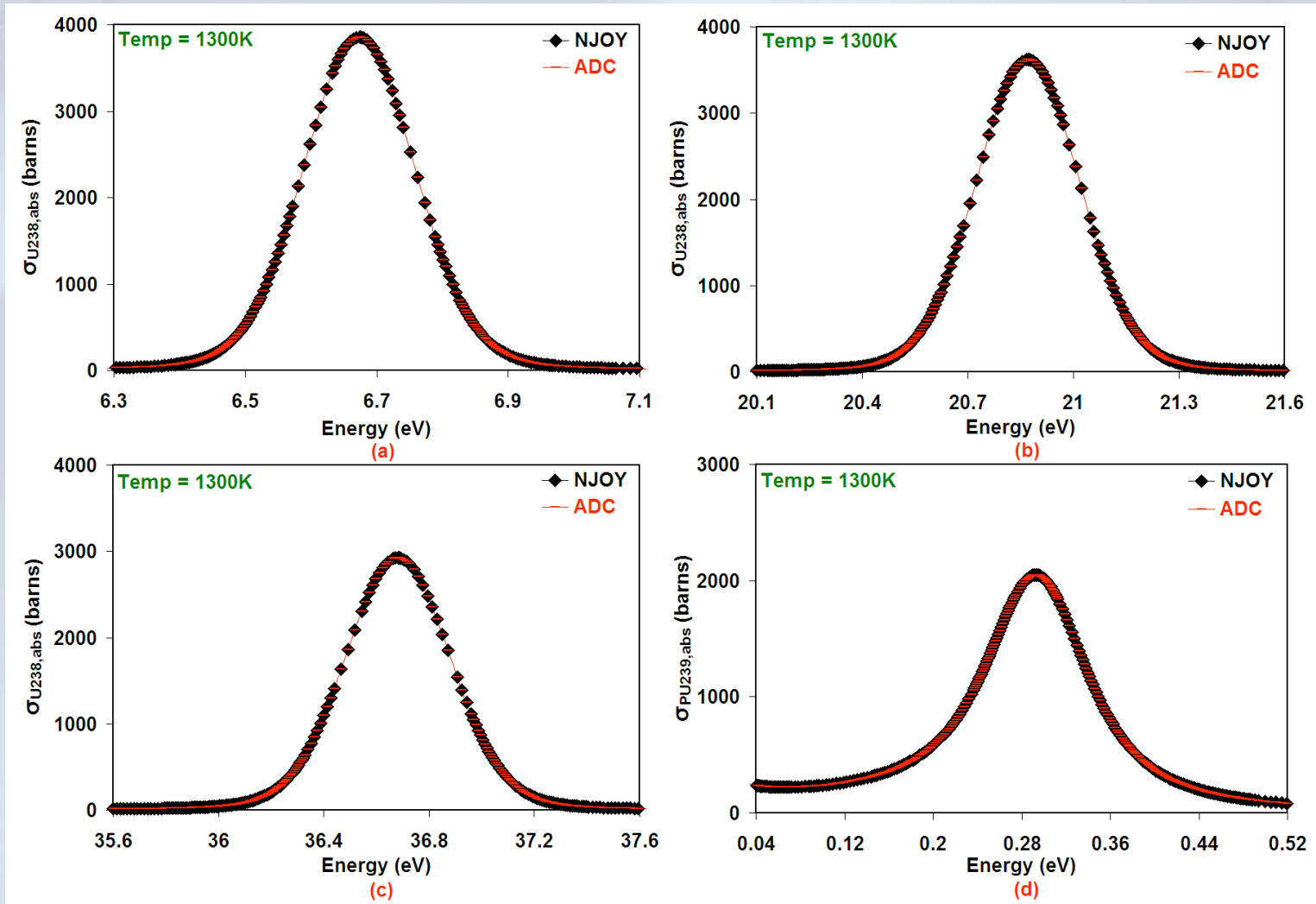
If a given interval converges for all temperature points in 77K-3200K within a given FT, the first grid point (marked with brown box) is recorded in a separate array to construct the union grid. If not, new grid points (marked with red) are continuously added.

Results - Union Energy Grid

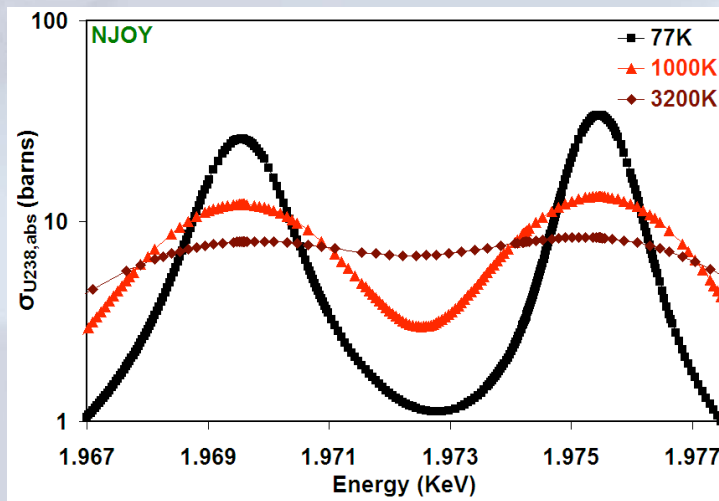
- Resultant energy grid points at a given temperature can get very high for some nuclides that have narrow, high-energy resonances, which don't need to be treated accurately in many applications.
- If the contribution to the resonance integral from any one interval gets small, the interval is declared converged. Resonance integral error was limited with 0.001 barns in ADC as in NJOY for a given FT of 0.1%. Since important resonance integrals vary from a few barns to a few hundred barns, this is a reasonable choice.

| | # of Union Grid Points for 77K-3200K with FT = 0.1% (U238) | | |
|----------------|--|---------------------------|--------------------|
| ΔT (K) | Res. Int. Err. = 0.001 b | Res. Int. Err. = 0.0001 b | Res. Int. Err. = 0 |
| 100 | 109,134 | 148,366 | 360,129 |
| 50 | 109,154 | 148,614 | 363,513 |
| 25 | 109,159 | 148,692 | 364,525 |

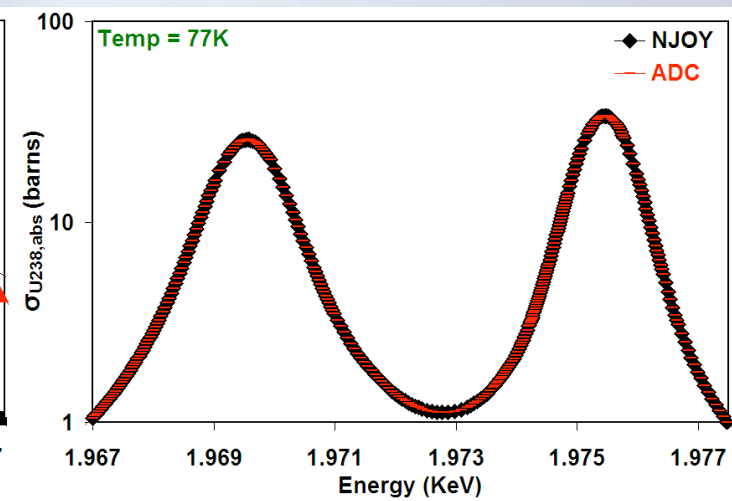
Results - Comparison of ADC with NJOY (1)



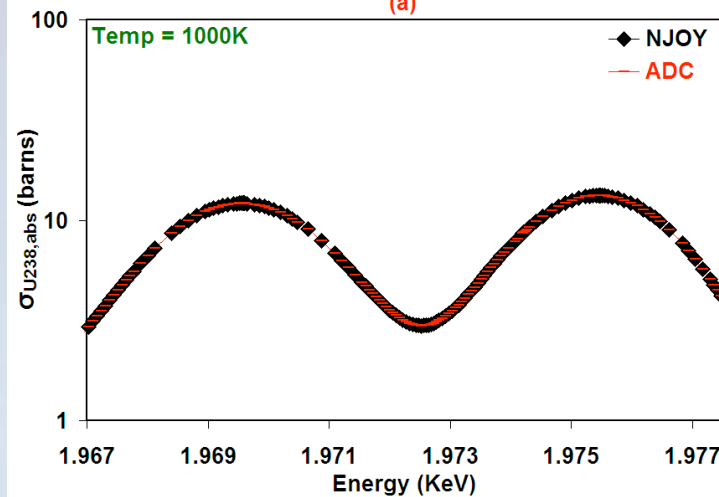
Results - Comparison of ADC with NJOY(2)



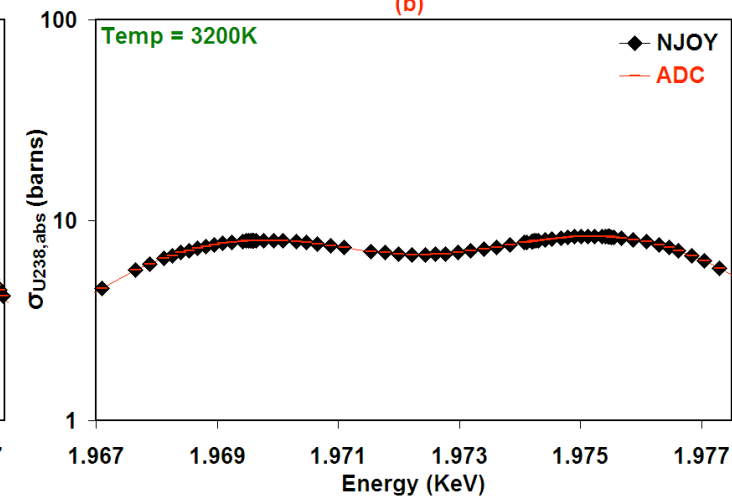
(a)



(b)

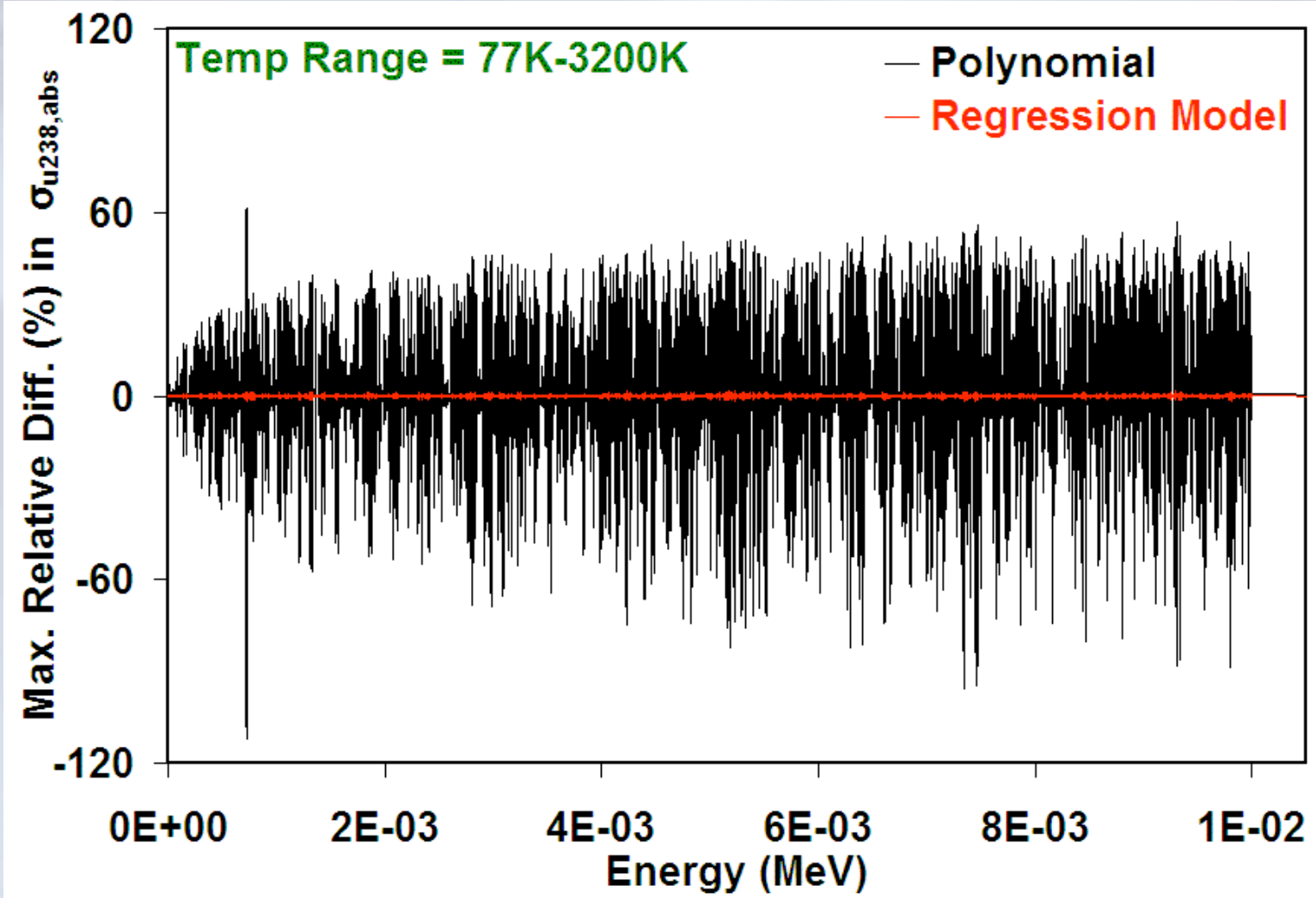


(c)

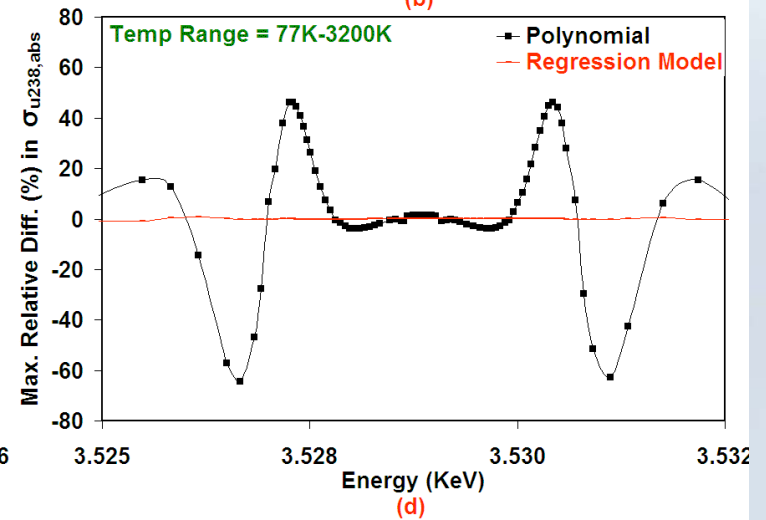
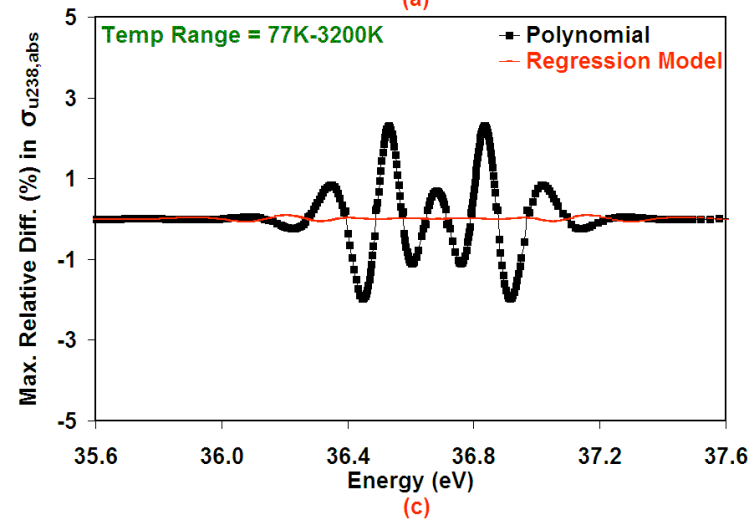
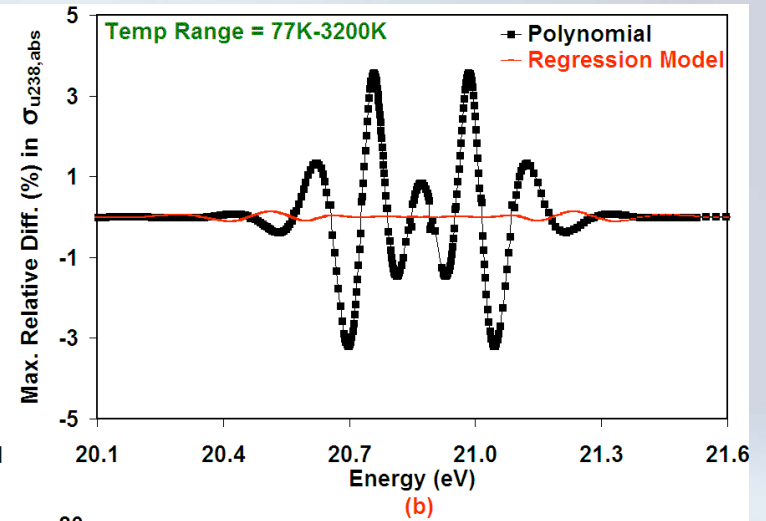
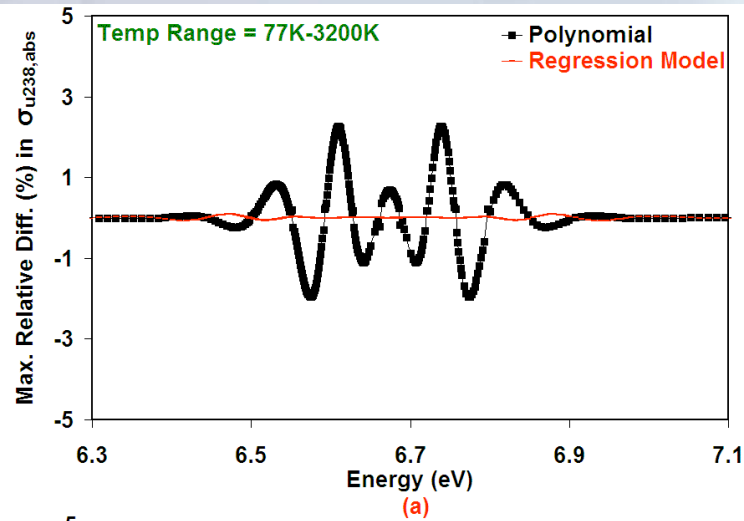


(d)

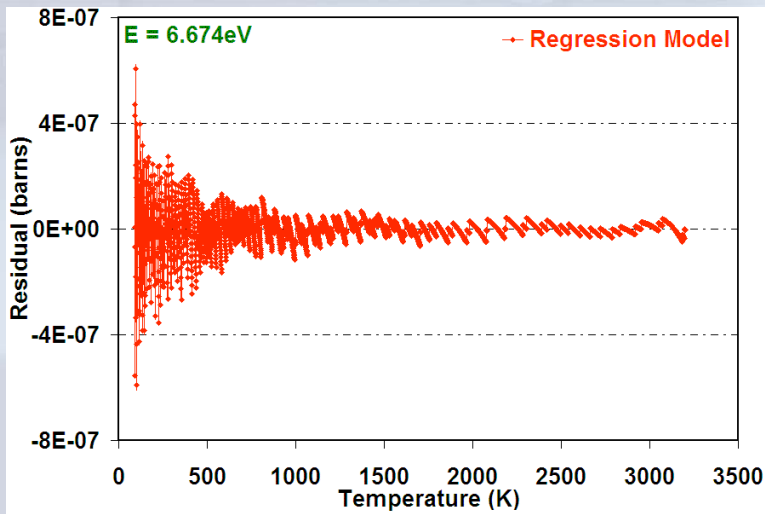
Results: Max. Rel. Diff (%) = $\frac{\sigma_a^{Exact}(T) - \sigma_a^{Model}(T)}{\sigma_a^{Exact}(T)} \times 100$



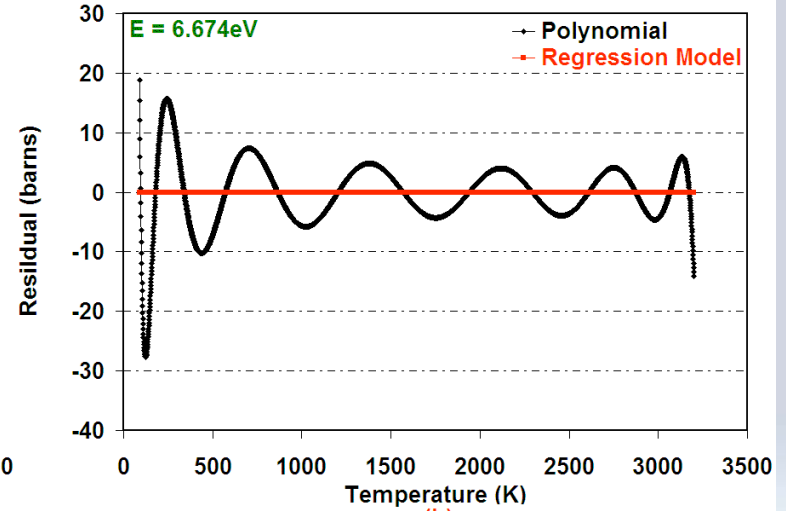
Results: Max. Rel. Diff (%) = $\frac{\sigma_a^{Exact}(T) - \sigma_a^{Model}(T)}{\sigma_a^{Exact}(T)} \times 100$



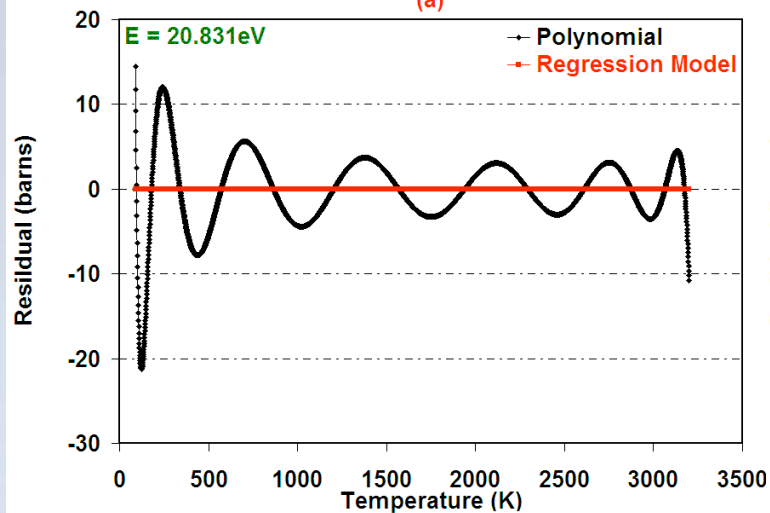
Results: Residual Scatter = $\sigma_a^{Exact}(T) - \sigma_a^{Model}(T)$



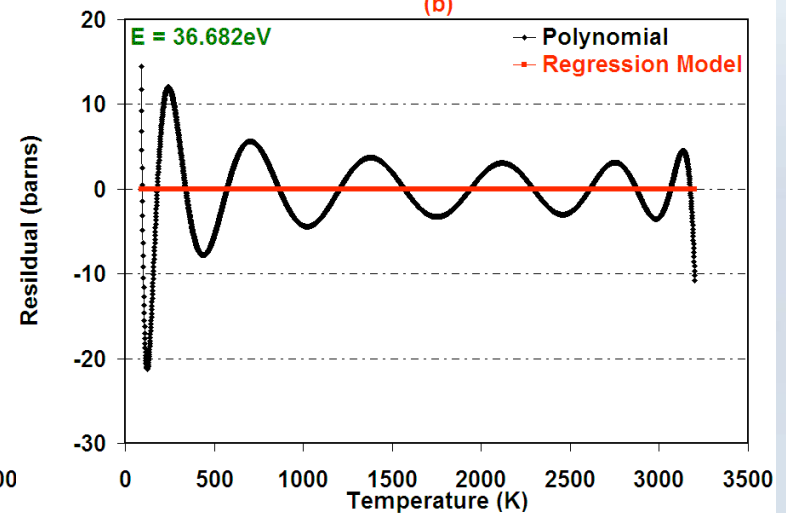
(a)



(b)



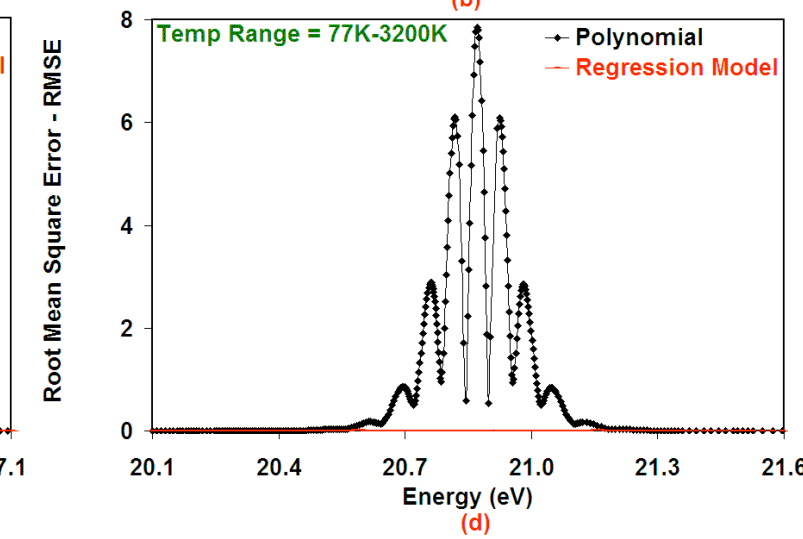
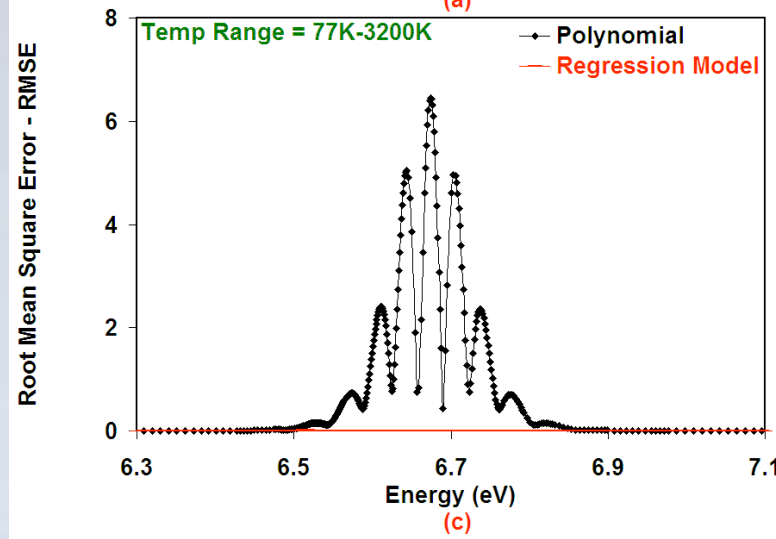
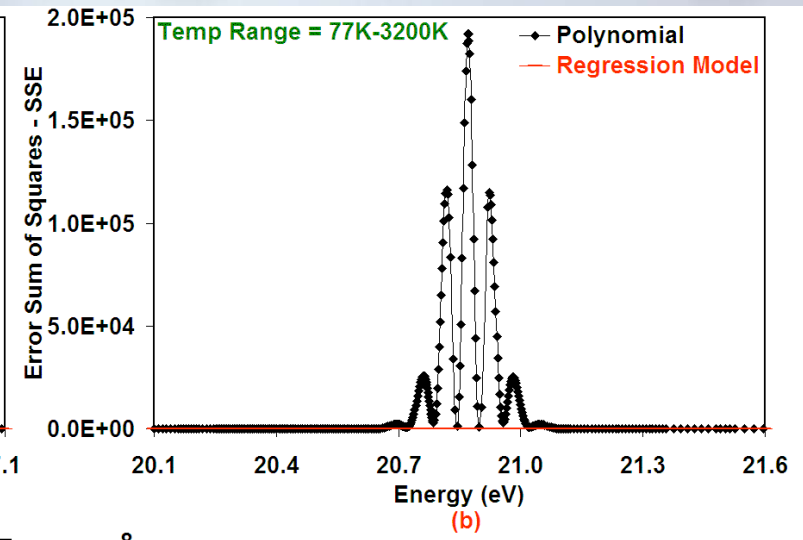
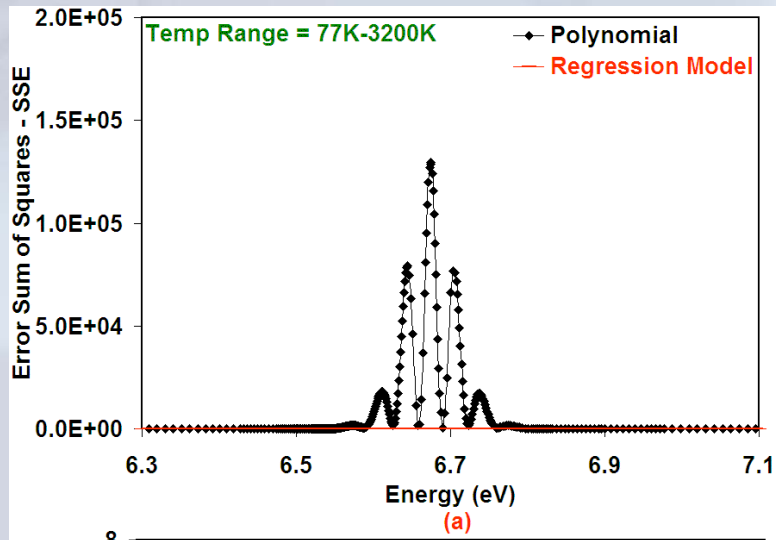
(c)



(d)

Results:
$$SSE = \sum_{T=77}^{3200} \left[\sigma_a^{Exact}(T) - \sigma_a^{Model}(T) \right]^2$$

$$RMSE = \sqrt{\frac{SSE}{v}}$$



Results: Monte Carlo Timing with On-The-Fly Doppler Broadening

- The free gas thermal model was applied to sample the motion of the target atoms in the medium in our Monte Carlo code. PDFs for target velocity and collision angle are sampled from;

$$f(x) dx = \frac{2}{3\sqrt{\pi}a^2} \frac{\left[(a-x)^3 - |a-x|^3 \right] x \exp(-x^2) dx}{\left(1 + \frac{1}{2a^2} \right) \operatorname{erf}(a) + \frac{1}{a\sqrt{\pi}} \exp(-a^2)} \quad f(\mu) = 3ax \frac{\left[a^2 + x^2 - 2ax\mu \right]^{1/2}}{(a+x)^3 - |x-a|^3}$$

$$\mu = \frac{1}{2ax} \left[a^2 + x^2 - \left[(x+a)^3 + \xi \left[|x-a|^3 - (x+a)^3 \right] \right]^{2/3} \right] \quad x = \beta v_t$$

- It was found that regression model can be used in Monte Carlo codes to Doppler broaden the cross sections on-the-fly with a computing cost less than 1% without keeping the broadened cross sections in the memory and letting an unlimited number of temperatures.



Conclusions

- ❑ The new regression model, derived based on the Adler-Adler multi level resonance representation, let us calculate the temperature dependent cross sections at the energy grid points with excellent accuracy.
- ❑ On-the-fly Doppler broadening of the cross sections have been successfully performed by using the combined regression model for the Monte Carlo codes for a modest computing cost.
- ❑ Doppler broadened cross sections during the random walks of the neutrons are newer kept in the memory, letting an unlimited number of temperatures.

Questions

